



**HAL**  
open science

# Surface modification of different materials for biological and environmental applications

Flavia Fioresi

► **To cite this version:**

Flavia Fioresi. Surface modification of different materials for biological and environmental applications. Organic chemistry. Normandie Université, 2020. English. NNT : 2020NORMR062 . tel-03141546

**HAL Id: tel-03141546**

**<https://theses.hal.science/tel-03141546>**

Submitted on 15 Feb 2021

**HAL** is a multi-disciplinary open access archive for the deposit and dissemination of scientific research documents, whether they are published or not. The documents may come from teaching and research institutions in France or abroad, or from public or private research centers.

L'archive ouverte pluridisciplinaire **HAL**, est destinée au dépôt et à la diffusion de documents scientifiques de niveau recherche, publiés ou non, émanant des établissements d'enseignement et de recherche français ou étrangers, des laboratoires publics ou privés.



Normandie Université

## THESIS

To obtain the doctoral degree

Specialty Chemistry

Prepared at the Rouen University

# SURFACE MODIFICATION OF DIFFERENT MATERIALS FOR BIOLOGICAL AND ENVIRONMENTAL APPLICATIONS

Presented and defended by  
**Flávia FIORESI**

Thesis publicly defended on december 17, 2020  
In front of the jury composed by

Dr Mohamed CHEHIMI	Directeur de recherche, Université de Paris Est-Créteil	Rapporteur
Pr Steeve REISBERG	Professeur des Universités, Université de Paris	Rapporteur
Pr Souad AMMAR-MERAH	Professeur des Universités, Université de Paris	Examineur
Pr Franck LE DERF	Professeur des Universités, Université de Rouen	Directeur de thèse
Dr Julien VIEILLARD	Maitre de conférences, Université de Rouen	Encadrant
Dr Nadine MOFADDEL	Maitre de conférences, Université de Rouen	Encadrant

Thesis directed by Pr. Franck LE DERF, COBRA laboratory



***À mon petit nourrisson Giuseppe Vincent FIORESI et à son papa.***



**SURFACE MODIFICATION OF DIFFERENT  
MATERIALS FOR BIOLOGICAL AND  
ENVIRONMENTAL APPLICATIONS**



## Remerciements

Je remercie tout d'abord Pr. Franck LE DERF mon directeur de thèse et aussi directeur de l'IUT et du campus d'Evreux, de l'Université de Rouen Normandie, pour m'avoir permise d'effectuer ma thèse dans son laboratoire et de m'avoir soutenue pendant toute ce période.

Je remercie tout particulièrement mon encadrant le Dr. Julien VIEILLARD, pour m'avoir accueillie dans son équipe au sein du laboratoire COBRA Evreux. Il m'a permis de découvrir puis de m'impliquer dans ce sujet pluridisciplinaire tout en me communiquant son enthousiasme. Je tiens aussi à remercier sa persévérance dans la période intermédiaire entre le démarrage de mon entreprise Fioresi Commerce, puis la naissance de mon bébé et la fin de ma thèse.

Je tiens aussi à remercier Dr. Nadine MOFADDEL ma Co-directrice de thèse et maitre de conférences, à l'Université de Rouen pour ses conseils, sa bienveillance et son encouragement.

Je remercie mon financeur, le programme EBW+ ERASMUS, qui a permis que ces travaux soient possibles.

Je tiens ensuite à remercier les membres du jury Dr. CHEHIMI, Pr. REISBERG et Pr. AMMAR-MERAH d'avoir accepté d'examiner mon travail de thèse, surtout dans ce moment compliqué à cause de l'épidémie de la COVID-19.

J'associe à ces remerciements les autres membres du groupe et collègues de travail de l'IUT d'Évreux qu'ont été très ouverts et accueillants depuis toujours pendant ces années de travail ensemble.

Bien sûr, cette thèse n'aurait pu aboutir sans le soutien, les conseils et les mots

d'encouragement de mon mari Everton FIORESI qui a toujours été présent avec son amour.

Mes remerciements vont aussi à ma famille au Brésil et mes amis pour tout leur soutien très important pour ma motivation et encouragement, avec des places particulières réservées à ma mère, mon père et ma sœur.

## Abbreviations

### A

**AWB** Agrowastes Biomass

### B

**BSA** Bovine Serum Albumin

### C

**CBD** 4-(Carboxymethyl) benzenediazonium

**COC** Cyclic Olefin Copolymer

### F

**IRTF** Fourier Transform Infrared Spectroscopy

**FET** Field-Effect Transistor

### G

**GC** Glassy Carbon

### H

**HF<sub>4</sub>** Tetrafluoroboric Acid

**H<sub>3</sub>PO<sub>2</sub>** Hypophosphorous acid

### I

**IM-MS** Ionic Mobility and Mass Spectrometry

### L

**LMSM** Laboratory of Microbiology - Signals and Microenvironment

### N

**nPTMS** n-propyl trimethoxysilane

## M

**M** mol L<sup>-1</sup>

## P

**PEI** Polyethylene Imine

**PBS** Phosphate Buffered Saline

## S

**SEM-EDX** Scanning Electron Microscope - Energy-dispersive X-ray Spectroscopy

**SPR** Surface Plasmon Resonance

**SAM** Self-assembled monolayer

**SPRi** Surface Plasmon Resonance imaging

## Summary

<b>GENERAL INTRODUCTION</b> .....	15
<b>CHAPTER I</b> .....	19
1. What is surface modification and why to study it? .....	20
1.1. Surface modification applied to the development of biosensors .....	22
1.1.1. For bio detection .....	25
1.1.2. To study bio interaction .....	26
1.2. Surface modification to remove pollutant from environment .....	26
1.2.1. Liquid phase .....	27
1.2.2. Gas phase .....	28
2. The chemistries used in surface functionalization .....	30
2.1. Physical treatment .....	30
2.1.1. Heat treatment .....	30
2.1.2. Gas treatment .....	31
2.2. Chemical treatment .....	32
2.2.1. Coating .....	32
2.2.2. Covalent grafting .....	33
2.3. Thiol .....	33
2.4. Silane .....	34
2.5. Diazonium salts .....	37
2.5.1. History .....	37
2.5.2. Synthesis .....	39

2.5.3.	Surface modification with diazonium salts .....	42
2.5.3.1.	Spontaneous grafting .....	42
2.5.4.	Chemical reduction.....	42
2.5.5.	Electrochemical reduction or oxidation .....	43
<b>CHAPTER II</b>	.....	<b>47</b>
1.	Introduction .....	48
2.	Presentation of the Surface Plasmon Resonance technique .....	49
2.1.	Modification of the SPR surface.....	53
2.1.1.	My strategy .....	54
2.2.	The choice of the diazonium salt.....	54
2.3.	The substrates selected to develop the SPR biochip .....	55
2.4.	The optical performance requested for a SPR biochip.....	56
3.	The SPR biochip developed.....	56
3.1.	Surface functionalization by chemical reduction .....	57
3.2.	Surface functionalization by electrografting.....	60
3.2.1.	Influence of the electroreduction parameters .....	62
3.2.2.	The characterization of the best candidate.....	67
3.2.2.1.	Cyclic voltammetry with ferrocene.....	67
3.2.2.2.	Infrared Spectroscopy (IRTF).....	68
3.2.2.2.1.	Description of the principle.....	68
3.2.2.2.2.	The ATR-IRTF (Attenuated Total Reflection) spectroscopy .....	69
3.2.2.2.3.	The surface characterization by ATR-IRTF.....	70

3.2.3. SPR Plasmon Curves.....	72
4. Application of the gold functionalized surface in SPR analysis .....	72
4.1. Antibody-antigen .....	73
4.2. The CNP-AmiC interactions.....	79
4.3. The next generation of biochip – Strip Gold Surface (SGS).....	81
5. Conclusion .....	86
<b>CHAPTER III.....</b>	<b>93</b>
1. Introduction .....	95
2. SCIENTIFIC PAPER I .....	98
3. SCIENTIFIC PAPER II .....	106
4. SCIENTIFIC PAPER III .....	113
5. Conclusion .....	124
<b>CONCLUSION AND PERSPECTIVES.....</b>	<b>127</b>
<b>EXPERIMENTAL PART .....</b>	<b>129</b>



## GENERAL INTRODUCTION

For almost a century, the researchers have been making important efforts in order to bring new properties to materials and nowadays surface modification of materials is more than ever a very attractive research subject related to a variety of promising industrial applications. The development of simple methodology to characterize biomolecular interactions has been, over the years, an indispensable technology to support researches in the areas of biology and microbiology due its high degree of sensitivity<sup>1</sup>. Various physical and chemical techniques were developed depending on the type and the nature of the material support. Surface modification by chemical coating is a promising solution to obtain well-defined properties such as optical reflectivity, antibacterial, self-cleaning, friction resistance, biocompatibility, anticorrosion, hydrophobicity etc... Thus, performant biosensor and membrane were developed.

That race against the time to develop that kind of device is due to the urgent necessity to expedite diagnoses, performed through support of complementary methods, to prevent the development of diseases. Specially disease resulting to the presence of opportunistic pathogens, such as bacteria<sup>2</sup>.

In development since the beginning of 1990<sup>3</sup>, biosensors are devices able to provide quantitative analytical information based on a biological recognition between two elements linked to a transduction system<sup>4</sup>. Biosensors are characterized by high selectivity and sensitivity, fast reaction process associated to a low cost device<sup>3,5</sup>. There is a wide range of biosensors in the research and development fields, and they can be classified in function of the transducer type<sup>4</sup>. This present study is focused on optical biosensors development due to its applicability in Surface Plasmon Resonance (SPR)<sup>4</sup>. That is a high-quality technique used to measure biomolecular interactions in real time in a label free environment. The ligand is covalently immobilized on the sensor surface and the analyte circulate in solution<sup>4</sup>. In few

decades, numerous studies have been developed in SPR due its possibility to carry out kinetics measurements of biomolecular interactions with a high degree of sensitivity<sup>1</sup>. The SPR analysis are mandatory performed on a flat substrate or a microfluidic device covered with a thin layer of gold. To be robust, an SPR chip should be sensitive, resistant to oxidation and experimental conditions, compatible with biomolecules, protect from unwanted adsorption and suitable for biomolecular grafting.

Until now, the development of robust SPR chip is still under investigation and in this thesis, I proposed to modify the gold surface of the chip with organic layers in order to increase the performance of the analytical tool. This organic layer shall facilitate the attachment of selected biomolecules and limited the unwanted adsorption. Our strategy will study the feasibility of gold solid surface functionalization using a chemistry based on aryldiazonium salts. These salts could be electro- or chemically reduced to obtain a radical moiety which could then covalently grafted to gold surface. This chemistry should be more stable than thiol adsorption used in existing SPR biochip.

Since many years, industrial activities are responsible for a pollution of the atmospheric gas concentration, the water and the soil pollution, drastically increasing the demand for sustainable energy<sup>6,7</sup>. Different methods such as gas adsorption on solid surface, bio sorbents for water heavy metal and dyes removal and different kinds of soil remediation are available to limit these pollutions. The presence some toxics gases in the atmosphere such as CO, CO<sub>2</sub>, H<sub>2</sub>S and hydrocarbons cause damage to the environment and public health<sup>8</sup>. Although different greenhouse gases were involved in atmospheric pollution, CO<sub>2</sub> is still one of the most important due its high concentrations in the atmosphere and due to its ability to induce serious health disease. The CO<sub>2</sub> capture on solid materials has become an interesting research topic for governments and industries in order to minimize the CO<sub>2</sub> quantity in the atmosphere.

Several studies in the literature have demonstrated that some adsorbents such as activated carbons, basic functionalized silica sieves, zeolites, etc.<sup>8</sup> are commercial but still sophisticated and expensive limiting their application. However, there is still a need to capture CO<sub>2</sub> for activities with limited operating cost.

The objective of this study is to promote the cocoa shell, an agrowaste resource ready to use and easy to modify, as low-cost materials for CO<sub>2</sub> adsorption, applying a chemical treatment to modify its physic-chemical properties. Another possible application of this treatment is using the cocoa shell to remove toxins from industrial waste in solution, such as heavy metals and paint residues, which is now one of the major challenges in the textile industries.

In chapter I is presented the bibliography part. The chapter II is mainly dedicated to surface functionalization of gold for application in the Surface Plasmon Resonance (SPR) technique. In the last chapter, I investigated the functionalization of two surfaces for different applications, the first one is a polymer, i.e. cyclic olefin copolymer, and the second one is an agrowaste material, i.e. cocoa shell.



# CHAPTER I

BIBLIOGRAPHIC STUDY

## 1. What is surface modification and why to study it?

Surface properties are responsible for the behavior of any material at the solid-liquid, solid-gas or solid-solid interface. The surface modification of the materials is the strategy that consist in modifying the surface to obtain different optical, mechanical or electrical properties<sup>9</sup>, as for example biocompatibility, adhesion, protection against corrosion, hydrophobicity/hydrophilicity, wear resistance, etc. (Figure 1).

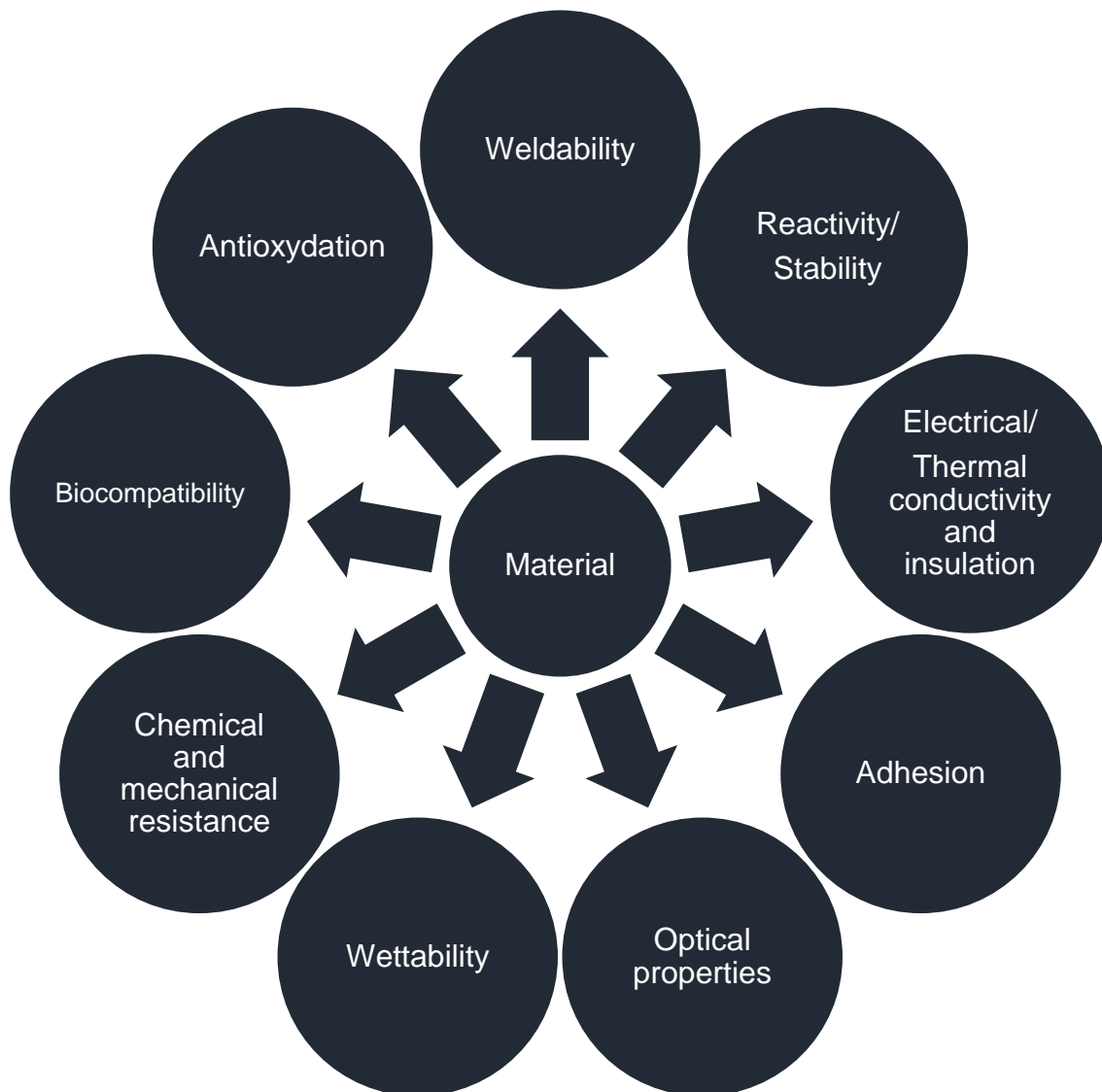


Figure 1: Properties obtained after surface modification.

The act of adding new characteristics to the preexisting properties of the material could help to valorize a material for any application.

There are many advantages of modifying a material (Figure 1) such as reduce corrosion impact through passivation step. Today, the world suffers great economic losses due to the effects caused by the corrosion of materials resulting from the pre-disposal of certain materials to the oxidation, as is the case of metals. Due to so many losses, scientists are constantly studying the development of techniques capable of reducing or avoiding corrosion, such as the use of protective paints<sup>10</sup>, the production of stainless steel<sup>10</sup>, galvanizing<sup>11</sup>, etc.

One strategy for the surface modification is to functionalize it, which means adding new chemical group suitable for different purposes. Thus, the way used for this purpose is to attach molecular species with specific functionality, in a controlled way, to the surfaces.

Surface molecular functionalization combines many challenges: from synthesize a modified material, characterize its properties, and validate its performance for the dedicated application.

The study of the surface properties of materials by organic coatings is of great interest from an industrial point of view, and a wide range of techniques have been developed over the years<sup>12</sup>. Among requirements for organic coatings, its stability under usage conditions is one of the most important parameters. There are different organic coating available, that are usually classified according to the type of interactions created between the substrate and the organic film<sup>13</sup>. Gathered as physisorption, these techniques giving only physical interaction (such as Van der Waals force) between the organic components and the substrate resulting in some case in limited stability<sup>12</sup>. On the contrary, chemisorption methods include grafting techniques in which the organic layer is covalently bound to the surfaces<sup>14</sup>. In this type of interaction we have two approaches, the “grafting to” or the “grafting from”<sup>15</sup>. The “grafting to” consist in adsorbing a polymer layer to form a covalent bond with a surface and the “grafting from” involves a mechanism of polymerization coming from the surface<sup>16</sup>.

Surface studies are very important because chemical reactions with closed environment of the

material occurred at interfaces. Various materials such as polymers<sup>17</sup>, gold<sup>18</sup>, bio sources<sup>19,20</sup>, among others can be modified by chemical grafting and used as supports for different applications.

## 1.1. Surface modification applied to the development of biosensors

The deposit of thin layers of molecular species on surfaces allows the formation of chemically defined surfaces and the control of surface functionality<sup>14</sup>. These types of modified surfaces are considered useful for a wide range of applications, such as biotechnology<sup>18,21</sup>, sensor development<sup>18,22</sup>, molecular electronics<sup>18,21</sup> corrosion inhibition<sup>23,24</sup>, among others. The use of modified surfaces to several applications is becoming increasingly popular and indispensable.

### **This study focuses on:**

- The functionalization of polymeric and metallic surface by diazonium salt to develop original biochip dedicated to characterization of biomolecular interaction.
- The functionalization of biomass by diazonium salt and silane to capture pollutants from the environment.

A biosensor is a device with a recognition mechanism designed to measure biological or chemical reactions<sup>3</sup>. It must be able to transform molecular recognition into a measurable physical signal through association between a biochemical component (antibodies, DNA, protein, cell, bacteria...) and a transducer<sup>25</sup>. The intensity of the measured signal is proportional to the concentration of the analyte<sup>8</sup>. This kind of devices are currently used in various fields such as medical (as for example glucose biosensor for diabetes), environment (as in pollutant measurements), food (as in safety control) and also in the military field (as in detection of explosives)<sup>8</sup>.

Biosensors play important roles in our daily processes, especially in health diagnostics, biomedical engineering, pharmaceutical analysis<sup>26</sup>. In the biomedical field, bio detection is a very important element in the fight against the COVID-19. Based on the rapid increase in the rate of human infection, the World Health Organization (WHO) has classified the COVID-19 outbreak as a pandemic<sup>27</sup>. Because no specific drugs or vaccines for COVID-19 are yet available at this date, early diagnosis and management are crucial for containing the outbreak<sup>28</sup>. Thinking about solving this problem, researchers of Korea developed a biosensor field-effect transistor (FET)-based biosensing device for detecting SARS-CoV-2 in clinical samples<sup>28</sup>. The biosensor was produced by coating graphene sheets of the FET with a specific antibody against SARS-CoV-2 spike protein.

The history of biosensors dates back to 1906, when M. Cremer studied the measurement of the potential difference through a glass membrane separating the unknown solution from a known reference solution, which is what we called nowadays of pH metro<sup>3</sup>.

Years later, in 1962, Leland C. Clark allowed the glucose level to be measured by oxidation using an enzyme attached to an electrode. The signal obtained was therefore a measurement of an electric current at the electrode<sup>8</sup>. However, only in 1975 the first commercial biosensor was developed by a company called Yellow Spring Instruments (YSI)<sup>8</sup>.

This tool consists basically of three components, the output system (display), the transducer part that provide measurable information, which will be chosen for its accuracy and compatibility with the target to be detected and then the detection part of the target, a biological detection system which will be chosen for its affinity with the target to be identified or detected in the analyte<sup>8</sup>. The transduction signal must be simple, sensitive and reliable, and may be of various nature. The selectivity and precision are two important features of a biosensor<sup>8</sup>. An ideal biosensor should be easy to use, small and with a minimal cost for easy large scale

development<sup>3</sup>.

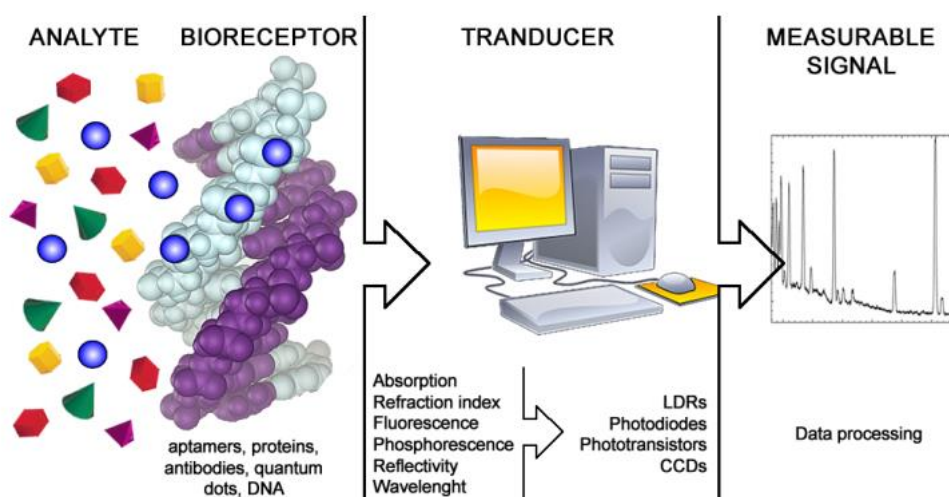


Figure 2. General Scheme of an optical biosensor <sup>29</sup>.

In the two distinct zones of the transducer, numerous combinations are possible, which will make it possible to have biosensors that are more or less sensitive to a particular target or even sensors that allow the simultaneous detection of several biological targets. To be selective for a specific biological compound, the surface of the sensitive interface has to be modified with the bioreceptor.

As described in Table 1, the transducer part of a biosensor can measure various physicochemical parameters that can be classified by families.

Types of transducers	Measured property
<b>Electrochemical</b>	Potentiometric, Amperometric, Conductometric, Nanotechnology and Bioelectronics
<b>Electrical</b>	Surface conductivity, Electrolyte conductivity
<b>Optical</b>	Fluorescence, Adsorption & Reflection, Surface Plasmon resonance
<b>Mass sensitive</b>	Resonance frequency of piezocrystals
<b>Light</b>	Bioluminescence

Table 1. Types of transducers used for biosensor applications <sup>29</sup>.

### 1.1.1. For bio detection

Biosensors are devices used for the detection and quantification of various biomolecules. Detections based on electrical transduction are generally based on conductometry and potentiometry. Conductimetric biosensors measure variation in the electrical resistance or impedance of the system due to the presence of the biomolecules, while potentiometric biosensors measure the electrical potential difference between a working and reference electrode in the presence of the analyte<sup>26</sup>.

Due the COVID-19 pandemic, the development of a highly sensitive and rapid biosensing devices has become increasingly important. Recently, a sensor was produced by coating graphene sheets of the FET with a specific antibody against SARS-CoV-2 spike protein<sup>28</sup>. The Figure 3 below shows how the capture and the analysis are carried out through the biosensor.

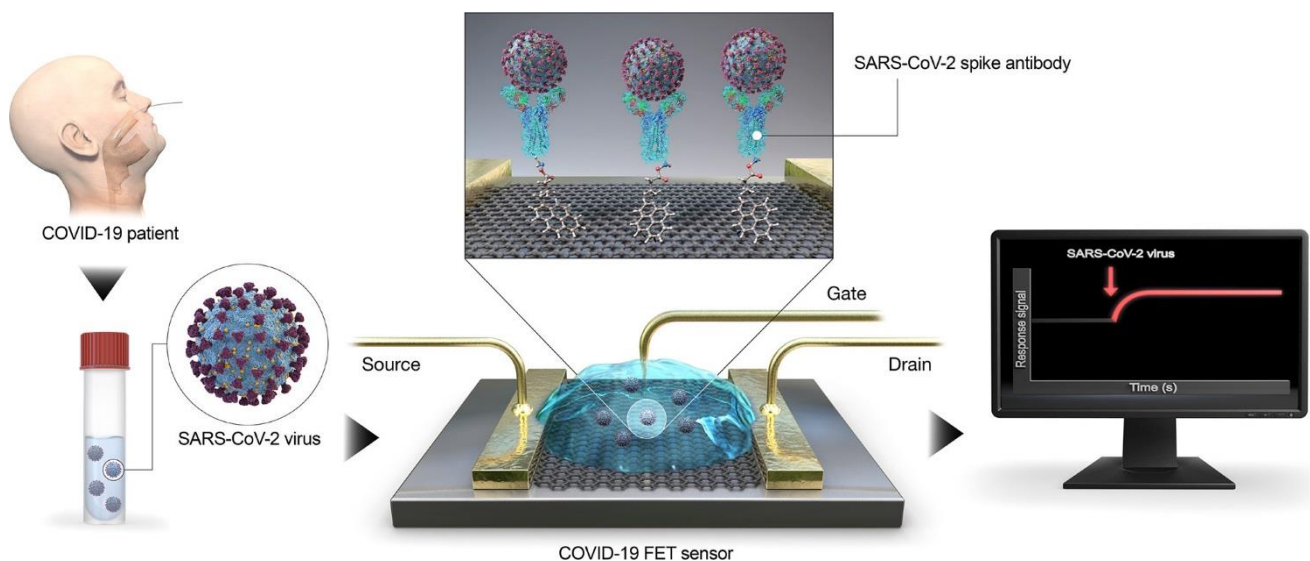


Figure 3. Schematic diagram of COVID-19 FET sensor operation procedure. Graphene as a sensing material is selected, and SARS-CoV-2 spike antibody is conjugated onto the graphene sheet via 1-pyrenebutyric acid N-hydroxysuccinimide ester, which is an interfacing molecule as a probe linker.

The performance of the sensor was determined using antigen protein, cultured virus, and nasopharyngeal swab specimens from COVID-19 patients<sup>30</sup>. Moreover, this technology of bio

detection could be adapted for diagnosis of other emerging viral diseases for example.

### 1.1.2. To study bio interaction

Life is based on biomolecular interaction! DNA, RNA, proteins, sugar chain... need to interact directly or indirectly to define complex answer (metabolism, immune defense...). To define medicine, we need to understand how these different species communicate together and identify if the signal is transferred through a direct interaction or mediated by another molecule. Among the biosensors, immunoassays are based on the direct interaction between antigen and antibody. These biosensors are sensitive, but both of the partners need to be known. DNA, RNA or protein chips could be also used as biosensors. They are interesting because they can be used for high-throughput screening of different targets in a complex solution (Serum, saliva, urine). Unfortunately, these techniques required a reporter strategy (fluorescent dye for instance) to see the interaction. In parallel of these biosensors, SPR biosensors are a promising alternative for quantitative analysis of molecular binding. These biosensors had the advantage of a label free technique, in real time, and ready for high-throughput screening.

## 1.2. Surface modification to remove pollutant from environment

In recent years, the potential of renewable sources to either produce energy or added value materials is a challenge in all fields of research. Focusing on biomass waste, its conversion into valuable products is particularly interesting, especially if the process allowing its transformation can be classified into the so-called green chemistry<sup>31</sup>.

The growth of science and technology over the world has led to the establishment of various industries which has helped the industrial, technological, and agricultural development of many nations. Environmental pollution from a variety of toxic derivatives, particularly heavy metals and minerals, aromatic molecules and dyes in wastewater posed a great danger to human,

plants, and aquatic creatures<sup>32</sup>.

A common example of a case that pollutes the environment are the organic dyes which can bring and firm color to other substances. Synthetic dyes usually have a complex aromatic molecular structure which possibly comes from coal tar-based hydrocarbons such as benzene, naphthalene, anthracene, toluene, xylene, etc. The complex aromatic molecular structures of dyes make them more stable and more difficult to biodegrade<sup>33</sup>. The conventional methods for dye removal from wastewaters include coagulation and flocculation, oxidation or ozonation, membrane separation and adsorption. Activated carbon is popular and effective dye sorbent, but its relatively high price, high operating costs and problems with regeneration hamper its large-scale application. Therefore, there is a growing need in finding low cost, renewable, locally available materials as sorbent for the removal of dye colors<sup>33</sup>.

### 1.2.1. Liquid phase

70% of the Earth's surface is covered with water and only a small fraction (2.5%) is freshwater compatible with terrestrial life.

Sustainable water supply is an increasing demand in today's world. In addition to water amounts needed for agriculture, water quality is fundamental for human life and the whole earth ecology.

According to the European Environmental Agency Report, only around 40% of surface waters (rivers, lakes, and transitional and coastal waters) are in good ecological status or potential, and 38% are in good chemical status.

An intensive use of chemicals in everyday activities and unrestricted access to medicines has resulted in increased waste production and an intense emission of typical as well as new organic compounds into the surrounding environment<sup>34</sup>. The impact of these chemicals on

living organisms is generally unknown but the experiments have proved their negative influence on vitality, life span, and reproductive success<sup>35</sup>.

Water treatments are most often based on biological processes which are now conveniently installed in all the developed countries. The main remaining problem concerns non-biodegradable compounds most often coming from industrial or agricultural activities. Besides very harmful dissolved heavy metal, most of these pollutants are organics, and may be very dangerous for human health.

Adsorption on activated carbon for achieving high water purification is widely used, and is often preferred as a post treatment as its cost would be excessive for concentrated pollution<sup>36,37,38,39</sup>. The main drawback of activated carbon is its cost, its regeneration has to be improved to become sustainable.

Various methods of preparation of activated carbon based on carbonization and post activation are described in literature.

### 1.2.2. Gas phase

The energy demand from our industrial way of life result in a huge increase in carbon dioxide emissions. Due to this, the capture of pollutants from the atmosphere has become an important field of research.

The pollutants are classified in two classes, the first one are called primary pollutants<sup>40</sup> that resulting from changes in natural emissions from the biosphere and are introduced directly into the atmosphere where many of them will react chemically, especially under the influence of solar radiation, and give rise to new constituents or secondary pollutants<sup>41</sup>, which are often more aggressive to the environment than those where they came from. These secondary

pollutants include strong acids, such as sulphuric acid and nitric acid, as well as strong oxidants such as ozone (O<sub>3</sub>). Thus, the atmosphere is the site of intense chemical activity, between compounds that are mostly in trace amounts.

The pollutants interaction causes serious environmental problems, such as haze, photochemical smog, acid rain etc., which can cause serious risks to human health and environmental ecology<sup>42</sup>.

According to World Health Organization (WHO) economic cost of the health impact of air pollution in Europe is the first assessment of the economic burden of deaths and diseases resulting from outdoor and indoor air pollution in the 53 countries of the Region.

Currently there are many technologies for air pollution control and gaseous waste treatment such as:

- The gas washing technology<sup>2</sup> that consists of transferring the gaseous pollution into a washing solution, then the pollutant passes from the gas phase to liquid where it is retreated.
- The treatment by recovery of solvents<sup>43</sup>, a technology that allows the recovery of solvents by adsorption-desorption on activated carbon, in this case the recovered solvents can thus be reused.
- The thermal/catalytic oxidation technology<sup>44</sup> which is a treatment consisting in thermally treating Volatile Organic Compounds (VOCs) by catalytic or regenerative route.
- The biofiltration technology<sup>45</sup>, where the gaseous compounds are degraded by bacteria fixed on an organic or inorganic medium.

- The adsorption technology, where we have the capturing polluting gases on an adsorbent support (such as activated carbon)<sup>46</sup>.

Our study is based on this last technology, where the operating principle is based on the adsorption of the pollutant on the surface of adsorbent. Thus, the polluted gas passes through an adsorbent mass made up of activated carbon, zeolite, biomass... The pollutant developed physical and chemical interaction with the surface of the adsorbent and then the cleaned gas is rejected. When the adsorbent is saturated with pollutant, it was extracted to be unload before next processing.

## 2. The chemistries used in surface functionalization

There are many different ways to activate or modify material surfaces to improve their properties. To be efficient, a surface treatment has to increase the energy level of the surface to facilitate chemical or physical interaction. The type of the interactions with the environment is mainly dependent of the chemical groups available at the surface. In function of the material used, surfaces could be physically activated using temperature, plasma or ozone treatment or directly chemically modified.

### 2.1. Physical treatment

#### 2.1.1. Heat treatment

Heat treatments (annealing, quenching, precipitation hardening, laser or electron tempering) are processes where the material is alternatively heated and cooled in order to modify its microstructure and significantly change its properties. Heat treatments are mainly applied with metal and organic biomass. The most common reasons that metals undergo heat treatment are to improve their strength, hardness, toughness, ductility, and corrosion resistance. In

general, such treatments could be applied at the surface but also in the core of the material. Heat treatment could be also combined with addition of other atoms which are allowed to diffuse to the surface of the material to modify it (carbonyl, nitride treatments of ferric sample for instance).

Pyrolysis and carbonization of organic materials could be also identified as a heating treatment because of the elevated temperature (600-900°C), inert atmosphere (nitrogen, argon) used and the irreversibility. Pyrolysis are used to convert carbonaceous sample (bamboo, cocoa, wood) in char residues with small pore and high surface area. In some cases, chemicals (such as salt, strong acid or base) are added before, during or after the thermal treatment to bring out new chemical group at the surface of the char. In this case, temperatures of carbonization are used in the range of 400 to 900°C<sup>47</sup>. Biochars could be also post-treated with chemicals to obtain functionalized biochar.

### 2.1.2. Gas treatment

Plasma treatment or corona discharge are used to clean and prepare surfaces prior to any coating or bonding. They are obtained when gas is exposed to a high energy source (electricity or microwave) and became a mixture of ions, electrons, radicals and other types of molecular fragments. It should be noted that in low pressure plasma treatment, just a limited elevation of temperature is required. When these molecules hit the surface material, they altered the chemical organization and composition of the surface. In corona discharge, the power and the density of the plasma is low could result in a short reactivity of the surface. Various material such as polymers, glass and ceramics could be treated by plasma treatment.

## 2.2. Chemical treatment

### 2.2.1. Coating

During coating, the attached molecules are simply held by physical forces such as Van der Waals forces. In this case, the heat of adsorption is low, and the adsorption process is reversible. The molecular coating could be achieved by a simple immersion in the corresponding organic solution (molecule, polymer). The organic solution could be also sprayed brushed or obtained by chemical reduction of ions to the surface. The thickness of the coating could range from nm to hundreds of  $\mu\text{m}$ . Thus, steel alloy could be galvanized by zinc in acidic bath. For aluminum foils, samples have to be immersed in a solution of chromium to be oxidized and then protected from corrosion. In some cases, electrical potentials are applied at the surface in addition to the acidic treatment to remove inorganic pollutant and obtain a sample polishing. In this case, the contaminants are converted in ions and the surface is cleaned.

Acidic and basic solutions are often used to treat lignocellulosic material in order to improve their adsorption properties. Thus, sugarcane and agave bagasse, radish cake, eucalyptus seed, carrot waste, leaves of *Melia azedarach L*<sup>48</sup> and Aleppo pine have been pretreated with acidic solutions (tartaric, nitric, sulfuric, citric or hydrochloric acid) to remove organic moiety from the environment.

If we are looking for an enhancement of the surface roughness and exposure, it is recommended to pretreat the natural fiber with basic solution (such as sodium hydroxide for instance). To complete, this overview, it should be note that some works investigate the performance of their fiber impregnated with small molecules (such as urea, EDTA (ethylenediaminetetraacetic acid), benzene, ethanol, methanol, formaldehyde, acetone) or with polymers (Polyethylene imine (PEI), k-carrageenan, polyaniline, polysiloxane triton X-100...)<sup>49</sup>.

Glass surface could be also coated with polymers (Polyethylene oxide (PEO), polyvinyl alcohol (PVA), PEI, polyacrylamide, polyamine) to limit unwanted molecular adsorption on capillary wall or modulate its charge density<sup>50,51,52</sup>.

### 2.2.2. Covalent grafting

Different methods were developed to immobilize functional groups on the surface of inorganic or organic substrates. For modification of metal, diazonium chemistry are well described<sup>53,54,55,56</sup>. For gold substrates, functional thiols could be also applied for various applications in biodevices (surface plasmon resonance (SPR), biochip, electrochemical biosensor). For cellulosic sample and oxides (silicon, alumina, titania... oxides), the surface reactivity is based on reaction with the hydroxyl groups present at the surface. So, the main covalent strategy is the covalent grafting of silane derivatives by silylation or silanization. Nevertheless, it could be note that diazonium salts have been also successfully grafted on cellulosic (cocoa shell, olive pit) and polymeric<sup>57, 58, 57, 59, 17</sup> (Cyclic olefin copolymer, Teflon, polyethylenterephthalate, polymethylmethacrylate) surface.

### 2.3. Thiol

Sulfur adsorption is suitable for modification of different noble metal such as gold, silver, palladium. Thiol deposition has been used to link organic, and biological materials to planar gold (Au) surfaces or gold nanoparticles (AuNPs). Indeed, alkanethiol are widely used on Au surfaces as a building blocks for the fabrication of different type of devices. One of the advantages of thiol adsorption is their organization at the solid-liquid or solid-gas interface. The gold-sulfur interaction is so important that thiolated molecules are organized as a Self-assembled monolayers (SAMs). In fact, SAM formation is a two- steps-process: Firstly, thiols are chemically adsorbed on gold and the molecules are lying parallel to the substrate. Then, when the surface coverage is increased, molecules stand up perpendicularly to the surface to

form dense and stable thiol lattice. In function of the nature of thiol (aromatic, number of carbon), the angle between gold substrate and molecules adsorbed could be different<sup>60</sup>. It is generally considered that thiol sorption on gold followed a chemisorption process due to the strength of interaction which is measured at 40-50 kcal.mol<sup>-1</sup>. In 2014, Xue et al. tried to measure the strength of the gold thiol interaction by measuring its rupture force. They found that the force was comparable to Au-Au bond at 1.4 nN <sup>(61)</sup>. The suggested process of chemisorption could be considered as an oxidative addition of the S-H bond to gold, followed by reductive elimination of the hydrogen.



But this hypothesis of chemisorption has been recently challenged by Inkpen et al. who estimate that gold-thiol is not a molecular junction but physisorption<sup>62</sup>.

In all of cases, thiol sorption is the main method used to functionalize gold surfaces for SPR applications<sup>18</sup>. Unfortunately, thiol sorption on gold is sensitive to certain physicochemical parameters such as temperature, solvent, etc<sup>21</sup>. So, diazonium salts could be an alternative to thiol-mediated immobilization because they are resistant to these physicochemical parameters<sup>21</sup> and graftable the metal surfaces<sup>63,18,23</sup>.

## 2.4. Silane

Organosilane coupling agents were studied since few decades<sup>64,65</sup>. As they are studied since a long time, there are many functionalized coupling agent commercially available with different functional groups (amino, alkane, thiol, methacrylic, epoxy...)<sup>66</sup>. These molecules are based on a silicon atom which is able to create 4 linkages (general formula: R-Si-(OR')<sub>3</sub>). To be useful the coupling agent should have different terminal groups at these ends. In general, the coupling agent is connect through a hydrocarbon chain to a pendant terminal functional group "R"

suitable for post-functionalization<sup>67,68</sup>. At the other ends, the coupling agent should have some alkoxy groups or halogen group R'. In presence of water or humidity, these groups are hydrolysable to create silanol group which are crucial for chemical grafting on the material surface. In presence of others hydroxyl groups from (organic or inorganic surface), a condensation step will be developed, and a linkage O-Si-O will be created. So, silanization is a two-step process where the leaving group depends on the initial composition of the linker (Cl, CH<sub>2</sub>-CH<sub>3</sub>, CH<sub>3</sub>). The performance of the silanization depends on experimental conditions (gas or liquid phase, concentration, pH, organic or aqueous phase, purity, temperature) and on the nature of the coupling agent (mono, di or trialkoxysilane). There is also some alkoxy silane with four alkoxy group but they are rarely used because not they are not suitable for orthogonal post-functionalization. (Figure 4) presents a surface silanization using a trialkoxysilane.

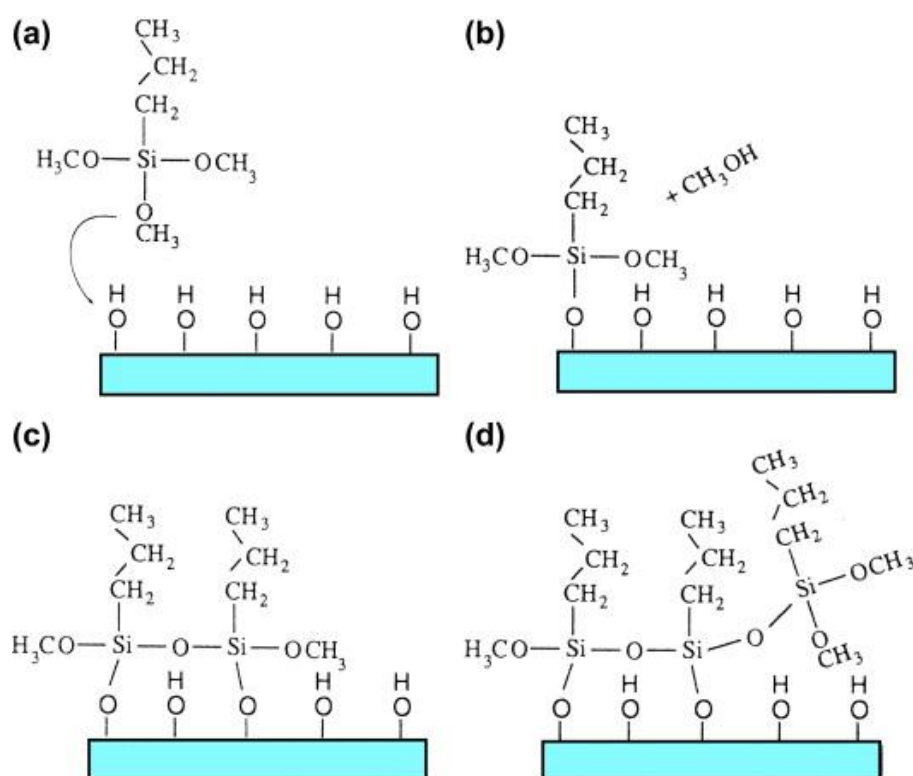


Figure 4: Modification of an hydroxyl surface by silanization: (a) a hydroxylated surface is immersed in a solution containing *n*-propyl trimethoxysilane (*n*PTMS); (b) one of the methoxy groups of the *n*PTMS couples with a hydroxyl group releasing methanol; (c) two of the methoxy groups on another molecule of the *n*PTMS have reacted, one with a hydroxyl group and the other with a methoxy group from the first *n*PTMS molecule; (d) a third *n*PTMS molecule has reacted only with a methoxy group. This molecule is tied into the silane film network, but is not directly bound to the surface<sup>69</sup>.

When the intermediate structure (Figure 4b) is fully condensate, the reaction stops. The reaction needs some pendant alkoxy or chlore group to continue and create some interaction with closed silane. In the best conditions, researchers are able to create a single silane monolayer at the surface of the material<sup>70</sup>. However, if the amount of water, the concentration of silane, the reaction time or the solvent are not well adapted a thicker silane layer can be formed consisting of both Si–O groups bonded to the surface, and silane units participating in a “bulk” 3D polymerized network.

It is interesting to note that the reactivity of amino-terminated silane is weakly affected by the experimental conditions and fully water-miscible. In this case, the amine group induced a self-catalysis leading to a good condensation of the molecule on the substrate used<sup>71</sup>.

One of the limitations of surface modified by silanization, is its weakness against hydrolysis which could reverse the condensation and free the coupling agent. It is important for coupling silane agents which are not miscible in water.

Even if, Gandini et al. showed that silane coupling agents that include an amino group at the R group display a good affinity toward cellulosic substrate<sup>72,73</sup>, the interaction between silane and hydroxyl group from cellulose is less evident and less described in literature than with silica. As cellulosic fibers are unreactive to many chemicals, the OH groups of the fiber have very low accessibility and weaker acidity<sup>74</sup>, the reactivity between cellulose and silane is limited even at high temperature. In general, researchers focused their works to ascertain the impact of these modifications on the mechanical properties of the ensuing composites. The group of Herrera is one of the first research group focusing his work to study the chemical reaction between cellulose derivates and silane<sup>75</sup>.

The strategy consists in activation of the alkoxy silane by hydrolyzing the alkoxy groups of the surface to form more reactive silanol groups. Thus, the following mechanism is generally

accepted to describe the chemical reaction. Some pre-hydrolyzed silanes (from diluted solution of silane coupling agent) adsorbed on cellulose surfaces. At this stage, silane simply covered the cellulose surfaces and it is only maintained by physical interactions. Hydrogen interactions between hydroxyl groups of silanes and those of cellulose should be the main interaction. So, if a cleaning step with ethanol is applied, all the silanes are removed from the surface. If the first step is followed by heat treatment (120°C, inert atmosphere), the condensation occurred between OH group from surface and from hydrolyzed silane giving Si–O–C and Si–O–Si couplings, respectively. These reactions ensured efficient and irreversible chemical bonding of the silane onto the cellulose surface.

## 2.5. Diazonium salts

Although the tendency to modify surfaces using thiol compound, the low long term stability due to the easy oxidation of thiol, the small electrochemical window (range -1 V to +1 V vs SCE) in the case of electrochemical reduction, and the lower bonding energy of S-Au with respect to the C-C bond has led to the use of diazonium as an alternative for the development of a stable surface based on covalent bonding<sup>8</sup>. This system offers the advantage of facile preparation, rapid reduction and the possibility of the introduction of different functional groups<sup>8</sup>.

In order to study all the advantages of this chemical compound, this present work is focused in the gold surface functionalization from diazonium salts.

### 2.5.1. History

A diazonium salt is an aliphatic, aromatic or heterocyclic compound, in which a  $-N_2^+$  group is covalently linked to a carbon atom ( $R-N^+\equiv N$ )<sup>76</sup>.

As showed in the (Figure 4), the aromatic diazonium compound  $ArN_2^+ X^-$  was developed by a

German industrial chemist and an early pioneer of organic chemistry called Johann Peter Griess at year of 1858 during the elaboration of a test for the detection of nitrite ions, by assaying with an amine which led to the formation of a colored compound<sup>11</sup>.

The conjugation of  $\pi$  electrons with the aromatic ring makes aryldiazonium ions much more stable than their aliphatic counterparts rarely used in classical organic chemistry. The diazonium group ( $N_2^+$ ) is known as the most electron-withdrawing substitute<sup>11</sup>.

The diazonium ions are most often formed by nitrosation of primary amines in an acidic medium<sup>76</sup>, however only the aromatic diazonium salts are stable in the medium term (several hours)<sup>76</sup>.

After its discovery the diazonium salts have been widely used for the preparation of azo dyes<sup>12</sup>, an important commercially compound on the textile, leather and foods industry.

It was mainly due to this discovery that Griess is considered an important figure in the formation of the modern dye industry.

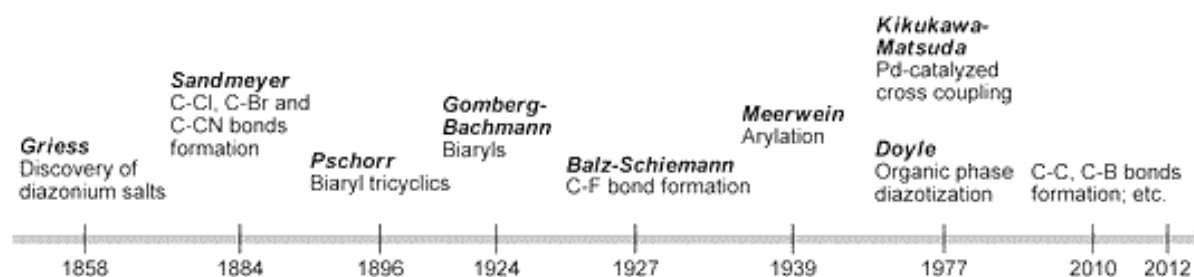


Figure 5: Brief history of the use of diazonium<sup>77</sup>.

Subsequently to the discovering of diazonium salts, these highly reactive chemical functions were used for the development of new synthesis of aromatic organic molecules (Figure 5)<sup>15</sup>.

The  $N_2^+$  is an excellent leaving group, it could be involved during various nucleophilic substitution reactions, as showed at the (Figure 5), such as the Sandmeyer reaction<sup>15</sup>

(halogenation, 1884), the Gomberg-Bachmann reaction<sup>10</sup> (benzyl coupling, 1924), the Schiemann reaction<sup>78</sup> (fluoridation, 1927), the Meerwein reaction<sup>79</sup> (arylation, 1939), among others.

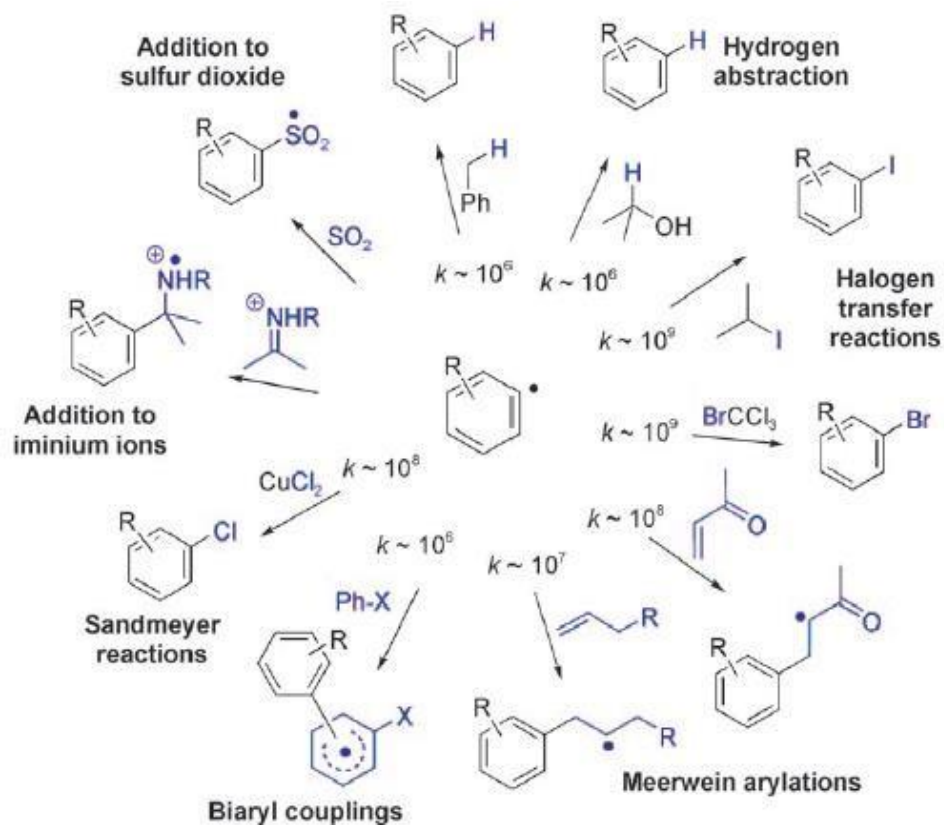


Figure 6: Scheme of the uses of aryl diazonium in organic synthesis ( $R$  = Substitute group,  $\bullet$  = Radical<sup>80</sup>).

## 2.5.2. Synthesis

Usually, two synthetic routes are used for the synthesis of aryl diazonium. The first route uses a counter-anion which stabilize diazonium and allow its isolation as a salt; the second route consist in the synthesis and the *in-situ* use of the diazonium function.

Different anions could be used to stabilize and isolate aryl diazonium salts:

1) The use of tetrafluoroboric acid in the presence of sodium nitrite allows to synthesize nitrous acid *in situ* and to carry out the diazotization reaction in an aqueous solution (Figure 7). This reaction is generally carried out between -5 and 0°C<sup>81,82,83,84</sup>. Then, the salts are stored at -20°C. The HBF<sub>4</sub> is known as a stabilizer to diazonium salts and as a catalyst for alkylations and polymerizations.



Figure 7: Synthesis of aryl diazonium tetrafluoroborate with HBF<sub>4</sub>.

2) The second method is to use directly the nitrosonium ion, provided by NOBF<sub>4</sub> in organic medium to obtain the desired product (Figure 8). This reaction, making it possible to overcome the presence of reaction by-products, but it required greater precaution because it is carried out at -40°C<sup>85,86</sup>.

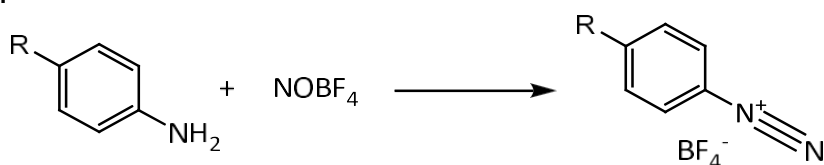


Figure 8: Synthesis of aryl diazonium tetrafluoroborate with NOBF<sub>4</sub>.

3) Another possible way to obtain stable salts is using the tosyl anion (*p*-TsO<sup>-</sup>) by using a dry mixture (*p*-TsOH/NaNO<sub>2</sub>) on aniline, mixing manually in a mortar<sup>87</sup>. According to these studies, these diazonium salts remain stable after one month at room temperature in a desiccator.

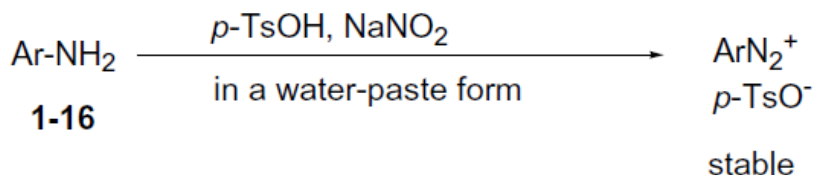


Figure 9: Synthesis of aryl diazonium tosylate salts (color).

These different synthesis routes allow to obtain the salts, which can be isolated, preserved and characterized.

But in the case where the diazonium function only serves as an intermediate for obtaining an aryl radical, it is then possible to dispense with a stabilizing counter-anion such as a chloride ion (introduced by the use of hydrochloric acid). This kind of synthesis is generally carried out in an aqueous solvent by reacting an acid (often HCl) with sodium nitrite. The presence of chloride ion, as counter-anion, is not sufficient to stabilize the diazonium cation, it will react quickly<sup>88,57</sup>. In an organic solvent, the use of *tert*-butyl nitrite will be preferred to sodium nitrite for better solubility for synthesis and *in-situ* use at room temperature<sup>89</sup>. This route can be considered when the aryldiazonium is poorly soluble in aqueous solvents.

The position and the nature of the functional groups on the benzene ring carrying the diazonium function influences both the synthesis of the aryldiazonium salts but also the formation of the products due to the electronic delocalization of the  $N_2^+$  function. The mesomeric and inductive effects affect the salt stability.

As showed in the Figure 10, the aryldiazonium salts can be also used for the grafting of aromatic layers on surfaces. Steric hindrance must therefore be taken into account when the aromatic ring is congested during a reaction between the molecule and a surface (S) that completely prevents grafting<sup>90</sup>.

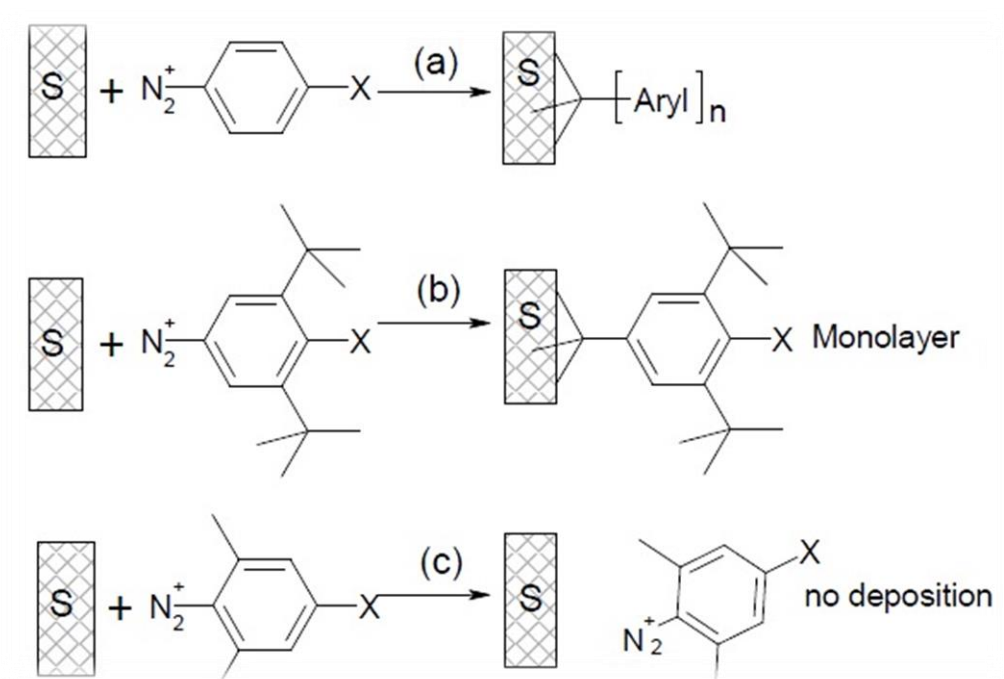


Figure 10: Influence of aromatic ring substitution on organic layer grafting on a surface<sup>91</sup>.

## 2.5.3. Surface modification with diazonium salts

### 2.5.3.1. Spontaneous grafting

There is the possibility of working without electric current, by spontaneous electroreduction, particularly with metallic surfaces. In this case, the atoms of the metallic surface gave the electrons required for the reduction of the diazonium salts and its grafting to the surface<sup>85,92,93,94, 94,95,96,97,98</sup>.

For non-conductive materials (as will be presented in the form of a scientific article in chapter III), electrons could not come from the surface, so some chemical reducing agent have to be added in the solution.

## 2.5.4. Chemical reduction

For aryl diazonium salts bearing a redox potential close to 600mV, the chemical reducers must have a lower standard potential (Figure 11)<sup>99</sup>. Among the different possible chemical reducers,

we use hypophosphorous acid ( $\text{H}_3\text{PO}_2$ ) which has a standard potential ( $E^\circ$ ) of  $-0.499 \text{ V/SHE}$ <sup>99</sup> providing two electrons during the reduction. It has been already described in literature to reduce aryldiazoniums<sup>100,101</sup>

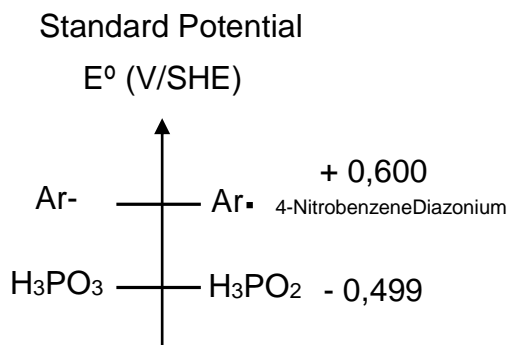


Figure 11: Standard potential of the species used.

### 2.5.5. Electrochemical reduction or oxidation

After a long period destined to be used almost exclusively as a dye, the electrochemistry of diazonium salts was described by Elofson, using mercury electrodes<sup>12</sup>. So, after 1992 the azo compounds began to be used to modify surfaces<sup>102</sup>.

The electrochemistry, by the supply of electrons in the medium, allows us to obtain radicals which are going to be formed by loss of a molecule of dinitrogen, and will thus react with the conducting surface which is used as a working electrode (Figure 12).

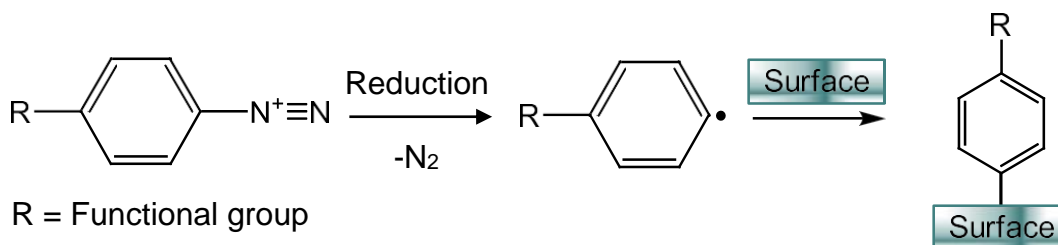


Figure 12: Electrodeposition of aryl nuclei on a surface.

The electrochemical reductions of aryldiazonium have been implemented with different conductive or semiconductor materials such as:

- Metals: Electroreduction on gold is often used<sup>103,84,86,88,57,104,105,106,107,108</sup> but we can also use it as a point of attachment to gold nanoparticles<sup>109</sup>. Other metals are also used such as iron<sup>110,111,112,113,114,115</sup>, steel<sup>116,108,117,118,119,120</sup>, silver<sup>120</sup>, palladium<sup>92</sup>, platinum<sup>121</sup>, titanium<sup>122</sup> or copper<sup>123,124</sup>.
- Carbon: We have at our disposal many forms of carbon such as vitreous carbon (GC)<sup>84,125,108,126,127,109,128,103,129</sup>, graphite<sup>130</sup>, in “printed” form<sup>131</sup> or in highly oriented pyrolytic form (HOPG)<sup>128</sup>. We also have in the form of nanotubes, directly or via the use of bulky paper (a kind of thin sheet composed of an assembly of nanotubes)<sup>132</sup> or even on microelectrodes printed in graphite<sup>133</sup>.
- Silicon, widely used in electronics, requires surface preparation, allowing the transformation of the passivation layer (Si-O-Si and Si-OH bonds) present on the surface into reactive Si-H functions<sup>92,134,93,135,94,95,96,97,98,99,136</sup>, (Figure 13).

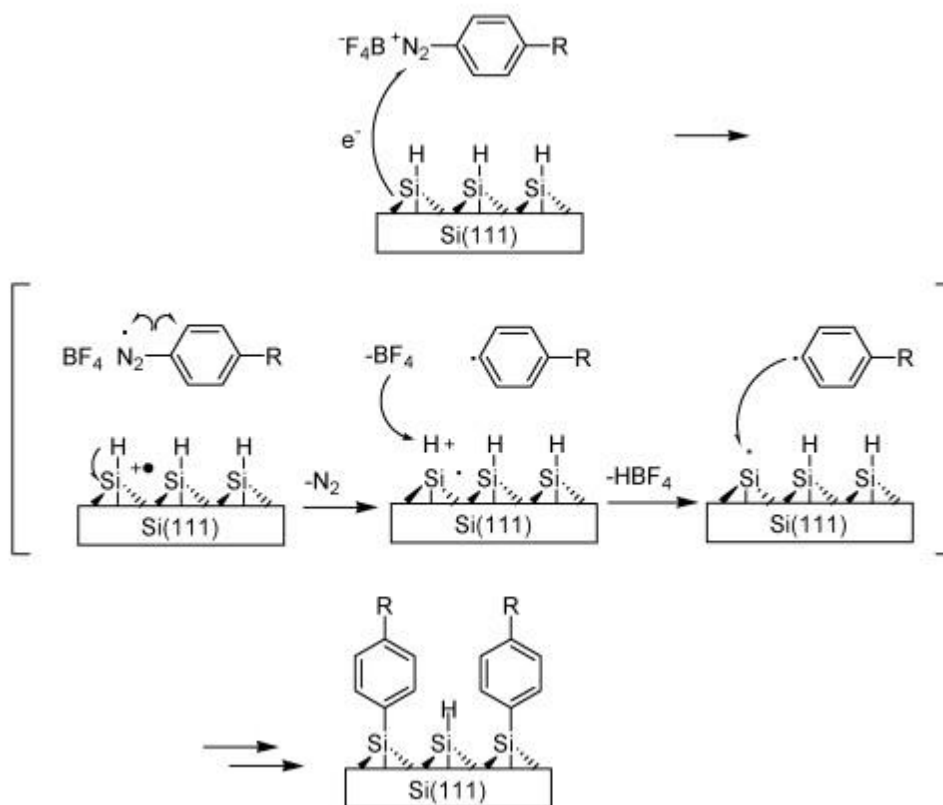


Figure 13: Reaction between an aryl radical and a silicon surface<sup>136</sup>.

- And other semiconductor materials, such as indium tin oxide (ITO)<sup>108,137</sup>, germanium<sup>138,139,93</sup>, titanium and its oxide (TiO<sub>2</sub>)<sup>135</sup>, or SiGe<sup>93</sup> and GaAs<sup>92</sup> alloys.

The electrochemical functionalization can be done by oxidation on vitreous carbon, platinum or gold<sup>140,141,142,143</sup>. However, the latter process is limited by the incompatibility of the surfaces with electro-oxidation. It is for this reason that the electroreduction pathway is more developed with vinyl compounds<sup>143</sup> and mainly with aryldiazonium salts<sup>144</sup>.

The main limitation of the electrochemical approach is the requirement of a conductive surface.

In this work, I will modify:

- Gold surface with diazonium salt to develop SPR biosensor (chapter 2);
- And organic surface with silane moieties and diazonium salts to develop CO<sub>2</sub> and organic sorbents (chapter 3).



# CHAPTER II

FUNCTIONALIZATION OF SURFACE APPLIED TO BIOCHEMISTRY

**Methodology and results**

## 1. Introduction

The chapter II is mainly dedicated to surface functionalization of gold surface for application in the Surface Plasmon Resonance (SPR) technique. Our strategy about this chapter was to modify gold surface with diazonium salts and then use it for SPR applications.

After a short presentation of the SPR technology and the different surface modifications involved for this application, I will present the 2 strategies of modification I applied: The electroreduction and the chemical reduction of the aryldiazonium salt. I will present the influence of different parameters (number of cycles in electrochemistry, diazonium concentration...) on the plasmon sensitivity. Then, I will demonstrate the proof of concept using a well-known antibodies/antigen couple. Finally, I will validate our strategy with an original application based on CNP-AmiC interaction. To conclude, I will present an innovative approach to develop a new biosensor suitable for the next generation of SPR instrument.

## 2. Presentation of the Surface Plasmon Resonance technique

Surface plasmon resonance (SPR) is a well-established technique for studying affinity between biomolecules at the liquid/solid interface<sup>145</sup>. The sensitivity of this real time technique is due to the gold sensing surface used. Thus, SPR succeeded in measuring the affinity constant between protein-DNA, protein-protein or small molecule-protein<sup>146,147</sup>.

The SPR physical process occur when a plane-polarized light hits a metal film under total internal reflection conditions<sup>4</sup>. In the process, a glass interface located between two very different refractive index media and a gold surface is illuminate with a polarized monochromatic light. Then, these conditions make it possible to obtain a phenomenon of total internal reflection due to the illumination of the surface with an angle of incidence greater than the limit angle (from which all the light is reflected). Thus, no refraction was obtained but an evanescent wave (electromagnetic component of the light) propagates perpendicularly to the interface over a distance equal to its wavelength. The presence of a metal surface will make it possible to obtain a resonance between the plasmons of gold and the evanescent wave by loss of light energy at the level of the beam reflected at a particular angle called the resonance angle (Figure 14).

For being use on the SPR technique, the metal must have construction band electrons capable of resonating with the incoming light at a suitable wavelength<sup>4</sup>. Metals that satisfy to this condition are silver, gold, copper, aluminum, sodium and indium. In addition, the metal on the sensor surface must be free of oxides, sulphides and not react to other molecules on exposure to the atmosphere or liquid. Of the metals, indium is too expensive, sodium too reactive, cooper and aluminum too broad in their SPR response and silver too sensitive to oxidation. This leaves the gold as the most practical metal.

This angle is sensitive to the refractive index of the medium in which the evanescent wave propagates. So, any modification on the gold surface will influence the propagation of the

evanescent wave. The use of the SPR technique for biosensor purposes has been proposed by Liedberg et al. in 1983<sup>4,148</sup>. The changes in mass on the surface of the sensor which take place during the association or dissociation of the biomolecular complex in the detection zone induce a modification of the angle of resonance of the incident light, see Figure 14.

Thus, to evaluate the interactions between two molecules, we have to immobilize a ligand into a microfluidic or planar surface and inject the analyte in a liquid phase. These systems make it possible to follow the mass changes on the gold surface, induced by the formation then the dissociation of molecular complexes, that allows to go back to the association and dissociation constant between ligand and analyte.

The SPR sensors can be coupled with image capture tools that allow observing in real time the changes induced by the differences on the surface, which we call SPRi (i for image generation)<sup>149</sup>. So, the advantages of the SPRi system is that analytical technique does not require a labeling of the targets, it is very sensitive (detection of the interaction from approximately 1 pg of protein), and the acquisition is done in real time.

The experimental analyzes were made on a SPRi-Plex II device from the manufacturer Horiba-Genoptics. We work with a bare crystal prism on which is placed a movable planar substrate including the functionalized metallic layer (in our case, a gold layer). The contact between the prism and the gold surface is ensured by a special optical oil with a refractive index equal to that of the prism. Once the sample holder is inserted into the instrument, the system is locked by the contact of a seal holding the system at its periphery, allowing the passage of the buffer solution (containing or not the analytes studied) without any leakage. The running buffer (Phosphate buffered saline (PBS buffer), 10 mmol L<sup>-1</sup>, pH 7.4) will go through the microfluidic circuit under a constant flow of 50  $\mu$ L / min to the gold surface and then be discarded. The reflectivity measurement is carried out at a fixed angle after defining the optimal working

angle<sup>150</sup>.

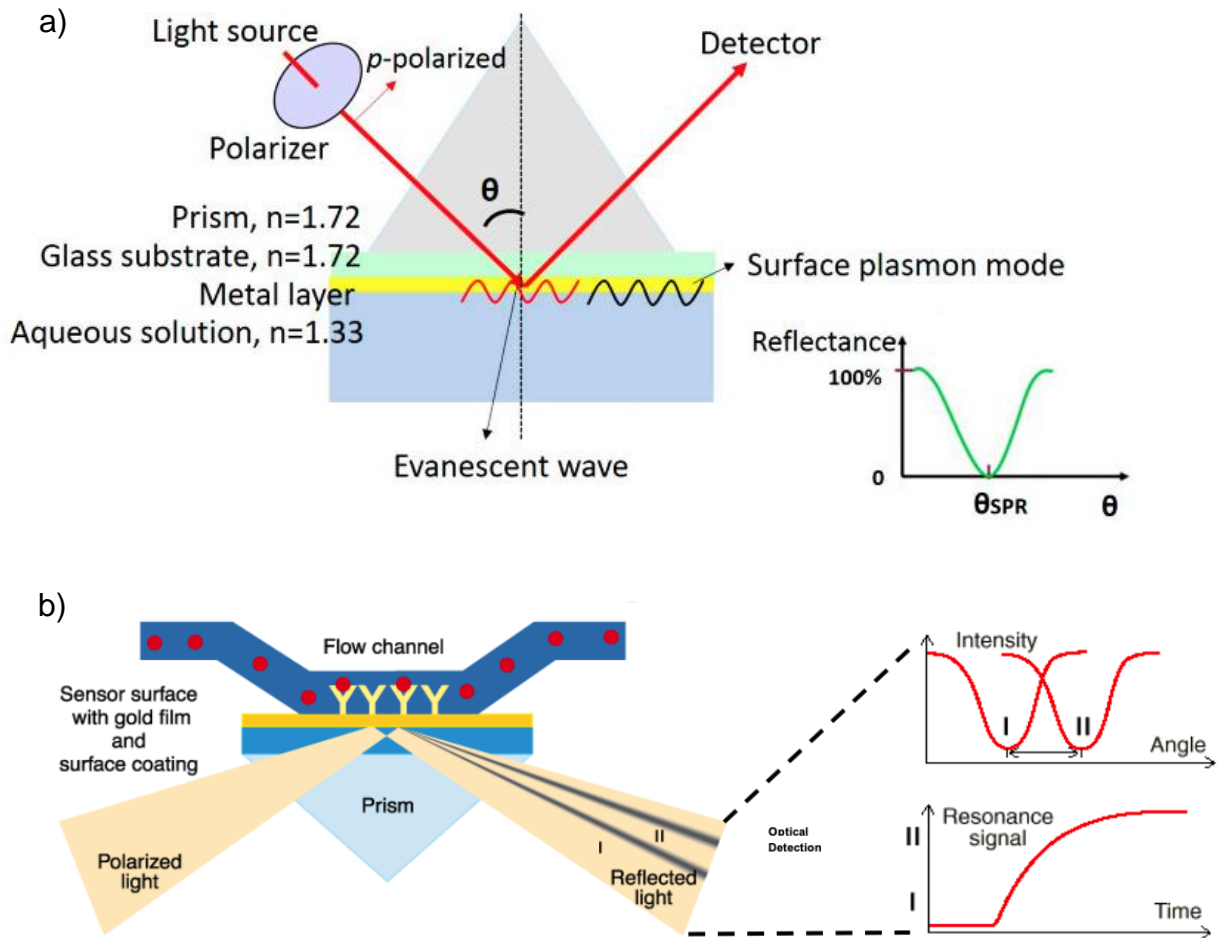


Figure 14: Principle of SPR measurement<sup>151</sup>. a) with HORIBA system; b) with BIACORE system<sup>152</sup>.

A Surface Plasma Resonance system basically works as follows (Figure 14), the excitation ray passes through a high density medium (a glass prism) which will modify the speed and the vector of the incident light wave ( $k_{in}$ ) as we can see in the Equation 1.

$$k_{in} = \frac{2\pi}{\lambda} \sin \theta \sqrt{\epsilon_p}$$

Equation 1: Equation of the incident light wave.

$\lambda$  is the wavelength of the excitation light,  $\theta$  is the angle of incidence and  $\epsilon_p$  is the dielectric constant of the prism<sup>153,154</sup>. We can describe the wave vector ( $k_{sp}$ ) of the surface plasmon propagating at the interface metal-prism by the following equation:

$$k_{sp} = \frac{\omega_{sp}}{c} \sqrt{\frac{\epsilon_m \epsilon_p}{\epsilon_m + \epsilon_p}}$$

Equation 2: Equation of the wave vector.

In the Equation 2 we have the angular frequency of the surface plasmon ( $\omega_{sp}$ ), the dielectric constant of the metal film ( $\epsilon_m$ ) and the speed of light  $c$ . So, that the plasmonic wave propagates at the metal and the insulator interface,  $k_{in}$  must correspond to  $k_{sp}$ . So that part of the photon energy is transferred to the surface. When a ligand is immobilized on gold surface, the dielectric constant of the metal film is modified. So, this constant is sensitive to the thickness of the molecular deposition and consequently to the interaction between ligand and analyte. During the experiment, we recorded the reflective intensity. Thus, we are able to monitor different event such as association/dissociation of the molecular complex (Figure 15).

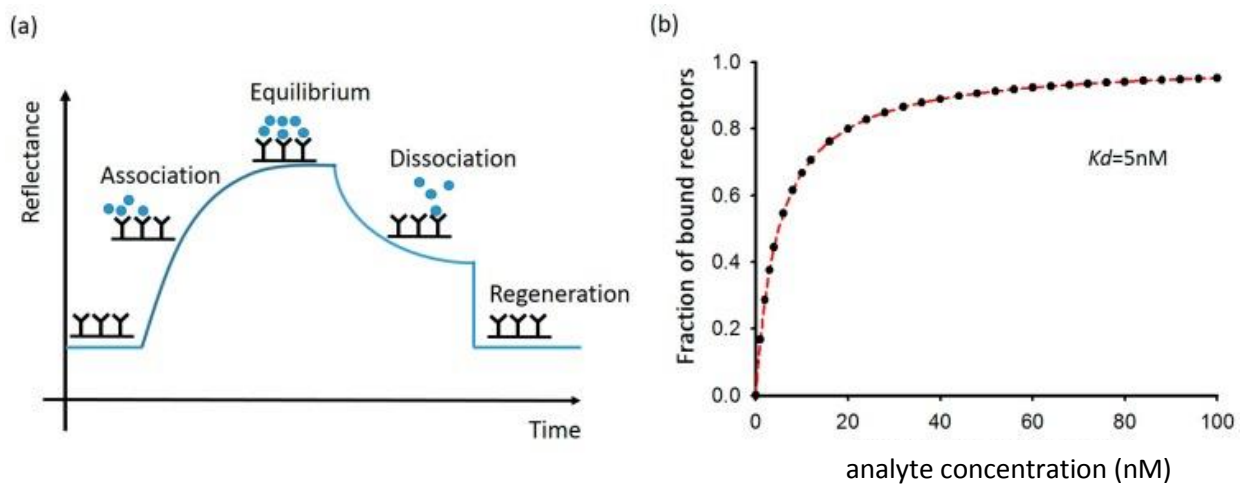


Figure 15: a) Kinetic of association and dissociation of the analyte/ligand complex. b) Variation of the SPR signal in function of the concentration of injected analyte<sup>152</sup>.

As SPR is a real time method, it is possible to monitor the kinetic of association and dissociation according to the modification of the dielectric constant of the surface (reflectance of the signal). Thus, the equilibrium constant  $K$  could be determined by the Equation 3. The concentration of the ligand-analyte complex (LA) is determined from the SPR signal, the concentration of the analyte (A) is defined by the user, and the concentration of total ligand grafted to the surface

(L) is obtained from the maximum SPR signal. This value is determined from Figure 15b when the curve fraction of bound receptor in function of analyte concentration reached saturation.

$$\frac{k_d}{k_a} = \frac{[L][A]}{[LA]} = K_D$$

*Equation 3: Steady state equation.*

The development of nanomaterials led to the appearance of the so-called localized SPR<sup>149,155</sup>. The plasmonic properties of nanoparticles of metals such as gold or silver make the optical signals obtained stronger and more controllable<sup>156</sup>. For example, a metallic film that comprises nano-orifices does not require an ATR to activate the SPR, a conventional light source and a microscope are sufficient to analyze this surface<sup>157</sup>. All of the latest advances in SPR biosensors have been reviewed recently by Singh et al<sup>158</sup>.

## 2.1. Modification of the SPR surface

Different strategies were investigated in the literature to immobilize biomolecules on gold surface such as physical adsorption, embedding in polymer, sol-gel entrapment, self-assembly method and layer by layer deposition<sup>159</sup>. Indeed, Biacore sell a commercial SPR biochip modified with carboxymethylated dextran hydrogel. Physical adsorption mediated by BSA and self-assembly methods are the most used in SPR. The alkanethiol chemistry was extensively studied because the sulfur-gold bond involved in the coating process formed spontaneously a densyl self-assembled monolayer (SAM) on the gold surface<sup>160</sup>. Even if, SAM helps to limit the non-specific adsorption of the analyte to the surface, unwanted adsorption is still a problem. To limit this interaction and enhance the S/N, the used of mixed SAM (with free and capped group), polymer coating and post-functionalization using protein or amino acid coating have been tested<sup>161</sup>.

Horiba sell some SPRi biochip pre-functionalized with SAM and dextran. Different free groups (thiol, amine, acid, alcohol) are available for covalent immobilization of the ligand. In comparison with other techniques, Thus, some carboxy-PEG based SAM were developed and present an oriented immobilization of the ligand and a limited nonspecific adsorption<sup>162</sup>. Despite its advantage, thiolated surfaces were still sensitive to experimental conditions because the gold-sulfur interaction is labile, yielding the coating unstable under specific condition. Thus, in 2002, Raitman et al. suggested to adsorb the electrografted-polyaniline polymer on gold surface and applied it in SPR experiment<sup>163</sup>.

### 2.1.1. My strategy

Commercial SPR biochips are really expensive and the chemistry available to immobilize molecule on gold surface were limited. The main objective of this work was to develop a new SPR biochip bearing a diazonium chemistry which is simple to produce and more stable than conventional commercial chip. As a proof of concept, different devices will be developed with carboxybenzene diazonium moieties in this thesis: Electrografted, chemically grafted, and strip electrografted biochip and these chips will be compared to thiolated biochip. The best device will be tested in collaboration with the Laboratory of Microbiology - Signals and Microenvironment (LMSM), EA 4312 in Evreux with a test complex Ovalbumine/anti-ovalbumine and an original complex AmiC/CNP.

## 2.2. The choice of the diazonium salt

On gold surface, the diazonium coating is promising as an alternative to the thiol coating because the carbon-gold interaction is more stable, and the electro-reduction is a fast process<sup>164,165,166,23</sup>. Although the diazonium salts being widely used to functionalize gold surface for electrode application, they are still few studies in SPR.

Aryldiazonium salts (Scheme 14) could be converted in an aryl radical by sonication, photoinduction, chemical or electrochemical reduction. Then, this radical react with the narrow surface incubated in the solution. In the literature, various surfaces have been modified by aryldiazonium salts<sup>57,167</sup>.

In this work, I would like to immobilize proteins, so I decide to functionalize the surface with a diazonium salt bearing a carboxylic acid. Then, the carboxylic acid will interact with NH<sub>2</sub> from protein to create an amide function. The stability of the carboxybenzenediazonium salts is limited so there are not commercially available. For this reason, I choose to synthetize my own diazonium salt from the reduction of the carboxyaniline (scheme 1).



*Scheme 1: The 4-Carboxybenzene diazonium synthesis*

I obtained the diazonium salt with a yield of 80%. It was characterized by IRTF, <sup>1</sup>H-NMR and then stored in the freezer until use.

### 2.3. The substrates selected to develop the SPR biochip

Gold is very resistant to oxidation and other atmospheric contaminants but is compatible with many chemical modification systems. The thickness of the gold should be ± 50 nm. The thickness of the metal layers is of great importance. Above an optimum, the dip in reflective light becomes shallow, bellow the optimum the dip becomes broader<sup>4</sup>.

The gold surfaces are purchased from Schott (Switzerland), Arrandee (Germany) and Horiba (France). These surfaces consist of a glass slide covered with an adhesion layer of chrome which then allows to deposit a layer of gold (Figure 16).

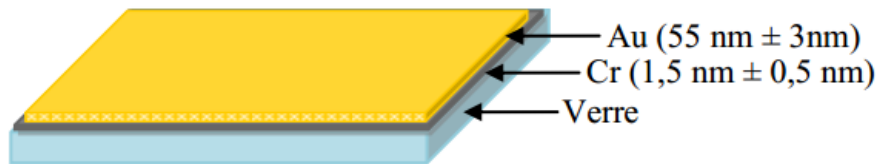


Figure 16: Composition of the gold support available.

## 2.4. The optical performance requested for a SPR biochip

Previously, we indicated that the plasmon which are confined to the plane of the gold film were parallel to the surface and sensitive to the liquid/solid interface<sup>4</sup>(Figure 17). To be efficient, an SPR biochip should have a prism/liquid interface limited to 300 nm<sup>4</sup> to be sensitive. So, the surface we developed should be relatively thin (around ~ 2 nm) to measure molecular binding. The reflectivity should be as high as possible (at around 25%), the plasmon angle should be as homogenous as possible and close to the optimal value at 60°. So, the developed biochip should respect these conditions.

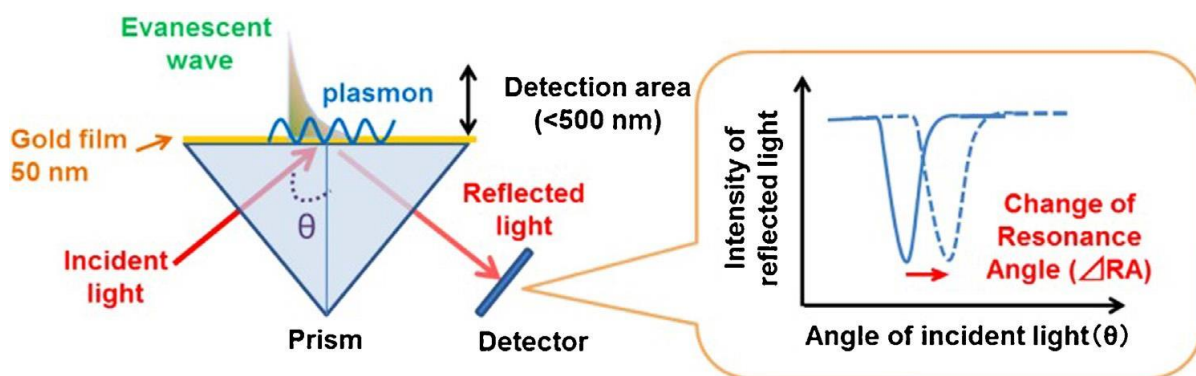


Figure 17: Diagram presenting the use of a surface plasmon<sup>168</sup>.

## 3. The SPR biochip developed

The grafting of diazonium salts on surfaces is fast and can be carried out by two techniques: chemical reduction<sup>169,19</sup> and electrochemical reduction<sup>63</sup>. Both of them will be presented in the next topics.

### 3.1. Surface functionalization by chemical reduction

During his PhD thesis Dr. F. Brisset<sup>17</sup> worked on polymeric and gold surfaces. He focused his work on the chemical reduction of diazonium salt to modify these surfaces. He demonstrated that a chemical reducer in acidic solution is enough to graft diazonium on gold while a UV irradiation has to be added for polymeric surfaces. I applied his conditions to evaluate if these conditions are suitable for the SPR analysis. The chemical reduction was realized as described in the experimental part. We tested 3 different initial concentrations of carboxybenzene diazonium (20, 50, 100 mmol L<sup>-1</sup>) and we fixed the other parameters (9 mL of HCl 0.5 mol L<sup>-1</sup>, 1 mL of hypophosphorous acid (50% H<sub>3</sub>PO<sub>2</sub> w/v) and 1 hour of reaction. During the experimental, the chemical reduction could be observed with the formation of gas (N<sub>2</sub>) (Figure 18) and a color change of the solution.

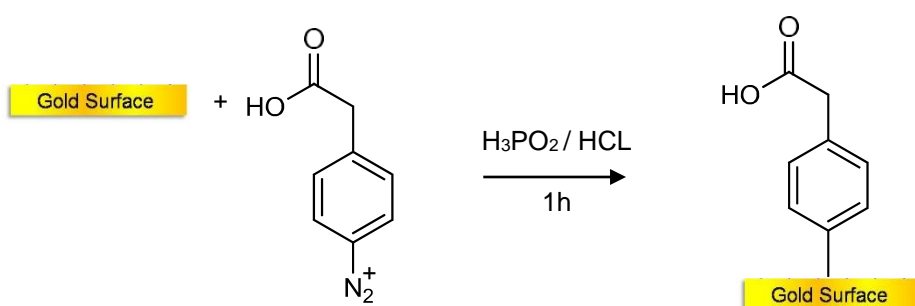


Figure 18: Chemical grafting of carboxybenzene diazonium on gold surface.

The conductivity is one of the characteristics of a metallic surface. Thus, we used cyclic voltammetry with a ferrocene redox system to compare the electrical performance of modified CBD biochip and unmodified gold biochip.

As we can see in Figure 19, the current intensity decreased when the concentration of CBD increased indicating that the surface was passivated by the organic layer. The passivation was maximum for 100 mmol L<sup>-1</sup> of CBD.

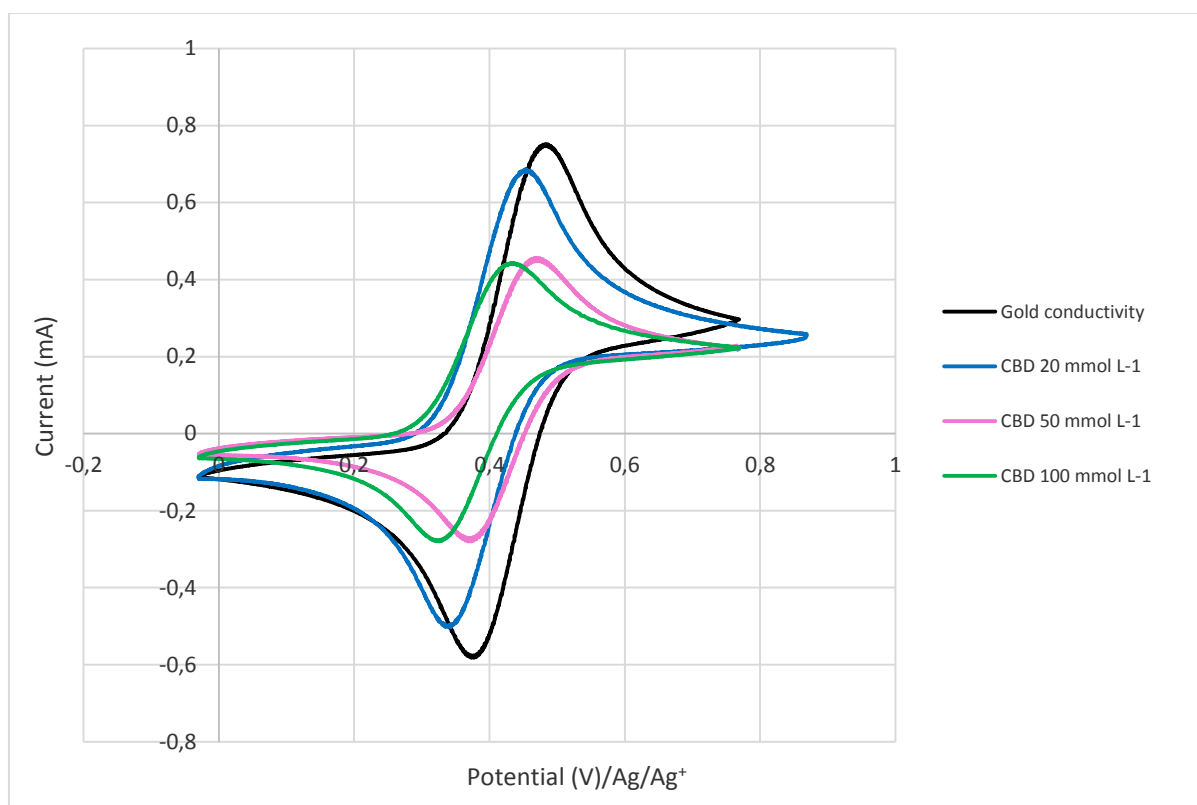


Figure 19: Cyclic voltammograms of ferrocene from the unmodified (black curve) and the CBD gold surface (blue curve = 20 mmol L<sup>-1</sup>; pink curve = 50 mmol L<sup>-1</sup>; green curve = 100 mmol L<sup>-1</sup>). Electrolyte: NBu<sub>4</sub>PF<sub>6</sub> 0.1 mol L<sup>-1</sup> in CH<sub>3</sub>CN; scan rate of 0.1 V/s from -0.3 to 0.5 V. Gold surface as work electrode, Platinum as counter electrode and Ag/AgCl as reference electrode.

So, the chemical reduction and its grafting of the diazonium on the gold surface is efficient. To become a SPR biochip, the CBD biochip should present a good plasmon signal (high reflectivity, and plasmon angle close to the unmodified surface). The plasmon curves obtained for the different biochips prepared with 100, 50, 20 mmol L<sup>-1</sup> of CBD are presented in Figures 20, 21, 22 respectively. The Figures 20a, 21a, 22a illustrate the surface of the biochip and we saw that the grafting doesn't seem to be homogenous with different traces and holes visible. For the plasmon analysis, we tried to select different area with similar appearance. The tested area is highlighted in Figure 20a, 21a, 22a. Despite this precaution, we observed in Figure 20b, 21b, 22b that the reflectivity and the plasmon angle are strongly modified. However, it could be noted on Figure 20b, that the distribution of the plasmon angle was lower with biochip prepared from 100 mmol L<sup>-1</sup> of CBD than the biochips prepared from 20 or 50 mmol L<sup>-1</sup> of CBD. It was probably because a high initial concentration of diazonium could be associated to a large

amount of aryl radical created and a fast adsorption and grafting. So, 100 mmol L<sup>-1</sup> of CBD should be preferred for to obtain SPR biochip. Then, to obtain sensitive SPR biochip, the intensity of the reflectivity is also important and has to be monitored. The 100 mmol L<sup>-1</sup> CBD-biochip had a reflectivity at around 43% which is much weaker than the wanted value at around 25%. For this parameter, biochip prepared from 20 or 50 mmol L<sup>-1</sup> of CBD will be better. Consequently, if we combined both of these parameters, the preparation of biochip by chemical reduction didn't seems to be adapted to develop efficient SPR biochip (at least in the tested conditions). The distribution of the values of the plasmon angle confirmed that the coatings were not homogenous all over the surface.

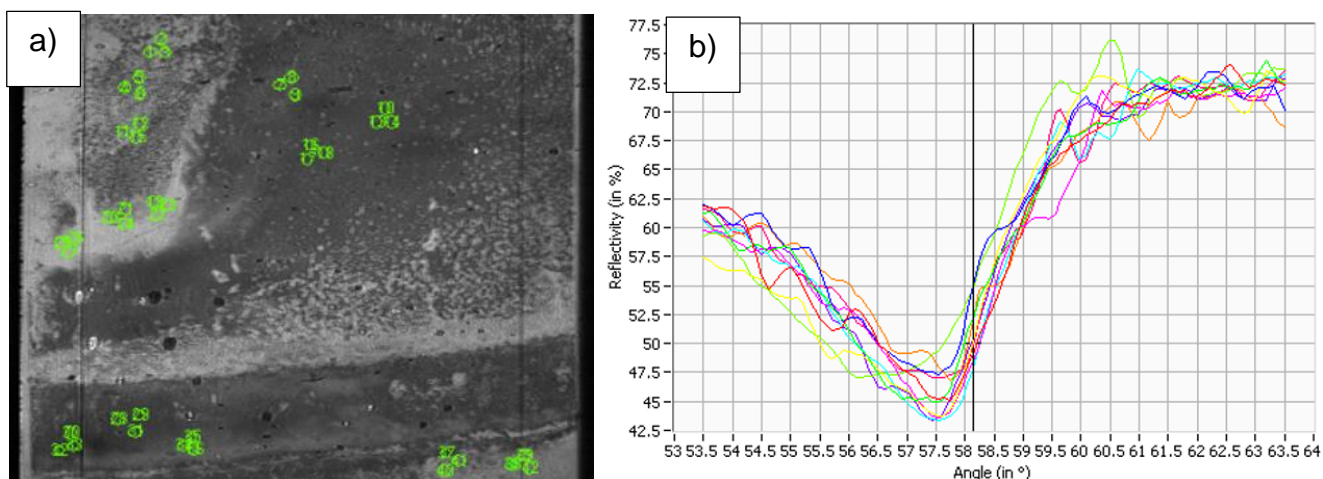


Figure 20: Microscopic image a) and SPR Plasmon curves b) for the biochip prepared by chemical reduction of CBD 100 mmol L<sup>-1</sup>.

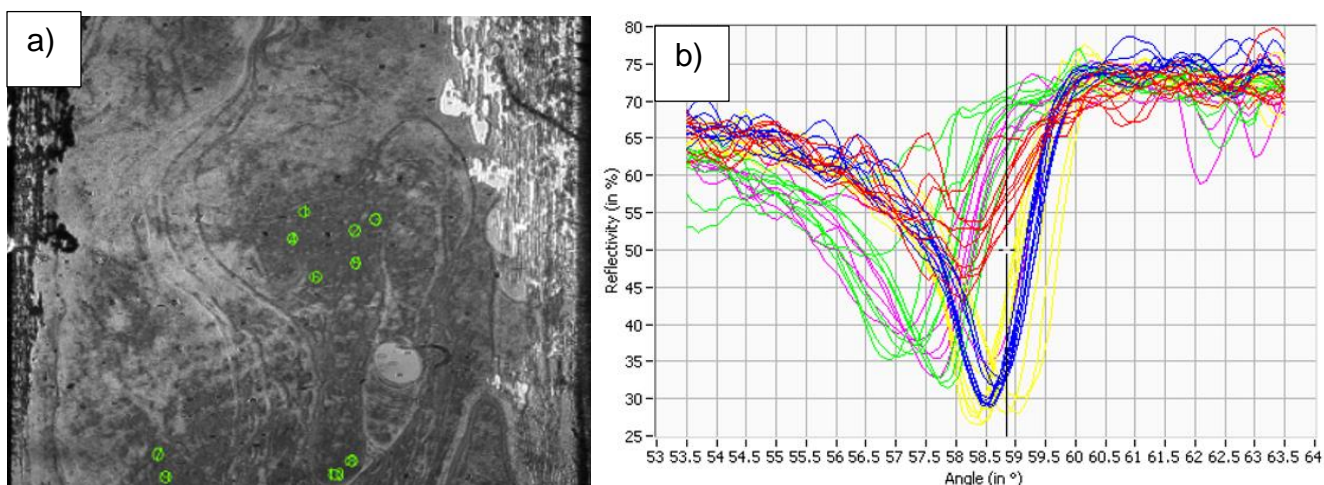


Figure 21: Microscopic image a) and SPR Plasmon curves b) for the biochip prepared by chemical reduction of CBD 50 mmol L<sup>-1</sup>.

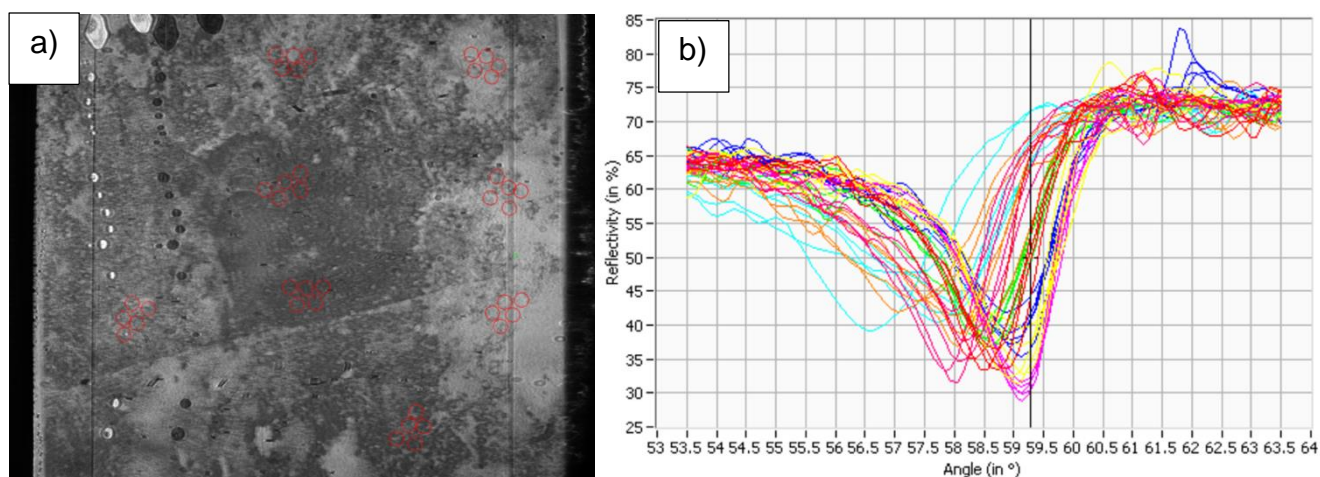


Figure 22: Microscopic image a) and SPR Plasmon curves b) for the biochip prepared by chemical reduction of CBD 20 mmol L<sup>-1</sup>.

### 3.2. Surface functionalization by electrografting

In this process, the surface to modify is used as the working electrode in a 3-electrode assembly. So, only conductive surface could be modified by this technique. To limit uncontrolled oxidation, the electrochemical reaction is mainly performed in organic solvents (acetonitrile in our case) and a potentiostat is used to apply current<sup>12</sup>. The details of the electroreduction of diazonium salt is described in the experimental part (annex). Briefly, a conventional three-electrode setup (Figure 23a) and a VersaSTAT3 potentiostat (Princeton Applied Research) are used.

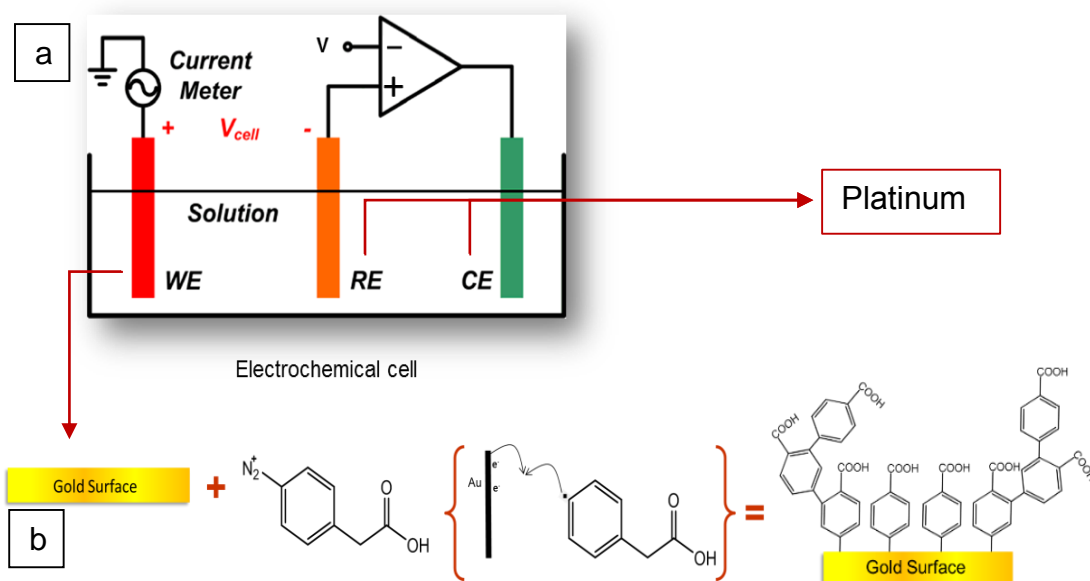


Figure 23: a) Electrochemical cell. b) 4-Carboxybenzene diazonium (CBD) reduction on the gold surface.

Platinum wires were used as auxiliary and reference electrodes whereas gold surface was used as working electrode. As we can see at the Figure 24a, only half of the surface is modified with aryldiazonium while the other half is kept intact. Thus, we have on the same device, a control and a study zone.

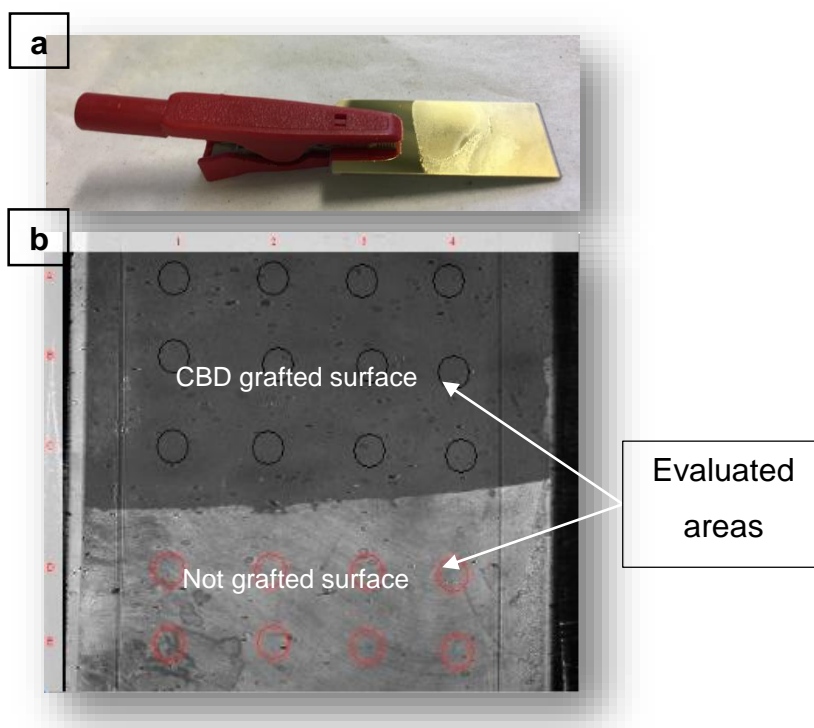


Figure 24: a) SPR biosensor obtained by electrografting. The dark side is unmodified by CBD and the bright part is modified by CBD. b) SPR biosensor observed by SPR camera.

The carboxybenzene diazonium salt is prepared at  $5 \text{ mmol L}^{-1}$  in an electrolyte solution of  $100 \text{ mmol L}^{-1}$  of tetrabutylammonium hexafluorophosphate (acetonitrile solution). Then, solution is degassed with  $\text{N}_2$  gas and cyclic voltammetry was performed at  $0.1 \text{ V/s}$ . For a specific electrical potential, diazonium salt was converted in an aryl radical which could react quickly with the electrode surface by a covalent bond<sup>170, 171</sup> (Figure 23b).

Under optimized conditions, it is possible to reach a single monolayer of benzene moieties but in the other cases, the aryl radicals will continue to attack the first layer formed and thus create multilayers of different thicknesses (Figure 23b). So, we developed different biochips by electroreduction of CBD.

### 3.2.1. Influence of the electroreduction parameters

To evaluate the influence of the CBD concentrations (5-20 mmol L<sup>-1</sup>) and the number of cycles during the electrochemical process (3-10 cycles) different experiments were driven. Figure 25 illustrated the reduction of CBD for different cyclic voltage. The broad peak starting at 0 V/Pt corresponding to a one-electron transfer with a redox potential at -0.331 V/Pt was typical for CBD reduction.

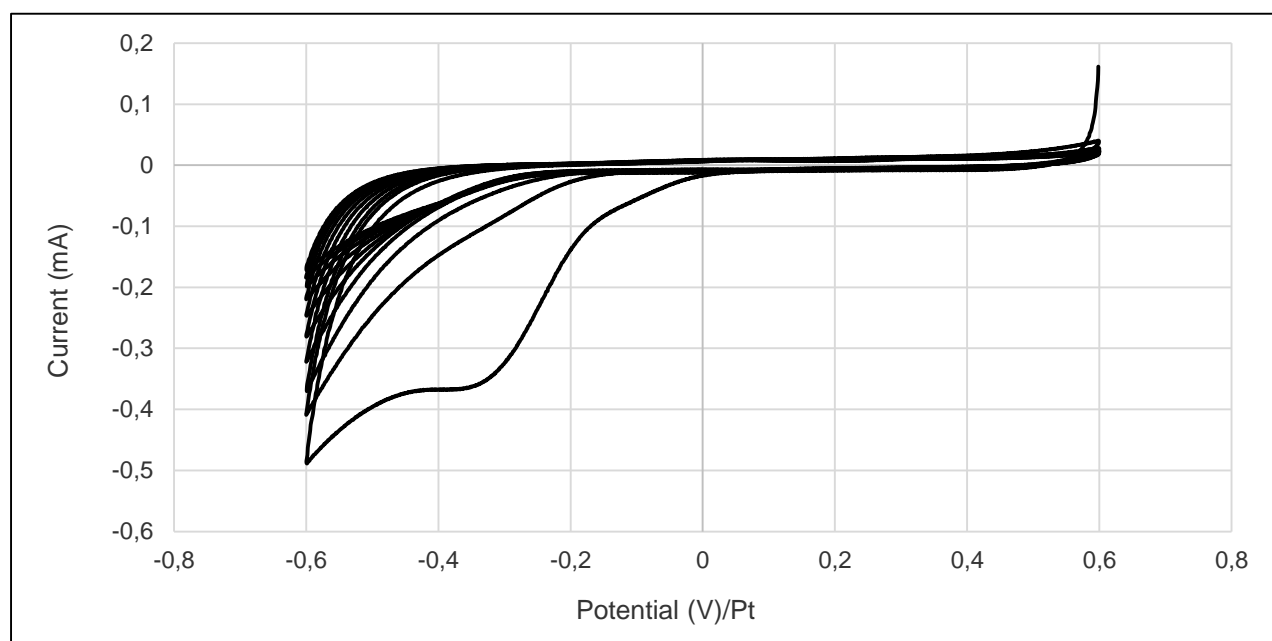


Figure 25: Electrodeposition of CBD 20 mmol L<sup>-1</sup> by cyclic voltammetry. Au surface as WE, Pt as CE and RE. Scan rate: 0.1 V/s vs. Pt from -0.6 to 0 V. Electrolyte: NBu<sub>4</sub>PF<sub>6</sub> 0.1 mol L<sup>-1</sup> in CH<sub>3</sub>CN.

To evaluate the influence of the number of cyclic voltages, we fixed the initial CBD concentration at 10 mmol L<sup>-1</sup> and we tuned the number of cycles from 3 to 5 and 10. The figure 26 illustrates that the higher is the number of cycles, lower is the current intensity. However, the decrease was limited and not proportional from 3 to 10 cycles. So, for an initial concentration of CBD 10 mmol L<sup>-1</sup>, it appeared that the number of cycles had a limited influence on the passivation of the electrode. Thus, the organic layer should be thin and mainly influenced by the first cycle of voltage.

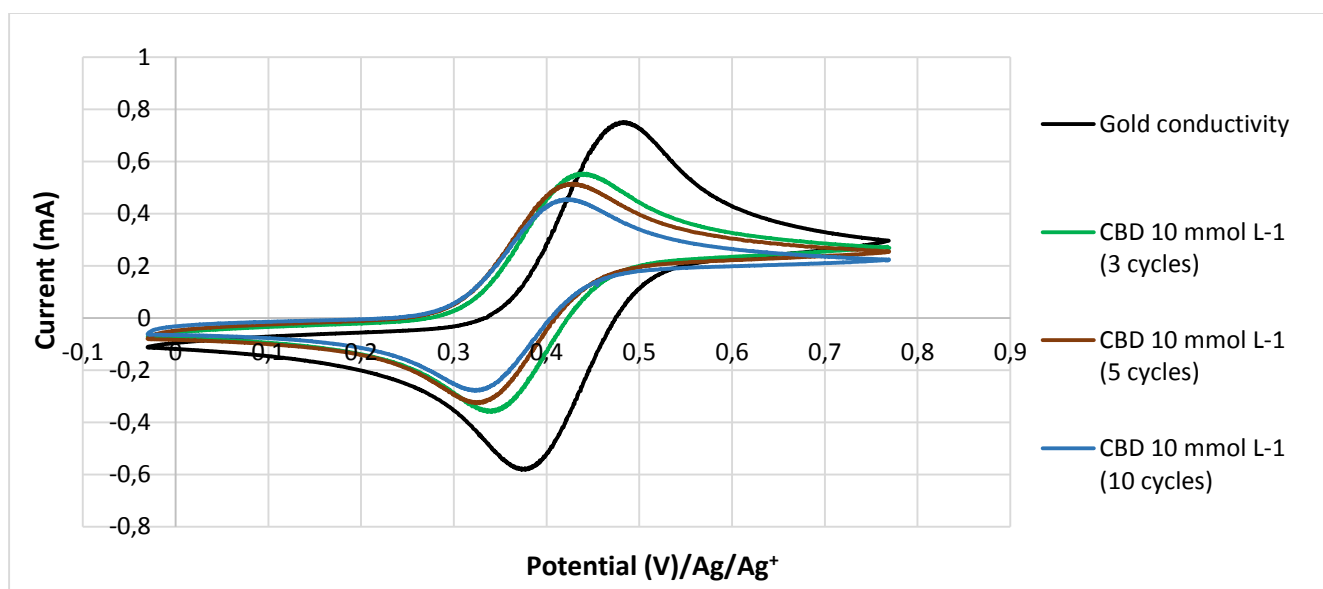


Figure 26: Cyclic voltammograms of ferrocene for the unmodified (black curve) and the modified gold surface from 3 (green curve) to 5 (purple curve) and 10 cycles (blue curve). The CBD concentration was fixed at 10 mmol L<sup>-1</sup>. Electrolyte: NBu<sub>4</sub>PF<sub>6</sub> 0.1 mol L<sup>-1</sup> in CH<sub>3</sub>CN; scan rate of 0.1 V/s from -0.3 to 0.5 V. Gold surface as work electrode, Platinum as counter electrode and Ag/AgCl as reference electrode.

To evaluate the influence of the initial concentration of CBD, we fixed the number of cycles to 3 and we modulated the initial CBD concentration from 5 to 20 mmol L<sup>-1</sup>. Results could be observed in Figure 27. It is clear that all the prepared biochips were correctly grafted because their current intensity were lower than unmodified biochip. The reduction of the current intensity was more important with the biochip prepared from 20 mmol L<sup>-1</sup> the other biochips. In fact, a larger concentration of diazonium salt during the first electrochemical reduction, generate a larger amount of aryl radical which react quickly with the molecules in their neighborhood. Thus, the aryl radical could bond covalently with the gold surface but also with the 4-carboxybenzene layer already attached forming a better coverage of the surface or a multilayer profile<sup>164,165</sup>. This conclusion fit well with the fast reduction process observed in Figure 25.

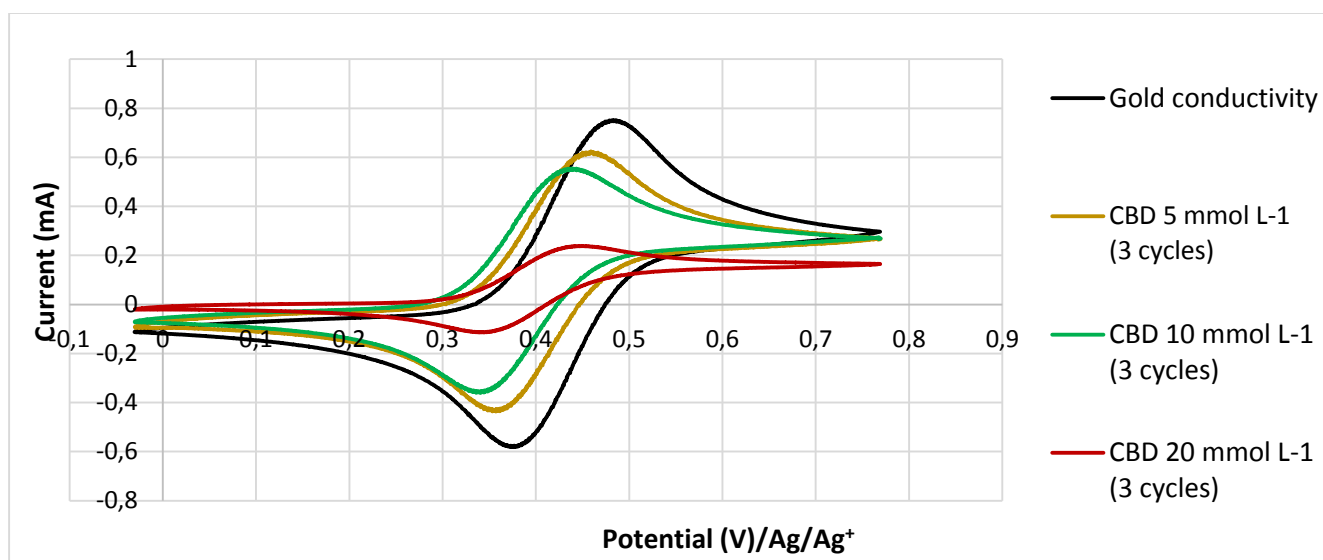


Figure 27: Cyclic voltammograms of ferrocene for the unmodified (black curve) and the diazonium modified gold surface (from 5 (yellow curve) to 10 (green curve) and 20 mmol L<sup>-1</sup> (red curve)).

Electrolyte: NBu<sub>4</sub>PF<sub>6</sub> 0.1 mol L<sup>-1</sup> in CH<sub>3</sub>CN; scan rate of 0.1 V/s from -0.3 to 0.5 V. Gold surface as work electrode, Platinum as counter electrode and Ag/AgCl as reference electrode.

To evaluate the influence of the previous parameters on the SPR signal, the plasmon signal was measured for the different conditions. We observed in Figure 28 that the shape of the reflectivity and the plasmon angle of the biochip surface was strongly modified when the initial concentration of CBD is higher than 10 mmol L<sup>-1</sup>. So, the liquid/solid interface is highly modified and measuring the biomolecular interaction at this interface in these conditions seems to be impossible. So, the concentration of CBD before electrografting has to be lower than (or equal to) 10 mmol L<sup>-1</sup> to keep a good reflectivity.

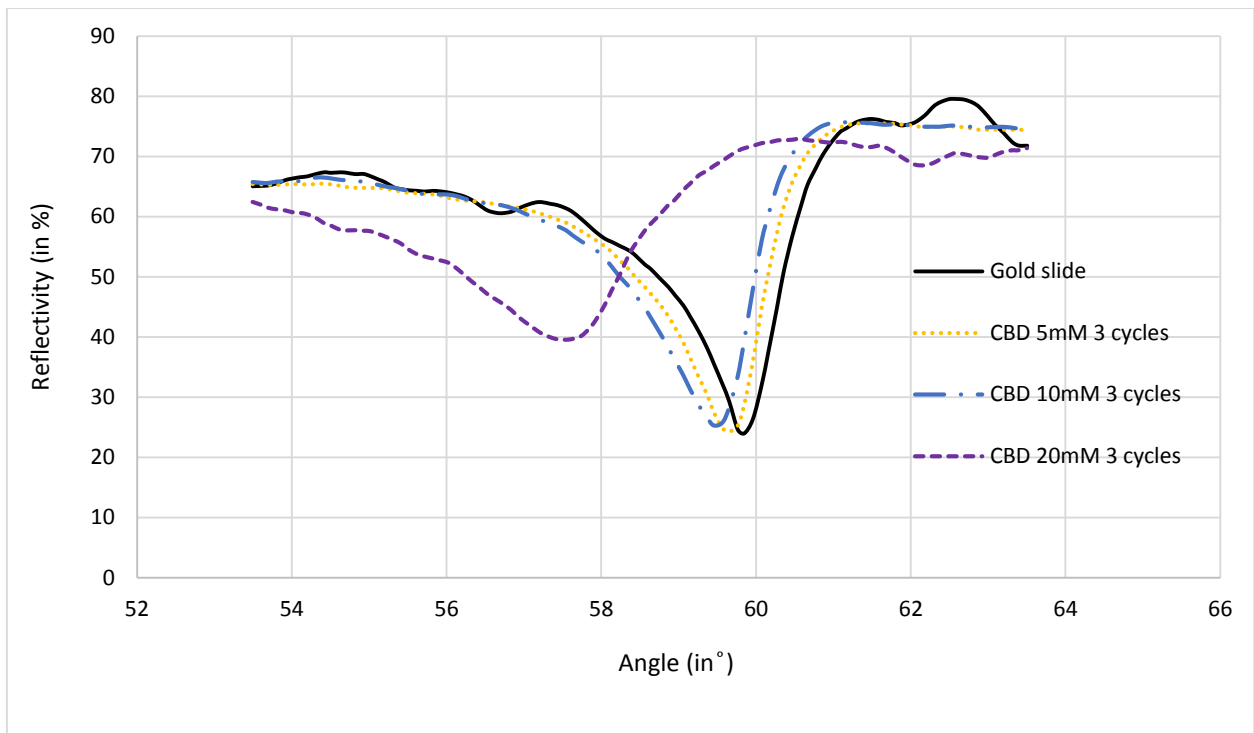


Figure 28: SPR Plasmon curves presenting the influence of the CBD concentration on the surface reflectivity at 3 cycles.

The influence of the number of cyclic voltages seems to be less important (Figure 29) than the influence of the initial concentration. As previously, the CBD-biochips present a shift of the plasmon angle to lower value as compared to the gold surface. For a low number of cycles, this shift is limited indicating that the 4-carboxybenzene layer is closed to a monolayer coating. When the concentration of CBD increased to 10 cycles, a multilayer coating was created modifying drastically the plasmon angle.

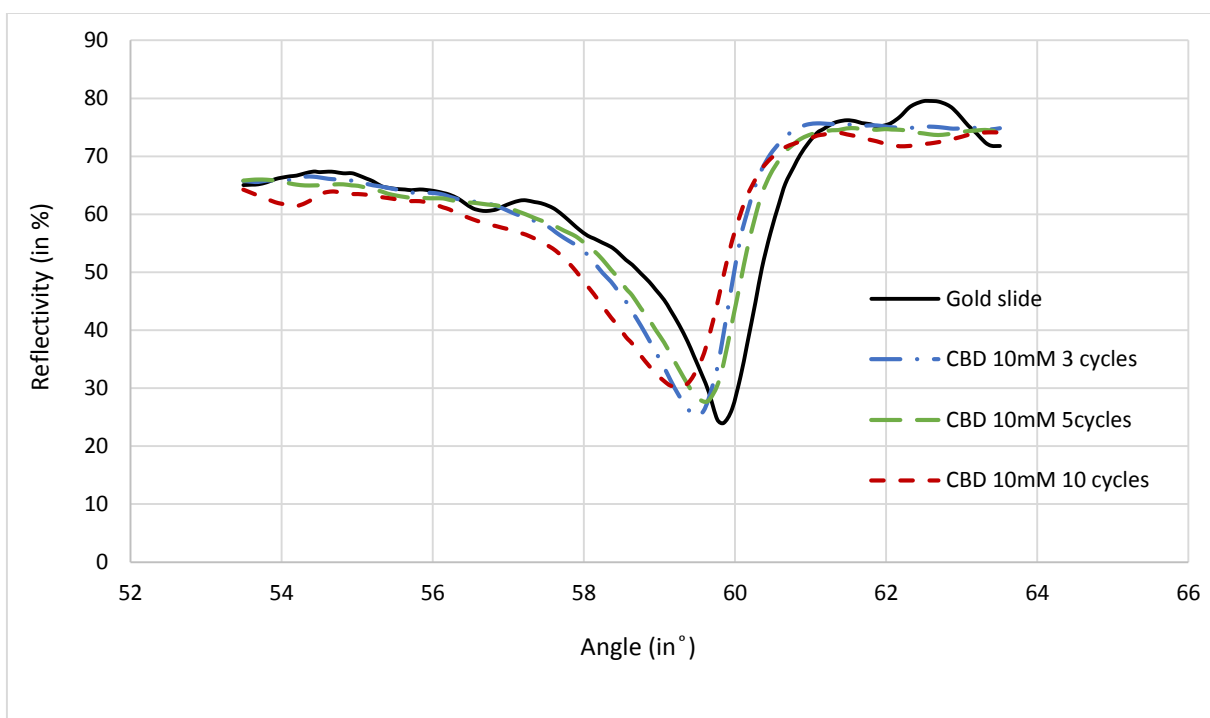


Figure 29: SPR Plasmon curves presenting the influence of the number of cycles on the surface reflectivity at CBD 10 mmol L<sup>-1</sup>.

Table 2 presents the different parameters important for SPR biochip. Clearly, the reflectivity and the plasmon angle stay close to unmodified gold surface if the surface coverage stays lower than 920 pg/mm<sup>2</sup> corresponding to 5 cycles of cyclic voltammetry applied on a 5 mmol L<sup>-1</sup> CBD solution. In these cases, the variation of reflectivity was limited to 0.5%. Then, for higher values of surface coverage, the plasmon angle and the intensity of reflectivity were strongly affected.

From all of these remarks and conclusions, I estimated that the best candidate biochip for SPR analysis should be prepared with 3 cycles of cyclic voltammetry and an initial concentration of 5 mmol L<sup>-1</sup> of CBD.

Concentration of CBD	Gold surface	5 mmol L <sup>-1</sup> 3 cycles	5 mmol L <sup>-1</sup> 5 cycles	5 mmol L <sup>-1</sup> 10 cycles	10 mmol L <sup>-1</sup> 3 cycles	10 mmol L <sup>-1</sup> 5 cycles	10 mmol L <sup>-1</sup> 10 cycles	20 mmol L <sup>-1</sup> 3 cycles	20 mmol L <sup>-1</sup> 5 cycles	20 mmol L <sup>-1</sup> 10 cycles
Angle (°)	59,9	59,7	59,6	59,6	59,5	59,5	59,3	57,7	57,4	53,8
Reflectivity γ (%)	24	24,3	24,5	27,4	25,3	27,8	30	40,2	48,8	40,5
ΔR <sup>a</sup> (%)		0,3	0,5	3,4	1,3	3,8	6	16,2	24,8	16,5
Γ <sup>b</sup> (pg/mm <sup>2</sup> )		55	920	626	239	699	1104	2981	4563	3036

Table 2: Experimental parameters extracted from reflectivity curves for unmodified and modified

CBD biochip. (<sup>a</sup>ΔR: variation of reflectivity; Γ<sup>b</sup>: molecules quantities per surface unit).

### 3.2.2. The characterization of the best candidate

To characterize the biochip prepared with 3 cycles of cyclic voltammetry and an initial concentration of 5 mmol L<sup>-1</sup> of CBD as a good candidate for SPR biochip, we studied the surface properties by cyclic voltammetry, IRTF spectroscopy and SPR analysis for instance. As previously, the biochip was prepared by electroreduction in a 3-electrode assembly (Figure 30).

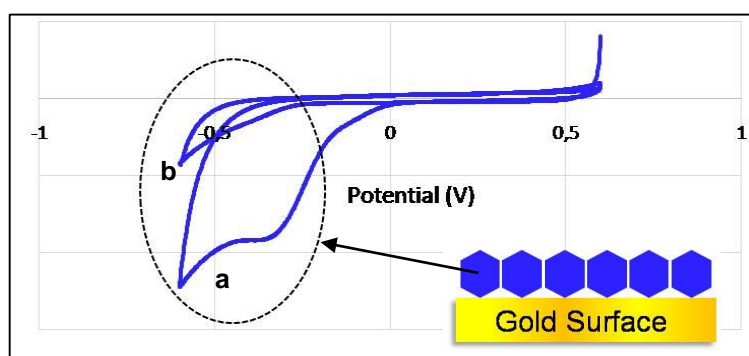


Figure 30. Cyclic voltammetry of carboxybenzene diazonium salt on gold surface. (a) first and (b) third cycle. Au surface as WE, Pt as CE and RE. Scan rate: 0.1 V/s vs. Pt from -0.6 to 0 V.

Electrolyte: NBu<sub>4</sub>PF<sub>6</sub> 0.1 mol L<sup>-1</sup> in CH<sub>3</sub>CN.

#### 3.2.2.1. Cyclic voltammetry with ferrocene

To confirm the surface modification, the biochip was used as a cathode to analyze the reference redox couple (Ferrocene/ferrocenium). The oxidation of this couple Fc<sup>+</sup>/Fc is reversible and could be investigated by cyclic voltammetry at 0.1 V/s. As we can see on the

voltammogram (Figure 31),  $\text{Fc}^+$  is reduced at 0.1 V/Ag/AgCl for modified and unmodified electrode. The intensity of the  $\text{Fc}^+/\text{Fc}$  system is lower with the modified biochip than with the gold surface indicating that the electron transfer is limited with the modified electrode. This result confirmed that the gold surface is passivated by the organic aryl layer after the electrografting of the diazonium salt.

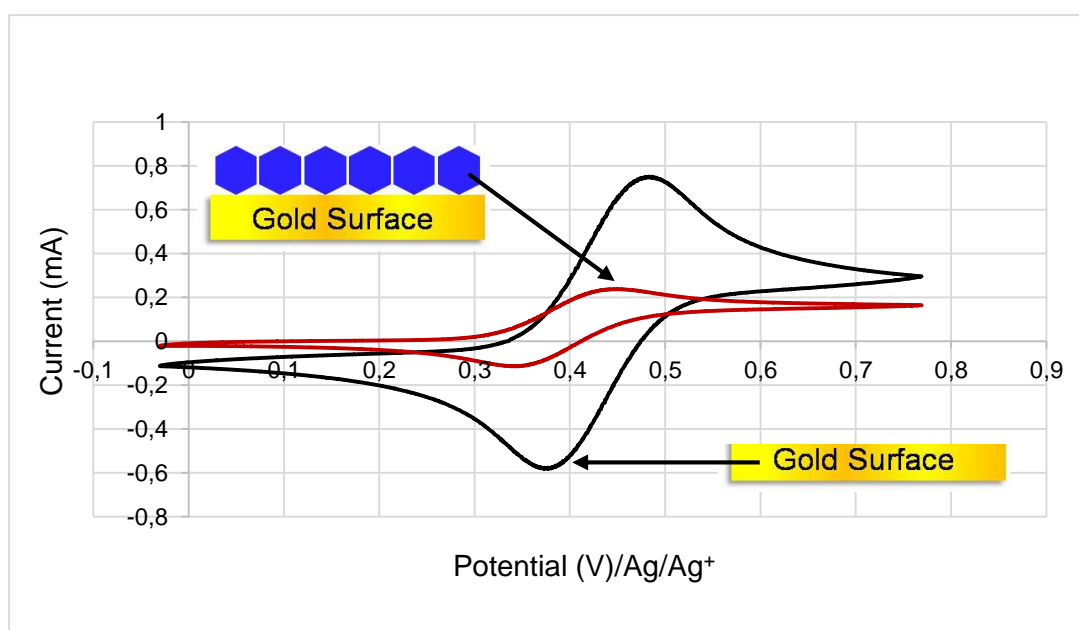


Figure 31. Cyclic voltammogram of  $1 \text{ mmol L}^{-1} \text{Fc}^+/\text{Fc}$  system with unmodified (black curve) and modified carboxybenzene (red curve) gold surface. Electrolyte:  $\text{NBu}_4\text{PF}_6$   $0.1 \text{ mol L}^{-1}$  in  $\text{CH}_3\text{CN}$ ; scan rate of  $0.1 \text{ V/s}$  from  $-0.3$  to  $0.5 \text{ V}$ . Gold surface as work electrode, Platinum as counter electrode and  $\text{Ag}/\text{AgCl}$  as reference electrode.

### 3.2.2.2. Infrared Spectroscopy (IRTF)

#### 3.2.2.2.1. Description of the principle

IR is a physico-chemical analysis technique based on the absorption of infrared radiation by interatomic bonds. Thus, IR spectroscopy is based on the excitation of vibrational and rotational energy levels of molecular bonds but not all vibrations give rise to absorption, it will depend on the geometry of the molecule and in particular on its symmetry. Spectrometers measure the attenuation of the incident radiation energy corresponding to the energy absorbed by the

molecule to change the vibrational or rotational state. Thus, it is possible to analyze the chemical composition of a sample and determine its chemical structure.

There are different variants of infrared reflection spectroscopy, such as polarization modulation infrared reflection-absorption spectroscopy (PM-IRRAS: Polarization modulation - infrared reflection-adsorption spectroscopy). It required a polarized light which is focused on the sample, a part of the signal is absorbed, and the other part is reflected and transmitted to the detector. This technique is interesting to characterize thin layers deposition and observe the orientation of these layers.

We used another variant of infrared spectroscopy, widely used for surface analysis, IR spectroscopy by attenuated total reflection (ATR-IRTF).

### 3.2.2.2. The ATR-IRTF (Attenuated Total Reflection) spectroscopy

The principle of this method is based on the total reflection of infrared radiation on the material analyzed. The analysis beam propagates through a crystal with a high refractive index, which is in contact with the sample to be analyzed. This beam is then fully reflected at the interface between the crystal and the sample. An evanescent wave is created at this interface, which will be absorbed by the surface of the sample. The attenuation of this wave will be transmitted to the reflected IR ray and then collected by the detector at the output of the crystal (Figure 32)

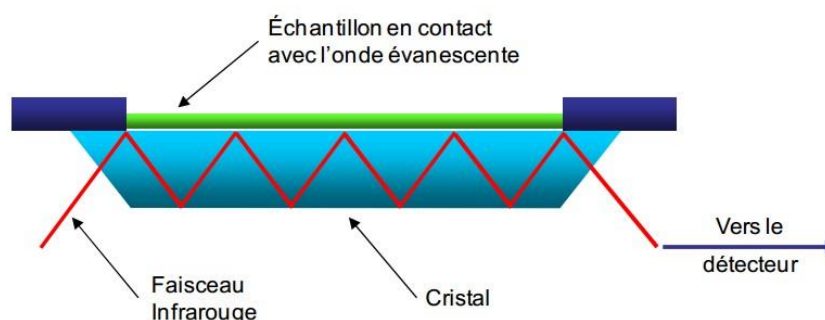


Figure 32 : Principle of multi-reflection IR-ATR spectroscopy<sup>103</sup>.

The contact between the sample and the crystal is very important because the evanescent wave only extends over a few microns (0.5  $\mu\text{m}$  - 5  $\mu\text{m}$ ). This optimal contact between the crystal and the sample is maintained by a press to allow the passage of the wave and therefore the transmission of vibrational and rotational information of the chemical groups of the sample. IR spectroscopy by ATR is therefore interesting for the analysis of flat surfaces and the monitoring of their chemical modification, but also for the analysis of liquids or powders directly placed on the crystal.

One of the limitations of this method is the penetration depth of the evanescent wave. Indeed, as the wave penetration is only a few microns on the sample surface, we do not have quantitative information on the whole of the substrate.

### 3.2.2.2.3. The surface characterization by ATR-IRTF

The measurements were carried out on a Tensor 27 spectrometer from Bruker-Daltonic equipped with an ATR germanium (Ge) crystal and a DTGS detector at room temperature. The spectra are acquired via the OPUS 6.5 software allowing spectra from 4000 to 650  $\text{cm}^{-1}$  to be obtained with a resolution of 4  $\text{cm}^{-1}$  (20 Scans). For our measurements, air was selected as a reference to remove  $\text{CO}_2$  and water contamination. To evaluate the surface modification, the surface of the SPR biochip was compared to the raw gold surface. The main digital processing is the automatic baseline correction, and in the case of very thin layers, an additional subtraction of  $\text{CO}_2$  and water vapor could be required.

IRTF spectroscopy was not a destructive technique but ATR tool required a very close contact between gold and crystal surface. So, the biochip has to be pressed and the physical contact could damage the aryl layer. For this reason, the device tested in ATR-IRTF can't be used for further test. Figure 33 represents the intensity of the transmittance peaks referring to the gold

surface before (green curve) and after (purple curve) the diazonium grafting.

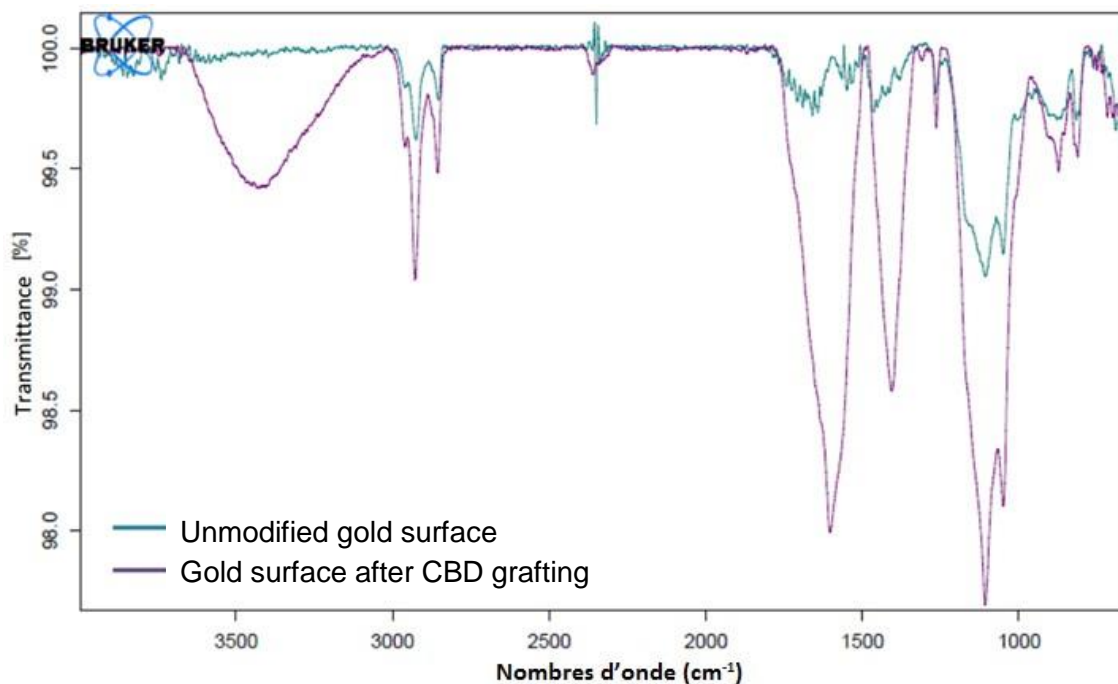


Figure 33: ATR-FTIR spectra for gold surface (green) and electrografted gold surface (purple).

We note the appearance of very intense bands on the surface (Figure 33) corresponding to:

- Large band between 3600 and 3200 cm<sup>-1</sup> ➡ O-H stretching vibration (carboxylic acid)
- Band around 1600 cm<sup>-1</sup> ➡ C=C stretching vibrations (aromatics)
- Band around 1440 cm<sup>-1</sup> ➡ O-H bending vibrations (carboxylic acid)
- Band around 1070 cm<sup>-1</sup> ➡ C-O stretching vibrations (carboxylic acid)

We can also notice that the band corresponding to N<sub>2</sub><sup>+</sup> usually observed at 2200 cm<sup>-1</sup> is not present on the electrografted surface confirming that diazonium salt is not just adsorbed. Thus, ATR-IRTF confirmed the grafting of the carboxybenzene moieties on the SPR biochip.

### 3.2.3. SPR Plasmon Curves

Plasmon curves were used to evaluate the homogeneity of the aryl layer grafted on gold surface. As only a part of the biochip was grafted with CBD, we were able to compare directly in one analysis the reflectivity and the plasmon angle between unmodified (yellow curve) and grafted surface (blue curve). It is important to note that these curves were a mean of different measurement points. In figure 34, we can see that the aryl layer deposit is really homogenous on the gold surface because there is no dispersion of the plasmon curves. The resonance angle was measured at  $59,8^\circ$  for the control part and it was characteristic for a commercial SPR biochip. This value was shifted to  $59,7^\circ$  for the CBD-treated surface confirming the modification observed by ATR-IRTF and cyclic voltammetry. This difference in reflectivity was associated to a surface coverage estimated at  $55 \text{ pg/mm}^2$ .

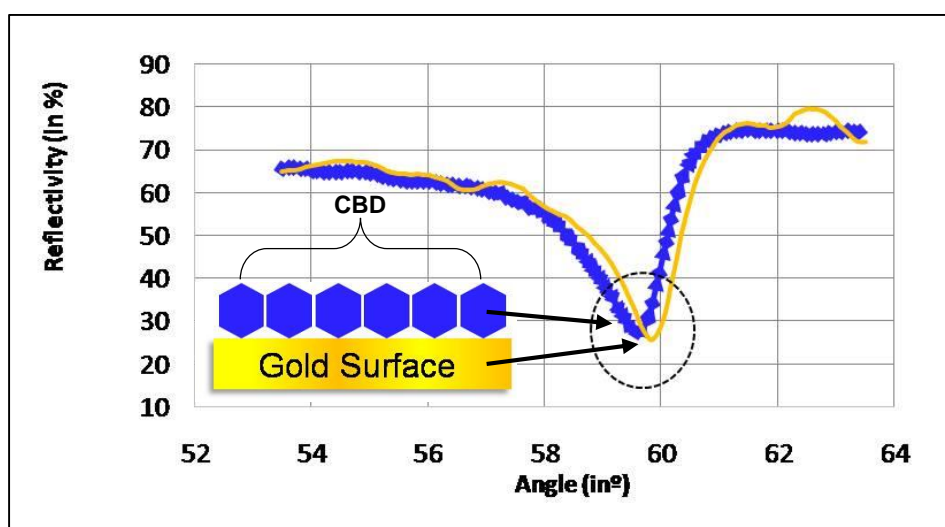


Figure 34: SPR Plasmon curves for the unmodified (yellow curve) and modified electrografted biochip (CBD  $5 \text{ mmol L}^{-1}$ , 3 cycles; blue curves).

## 4. Application of the gold functionalized surface in SPR analysis

The CBD-biochip were tested with different molecules to evaluate its performance in SPR analysis. To obtain a real time analysis, we need to immobilize a partner on the solid surface

and the target biomolecules has to be injected in solution. As a proof of concept, we started with a classical antibody/antigen interaction and then we tested an unknown protein/peptide interaction.

#### 4.1. Antibody-antigen

SPR is a relevant technique to identify the presence of an antigen in a complex solution. So, the antibody has to be immobilized at the biochip surface. In this experiment, we choose to immobilize the anti-ovalbumin immunoglobulin G (anti-OVA) and we perfused the ovalbumin (OVA) in a liquid phase.

The developed SPR biochip was prepared with a carboxybenzene surface, so different chemical group such as (primary amine, hydroxyl or thiol group) could be aimed to immobilize the anti-OVA by covalent linkage. In this work, we decided to aim the primary amine of the antibody because it was presented at the N-terminal of the peptidic chain and at the end of the lysin.

To increase the reactivity of the carboxylic surface, we have to activate the carboxylic acid to obtain an activated ester. This intermediate could be easily replaced by primary amine through nucleophilic attack. Thus, an amide bond (a kind of cross-link<sup>164</sup>) is obtained between the surface and anti-OVA. In our case, we choose to work with carbodiimide (EDC) as activating agent but as the Acylisourea intermediate is unstable we also used sulfo-N-hydroxysuccinimide (NHS) as a coupling agent. This second agent gave a NHS ester which is more stable. Moreover, the presence of the SO<sub>3</sub> group improve the water solubility of EDC. The activation was achieved after an incubation of 30 minutes in phosphate buffer (PBS) at pH 7.4 and at room temperature. Then, anti-OVA was prepared at 200 µg/mL in NaAcetate buffer and incubated at different spots for 30 minutes (Figure 35). In order to optimize this step, different antibodies concentrations (50; 100; 200; 300 µg/mL) and pH (4; 4.5; 5; 6) were tested.

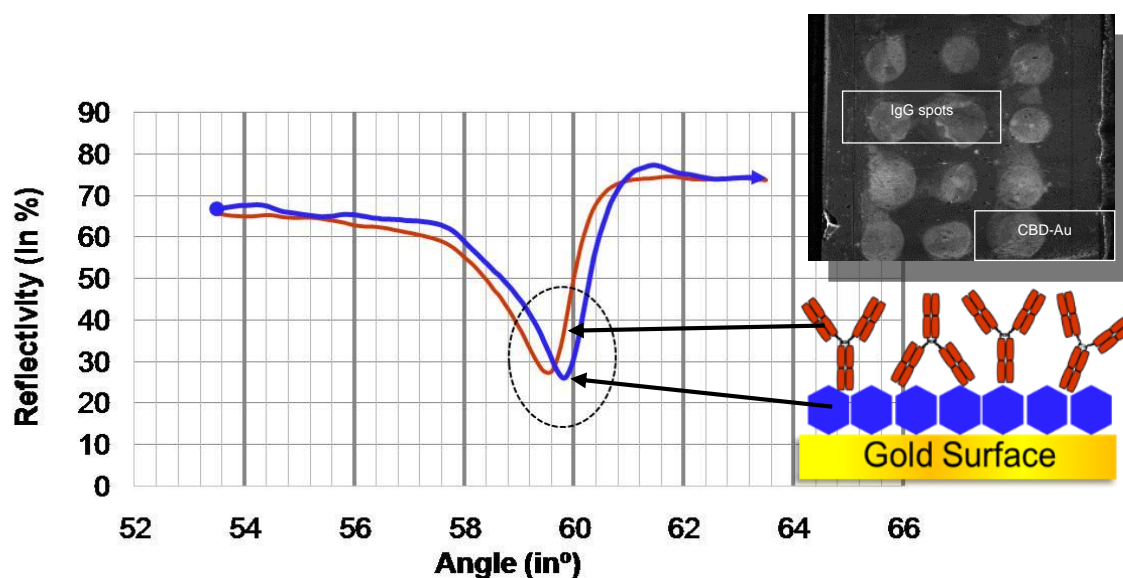


Figure 35. SPR plasmon curves of anti-OVA (IgG) spots (red curve) and negative CBD surface (blue curve).

*Antibodies were immobilized at 200  $\mu\text{g/ml}$  in NaAcetate 10  $\text{mmol L}^{-1}$  pH 4.5.*

To limit the antigen adsorption out of the defined spots, different active or passive strategies were described in literature<sup>172</sup>. In our case, we choose to work with Bovine serum Albumin (BSA) as a blocking protein. This protein was selected because it was accessible and inexpensive. The blocking was achieved after 30 minutes of incubation with bovine serum albumin (BSA) at 200  $\mu\text{g/mL}$  in PBS 10  $\text{mmol L}^{-1}$ <sup>173</sup>. We also deactivate the unreacted carboxylic groups on the surface with ethanolamine.HCl (ETA) at 1  $\text{mol L}^{-1}$  pH 8.5 during 30 minutes<sup>174</sup>. For this work, we decided to select the CBD-gold surface to use as a negative control. It can be observed in Figure 35 that after anti-OVA incubation, the plasmon angle was shifted to lower value confirming that anti-OVA was correctly immobilized on the defined area.<sup>5</sup>

When the preparation of the anti-OVA-CBD biochip was finished, we started the kinetic experiment. As SPR imaging was a real time technique, it was possible to monitor the association/dissociation between the immobilized anti-OVA and OVA. If there are no difference in response on Figure 36 after OVA injection, it means no interactions were observed.

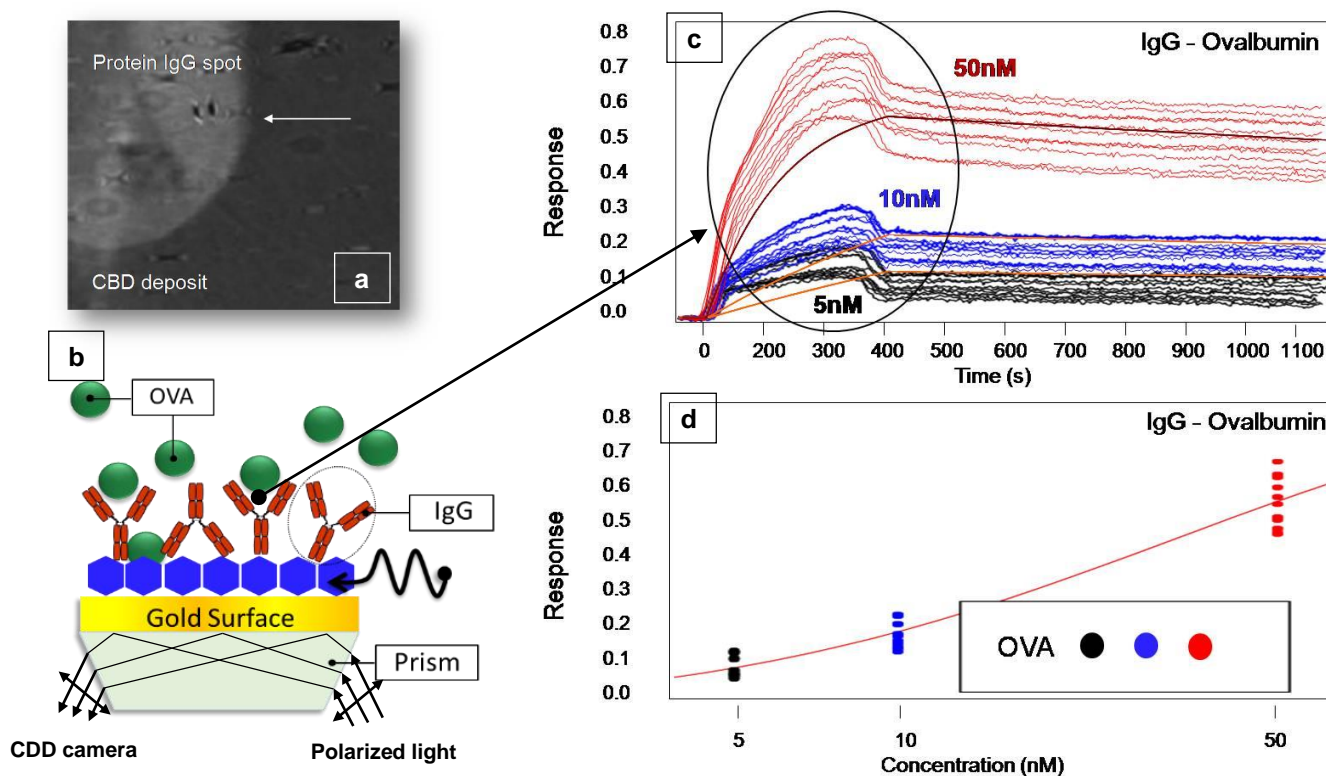


Figure 36. (a) SPRi images of anti-OVA spot (200  $\mu\text{g/ml}$ ) on the CBD-Au grafted SPRi biochips at 5  $\text{mmol L}^{-1}$ , 3 cycles. (b) Scheme of the anti-OVA grafted onto the CBD-surface in interaction with the circulating ovalbumin (OVA). (c) Kinetics reflectivity for different concentrations of injected ovalbumin. (d) dose-response curve of different antigens concentrations.

The biomolecular interactions are performed under a flow rate of 50  $\mu\text{L/min}$ . The running buffer consisting in PBS 10  $\text{mmol L}^{-1}$  pH 7.4. The injections are carried out with 200  $\mu\text{L}$  sample loop injection (240 s) containing ovalbumin from chicken egg white (OVA). Different concentrations of OVA were injected and as we can see in Figure 36c, the reflectivity responses during the association step increased with the injected concentration. It indicated that more molecules of OVA were present at the solid/liquid interface when the concentration of OVA increased. The dissociation part (after 400 s) is also informative because it indicates that some molecules of OVA are still present at the interface after washing with the buffer. So, there is a direct interaction between OVA and anti-OVA at the solid/liquid interface. From these SPR kinetics (Figure 36c), it was possible to extract some important data such as the association rate constant ( $k_a$ ) and the dissociation rate constant ( $k_d$ ). The reflectivity responses were expressed in % of reflectivity, where 1% of reflectivity corresponding to 185  $\text{pg/mm}^2$  following Horiba Scientific-Genoptics instructions<sup>175</sup>. So, it was possible to extract some information to estimate

the dissociation constant ( $K_D$ ) (Figure 36d) because the reflectivity responses were increased with the concentration of OVA during the association and the dissociation steps. A  $K_D$  of  $1.09 \text{ nmol L}^{-1}$  was obtained with our CBD-biochip. This value was comparable with the previously reported by HORIBA and in literature with thiol biochip<sup>176,177,178</sup>. Antibody orientation is important to obtain a correct binding to antigen (Figure 36b). Brogan et al. demonstrated that the dissociation rate constant is more important on thiol biochip with randomly orientated antibodies than orientated antibodies resulting in a poor binding efficiency. In this study, the  $k_d$  of  $1.88 \times 10^{-4} \text{ s}^{-1}$  was obtained with antibodies randomly attached to the diazonium surface. This result was comparable to the  $1.88 \times 10^{-4} \text{ s}^{-1}$  described in literature for protein A immobilized immunosurface<sup>178</sup>.

In SPR, a biochip should be available for successive analysis, so, the complex OVA/ Anti-OVA obtained from a previous experiment has to be displaced to obtain a ready to use anti-OVA surface. For this regeneration, different solutions (Sodium Dodecyl Sulfate, Octyl-Glucoside, Glycin) were tested<sup>179</sup>. SDS was recommended to remove hydrophobic interaction and Glycin was advised for acidic interaction. The best regeneration solution should displace OVA without damaged the surface chemistry and the anti-OVA immobilization.

As we can see in the Figure 37, three different zones were tested (anti-OVA spot; BSA passivated area; CBD-Au surface).

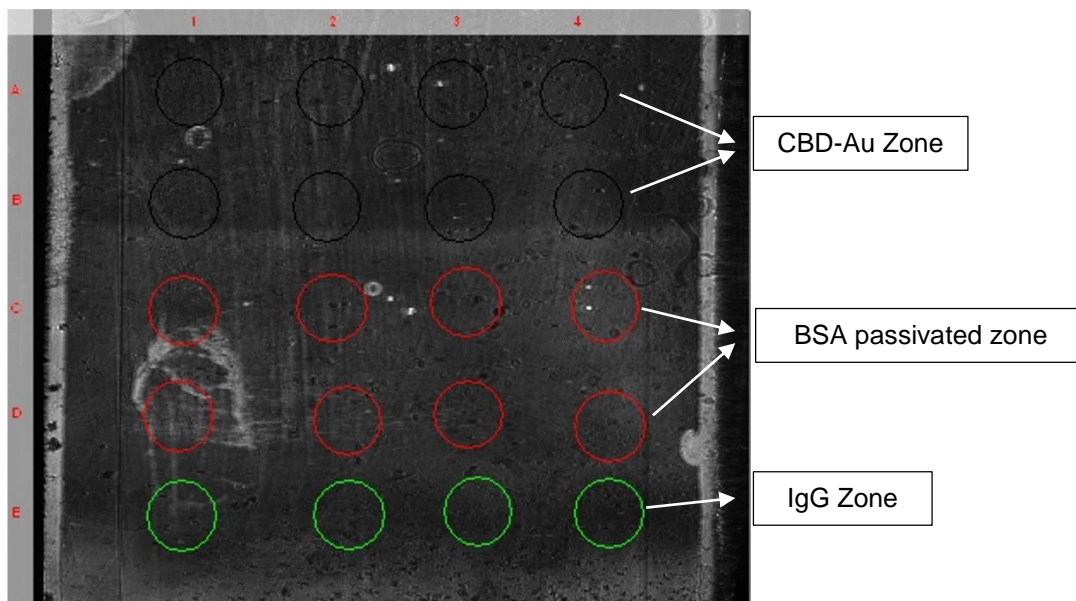


Figure 37: Microscopic images for anti-OVA (green spot), BSA (red spot) and CBD areas (black spots).

The Figure 38 show the kinetics associated to the injected SDS and OG solutions. As we can see the surface chemistry and also the antibodies immobilized on this surface did not changed in function of the injections. It means that these solutions didn't damage the CBD chemistry surface and the BSA passivated surface. Unfortunately, these solutions were not strong enough to displace OVA and regenerate the anti-OVA surface.

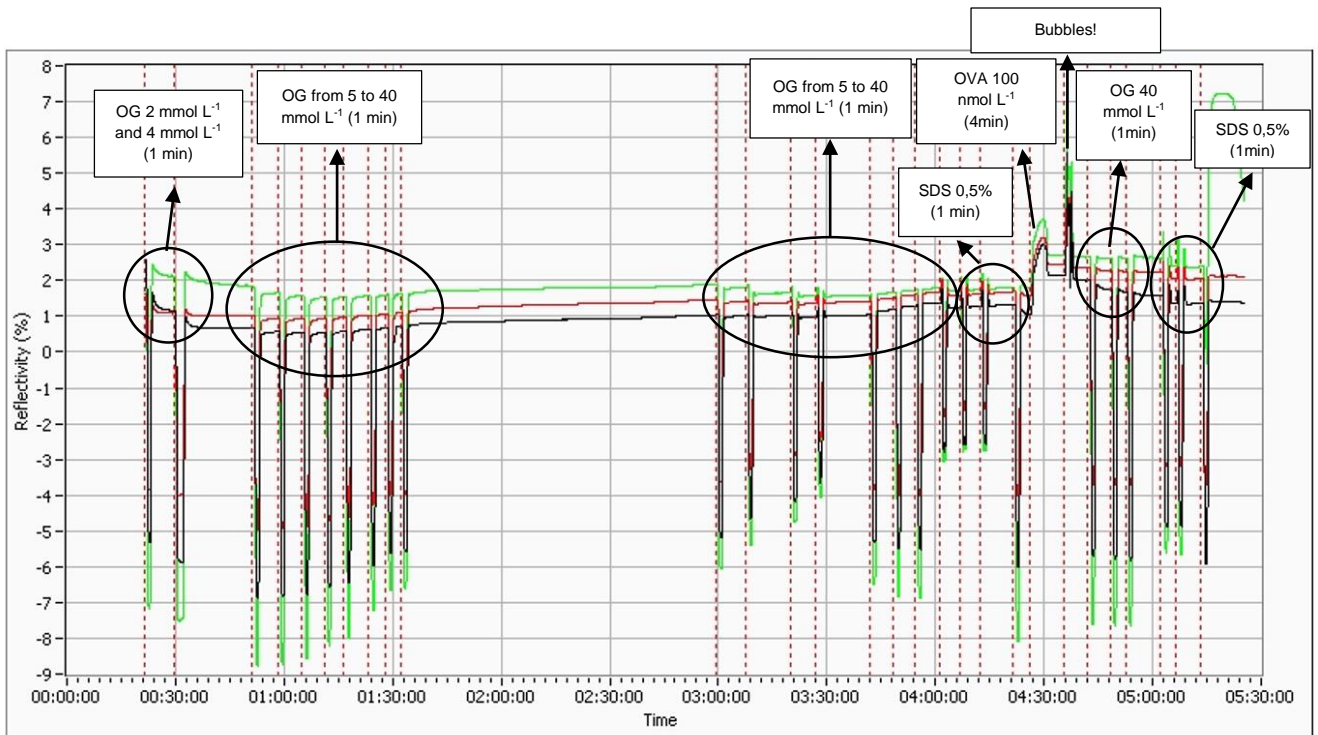


Figure 38: Kinetics reflectivity variation of the three studied areas (Green curve: Zone of immobilized IgG protein. Red curve: Zone passivated with BSA. Black curve: Zone of the CBD-Au). Injections of different detergents and Ovalbumin.

Figure 39 present the surface regeneration with glycine<sup>23, 4</sup> at 10 mmol L<sup>-1</sup> pH 2.5. As the glycine solution is acide, the global charge of anti-OVA and OVA should change resulting in a dissociation of the complex.

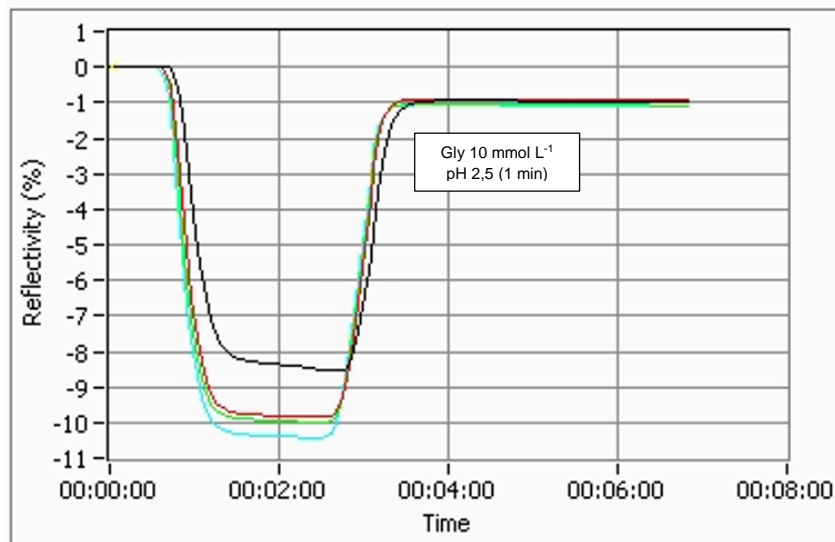


Figure 39: Kinetics reflectivity on different areas after injection of Glycine 10 mmol L<sup>-1</sup> pH 2,5 during 1 min.

## 4.2. The CNP-AmiC interactions

*Pseudomonas aeruginosa* is an opportunistic pathogen involved in a large number of diseases such as septicemia, urinary tract infections, pancreatitis, dermatitis, and keratitis mostly in immunocompromised patients<sup>2</sup>. These bacteria had a high adaptability and became resistant to antibiotherapy. So, new therapeutic approach has to be developed. The team of Pr. Olivier Lesouhaitier from LMSM is strongly involved in the research of new strategies and they recently focused their work on the role of the natriuretic peptide in the process of adaptation. Thus, they demonstrated in 2015 that *Pseudomonas aeruginosa* are able to detect the presence of these eukaryotic hormones and to adapt their virulence as an answer<sup>2</sup>. This detection could be mediated by different interaction or induced by a direct interaction with a specific receptor. They identified the bacterial receptor AmiC as a candidate. indeed, when the bacterial DNA was mutated to block the production of this receptor, the bacteria was not sensitive to natriuretic peptide. So, AmiC was a good candidate but they have to control if the interaction was direct or mediated. So, we used our CBD-SPR biochip to measure this potential interaction between the C-Type Natriuretic Peptide (CNP) and the bacterial protein AmiC. Our results will be compared to datas obtained by Microscale Thermophoresis (MST).

In this study, we choose to immobilize the CNP to the surface and to inject the bacterial protein AmiC prepared by LMSM team. As previously, CBD surface were activated with EDC/SulfoNHS for 30 minutes and then CNP were incubated for 30 minutes. To evaluate the influence of the pH, CNP solutions were prepared at pH 4 (green spots), 5 (blue spots) and 6 (red spots on Figure 40). Finally, the surface was blocked with BSA and deactivated with ethanolamine.

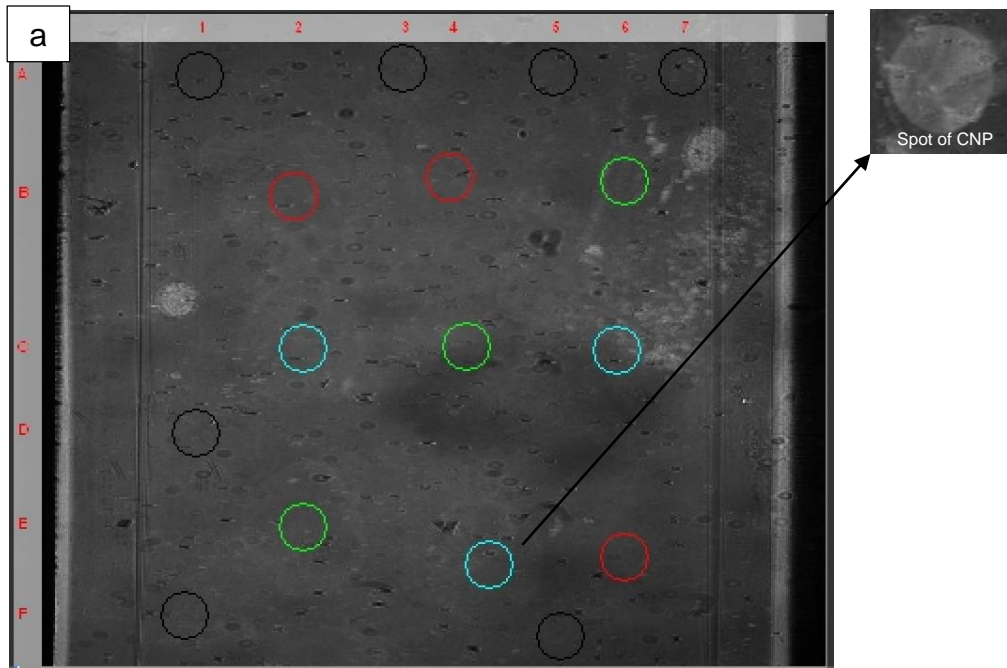


Figure 40. (a) SPRi images of the immobilized CNP prepared at pH 4 (green spots), 5 (blue spots) and 6 (red spots). Black spots were used as negative control.

After immobilization, blocking and deactivation, the plasmon angle was evaluated to check the sensibility of the sensor. The (Figure 41) below show the SPR Plasmon curves corresponding to the spots of CNP and we can see a reflectivity next to 20% and an incident angle of 58,8°, which are well adapted for a SPR analysis.

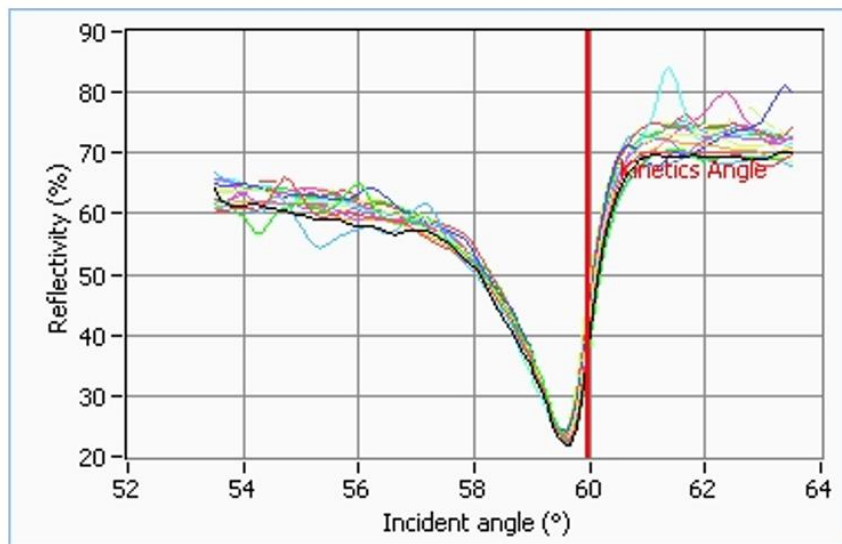


Figure 41. SPR plasmon curves of immobilized CNP hormone spot at 100  $\mu\text{g/mL}$  on the CBD-Au grafted SPR biochip.

The biomolecular interactions are performed under a flow rate of 50  $\mu\text{L}/\text{min}$  with a running buffer of PBS 10  $\text{mmol L}^{-1}$  pH 7.4. The injections are carried out with a 200  $\mu\text{L}$  sample loop injection (240s) containing the bacterial protein (AmiC).

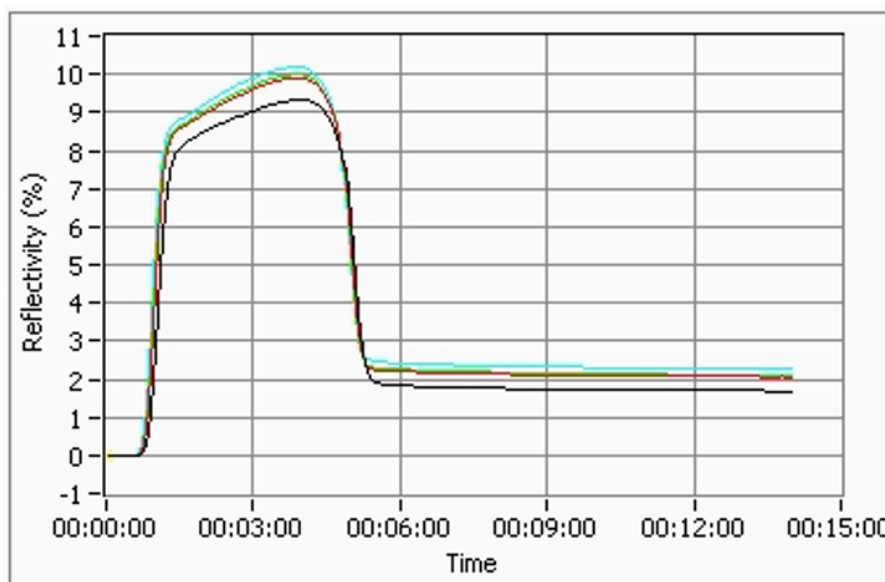


Figure 42. Kinetics reflectivity of the studied couples (CNP/AmiC). Different concentration of AmiC were injected. CNP was immobilized at 100  $\mu\text{g}/\text{mL}$ . Injection volume: 200  $\mu\text{L}$ , flow rate: 50  $\mu\text{L}/\text{min}$ .

Kinetic constants were obtained with the AmiC concentration of 1  $\mu\text{mol L}^{-1}$  after background subtraction of the signal from the CBD-Au surface. Responses were expressed in % of reflectivity, where 1% of reflectivity corresponding to 185  $\text{pg}/\text{mm}^2$  following Horiba Scientific-Genoptics instructions<sup>175</sup>.

The CNP/AmiC capture was correct with a reflectivity of  $\sim 2\%$  for all of the three different pHs tested. The equilibrium dissociation constant ( $K_D \sim 2.0 \mu\text{mol L}^{-1}$ ) obtained is compatible with the  $K_D$  value of  $2.0 \pm 0.3 \mu\text{mol L}^{-1}$  obtained by Rosay et al<sup>2</sup> by MST technique.

### 4.3. The next generation of biochip – Strip Gold Surface (SGS)

One of the limitations of SPR technique came from the plasmon angle. Indeed, this angle has to be correctly selected before any experiment to obtain a good sensitivity. Consequently, it was impossible to work with different plasmon angles at the same time except if we selected

one angle at the expense of the other or a mean value which is correct for no one. To solve this problem, Horiba developed a new generation of SPR instrument called Xelplex. This instrument is a multiplex platform allowing to work simultaneously with different plasmon angle. So, it was possible to define a specific plasmon angle for each spot to obtain the best sensitivity for each area. Therefore, this instrument is well adapted to work with diazonium chemistry. To go further, we choose to define a new design for a SPR sensor. One of the limitations of diazonium or thiol chemistry is the difficulty to graft different chemical groups in defined area. So, we worked with Dr Rabah ZEGGARI from Femto engineering to design a new “Strip Gold Surface” (SGS) (Figure 43). This biochip had two non-interconnected metal parts, that means, separated by an insulating medium (glass). So, it was possible to electrograft different diazonium salts on each gold surface or test two conditions of grafting in one analysis. This SGS biochip is perfectly adapted for the Xelplex system. So, I contacted (with the help of Dr. W. Boireau), Karen Mercier and Nathalie Volmer from the research center of Horiba to test our SGS biochip.

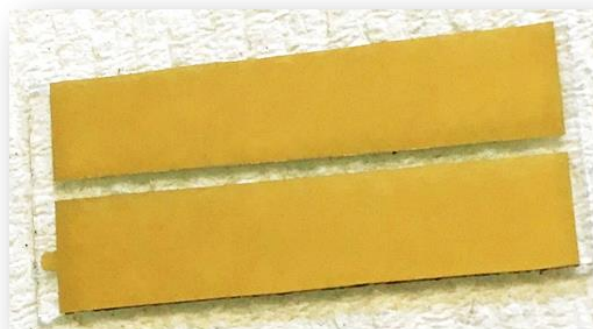


*Figure 43: Strip gold surface (SGS).*

In this proof of concept, we tested two different conditions of CBD electrografting (Figure 44): 6 (Zone A) and 4 cycles (Zone B) of electroreduction of CBD by cyclic voltammetry.

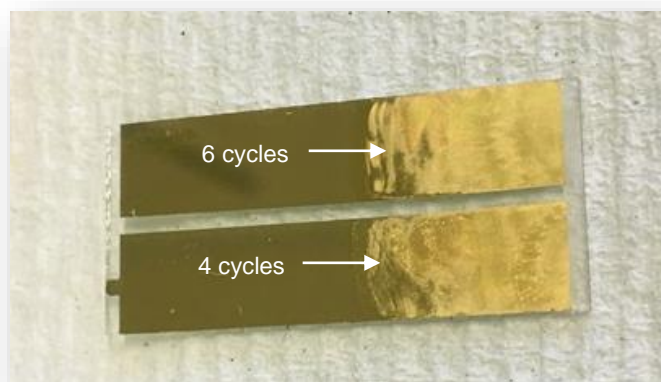


Figure 44: Strip gold surface (SGS) grafted with CBD 5 mmol L<sup>-1</sup> at 4 and 6 electrochemistry cycles.

As previously, we used OVA and anti-OVA to evaluate the potential of SGS biochip for SPR analysis. Here, as showed in the Figure 45 we tested simultaneously 2 different concentrations of anti-OVA (100 µg/mL (spot IgG 2A and IgG 2B) and 200 µg/mL (spot IgG 1A and IgG 1B) on two different surfaces (areas A: 4 cycles of reduction; areas B: 6 cycles of reduction). This design was impossible to use with conventional SPR system.

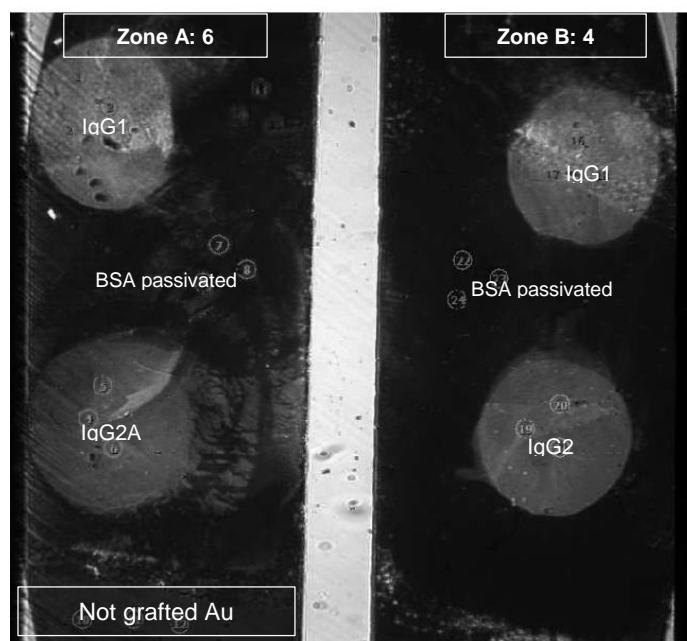
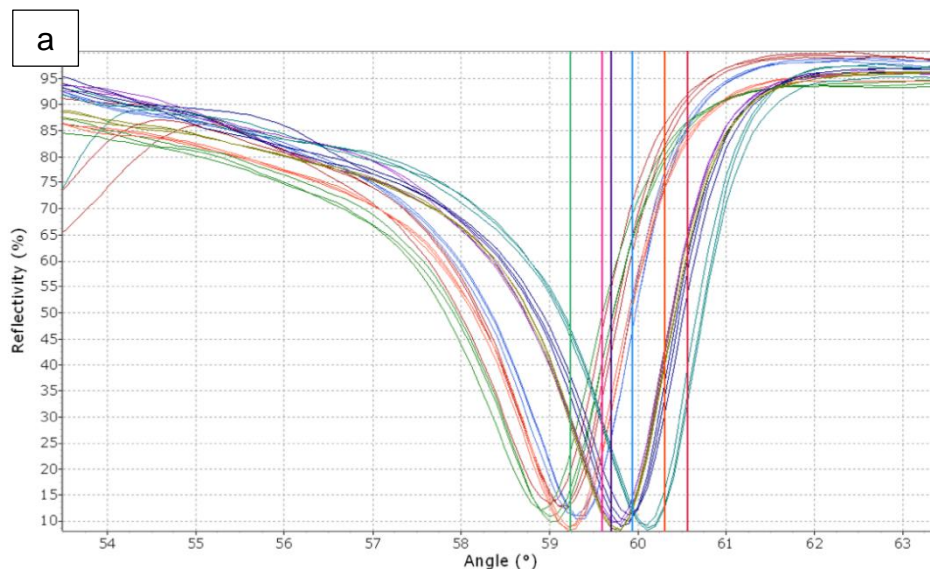


Figure 45: SPRi images of immobilized anti-OVA spot at 100 (2A; 2B) and 200 µg/ml (1A; 1B) on electrografted CBD surface prepared with 6 (Zone A) or 4 cycles (Zone B) of reduction.

As it was presented in Figure 46a, the Xelplex instrument is able to monitor different plasmon curves and kept the best angle for SPR kinetics (Figure 46b).



Nº	Angle (°)	Color	Zones
1	59,24°	Green	IgG2B
2	59,60°	Magenta	IgG1B
3	59,7°	Purple	IgG1A
4	59,93°	Blue	IgG2A
5	60,30°	Orange	BSA Passivated Zone A
6	60,57°	Red	BSA Passivated Zone B

Figure 46: SPR Xelplex plasmon curves (a) and the selection of the studied angles (b).

Then, the kinetic are carried out under a flow rate of 50  $\mu\text{L}/\text{min}$  in PBS 10  $\text{mmol L}^{-1}$  pH 7.4. The injections are carried out with 200  $\mu\text{L}$  sample loop injection (240s) containing OVA. Figure 47 present the multiplex Kinetics analysis where all the spots are evaluated separately but during the same time. Thus, the SPR analysis became much faster and economic than conventional technique. So, the SGS biochip is ready to use with this new technology.

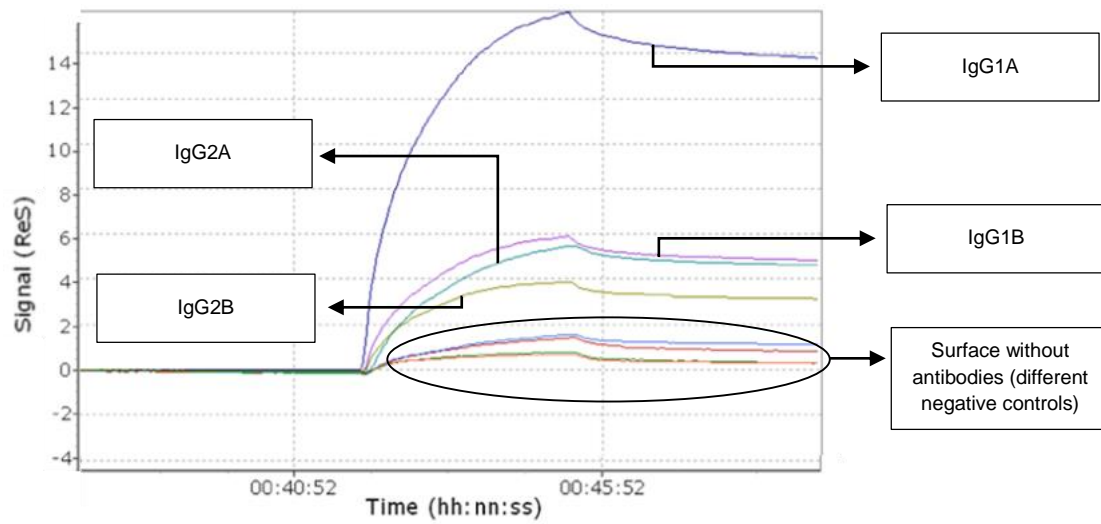


Figure 47: Kinetics reflectivity of the studied couples (anti-OVA/OVA) with the SGS biochip and the Xelplex system. Injection volume: 200  $\mu$ L, flow rate: 50  $\mu$ L/min.

## 5. Conclusion

Biosensors became essential analytical tools due to their higher performances compared with currently available diagnostic devices. The refinement studies for this type of technology are becoming necessary in today's world to answer the challenges of the medical and pharmaceutical areas.

This project implements that the aryldiazonium chemistry was an efficient alternative to prepare SPR biochip. I demonstrated that the use of diazonium salts for biosensors development is convenient, simple, fast and low cost. Diazonium with different organic function could be grafted and in this work, I demonstrate the proof of concept with carboxylic acid. I demonstrated that the grafting could be achieved by chemical and electrochemical grafting on gold and that only the electrochemical grafting was suitable for SPR experiment. After optimization of the experimental conditions of electrografting, I was able to obtain a surface with optical characteristics close to commercial biochip. Then, I demonstrated through two different applications that my biochips were available to study antigen/antibody and protein/peptide interaction. This diazonium approach was so promising that Horiba decided recently to commercialize SPR biochip prepared by electro addressing of diazonium salt.

For biologist, SPR is interesting but complicated and too long because one of the partners has to be immobilized onto the surface and some optimization step are requested. Recently, the Microscale Thermophoresis (MST) technique gave some attention and we demonstrated in this work that comparable result could be obtained by both of these techniques.

To develop SPR techniques, HORIBA developed a new multiplex platform. This platform permits to test different conditions simultaneously reducing time and cost. The commercial biochip available at this date are not adapted for this new technology so, we developed a new SGS biochip and we demonstrate its potential for multiplex experiment.

The perspective of this SPR biochip development will be:

- To improve the regeneration step to emphasize to work with different injected solution in one biochip.
- We have also to evaluate our chemistry with more complex solution such as blood, saliva, etc....
- We have also to develop the potential of the SGS biochip. Different diazonium salts could be grafted to obtain different chemical group at the surface to immobilize a protein with different orientation. This approach could be also used to evaluate the affinity for different antibody using orthogonal chemistry.



SURFOCAP 2017

## Electrografting of diazonium salt for SPR application

F. Fioresi<sup>a</sup>, A. Rouleau<sup>b</sup>, K. Maximova<sup>b</sup>, J. Vieillard<sup>a\*</sup>, W. Boireau<sup>b</sup>, C. Elie Caille<sup>b</sup>,  
C. Soullignac<sup>a</sup>, R. Zeggari<sup>b,d</sup>, T. Clamens<sup>c</sup>, O. Lesouhaitier<sup>c</sup>, N. Mofaddel<sup>a</sup>, F. Le Derf<sup>a</sup>

<sup>a</sup>UMR CNRS 6014 COBRA, Université de Rouen Normandie, 55, rue Saint Germain, 27000 Evreux.

<sup>b</sup>Institut FEMTO-ST, UMR CNRS 6174, Université Bourgogne Franche-Comte, 15B avenue des Montboucons, 25030 Besançon, France

<sup>c</sup>UPRES EA 4312 LMSM, Université de Rouen Normandie, 55, rue Saint Germain, 27000 Evreux

<sup>d</sup>Femto Engineering, Centre de Développement Technologique de Femto-st, 15 B avenue des Montboucon, F-25030 Besançon

---

### Abstract

A general method to develop diazonium-based biochip for SPRi analysis is presented. The electrografting of carboxybenzene diazonium salt is optimized in order to fit with the requirement of the SPR technology. The influence of the surface preparation on plasmon quality is discussed and the performance of this original modified biochip is investigated for determining the binding constants between circulating ovalbumin and spotted anti-ovalbumin antibody. The kinetic constants are calculated and compared with literature and similar performances are reached confirming that diazonium based biochip is a good complement to commercial SPRi sensor.

© 2018 Elsevier Ltd. All rights reserved.

Selection and/or Peer-review under responsibility of SURFOCAP 2017.

*Keywords:* Diazonium salt, Surface plasmon resonance, affinity constant, ovalbumin, electrochemistry, SPRi

---

### 1. Introduction

Surface plasmon resonance (SPR) is a well-established technique for studying affinity between biomolecules whose interaction takes place in a liquid/solid interface [1]. The sensitivity of this real time technique is due to the gold sensing surface used. Thus, SPR succeeded in measuring the affinity constant between protein-DNA, protein-protein or small molecule-protein [2-4]. However, working with a solid surface has some drawbacks.

\* Corresponding author. Tel.: +33 2 32291536;

E-mail address: [julien.vieillard@univ-rouen.fr](mailto:julien.vieillard@univ-rouen.fr)

Indeed, SPR is a technique based on a refractive index, so it is highly sensitive to biomolecular adsorption [5]. In this context, different strategies were investigated for coating gold surface. Dextran polymer and polyethylene glycol chemistry were interesting for limiting the nonspecific adsorption from complex protein matrix but their utilizations in SPR were limited by the need of acidic post-functionalization [6, 7]. In 2002, Raitman *et al.* showed that the electrografted-polyaniline polymer could be adsorbed on gold surface and applied for SPR experiment [8]. Then, alkanethiol chemistry was extensively studied because the sulfur-gold bond involved in the coating process formed spontaneously a densyl self-assembled monolayer (SAM) on the gold surface [1]. Despite its advantage, thiolated surfaces were still highly sensitive to nonspecific adsorption and some post-functionalization using protein or amino acid coating could be required [9]. Moreover, the gold-sulfur interaction is labile, yielding the coating unstable under specific condition. Aryldiazonium chemistry is a convenient method to modify conductive or polymeric surfaces by electro-reduction or chemical reduction respectively. During the electrochemical process, the diazonium salt is reduced to an aryl radical which interacts with sulfur to form a covalent bond. On gold surface, the diazonium coating is promising as an alternative to the thiol coating because the carbon-gold interaction is more stable and the electro-reduction is a fast process [10-13].

Two strategies are investigated for the protein immobilization through diazonium chemistry. In one case, surface is firstly modified by aryl diazonium and then proteins are attached by peptide coupling [14]. In the other case, the protein is firstly conjugated with the diazonium salt then immobilized onto the surface. In both case, the diazonium coating presents a better antifouling activity than thiol SPR chip [13, 15].

In this paper, the use of an electrochemical diazonium grafting to obtain a SPR sensing layer is reported. The influence of the cyclic voltammetry parameters and the initial concentration of diazonium salt on the quality of the sensing layer are discussed. The potentialities of diazonium sensing layer to characterize affinity constant between ovalbumin and its antibody (anti-OVA) are emphasized and compared to literature.

## 2. Material and methods

### 2.1. Cyclic voltammetry

The electroreduction of the diazonium salts was performed as described elsewhere [13], using a conventional three-electrodes cell setup and a VersaSTAT3 potentiostat (Princeton Applied Research). Platinum wires were used as auxiliary and reference electrodes whereas gold surface (Schott) is used as working electrode.

### 2.2. SPR analysis

Following the diazonium grafting, acidic functions were activated by EDC/SulfoNHS (4:1 V/V) coupling during 10 minutes. Then, the antibodies were directly grafted inside the SPR apparatus at 20  $\mu\text{L}/\text{min}$ . In order to limit nonspecific interaction on antibodies free area, the surface was blocked with bovine serum albumin (BSA, 200  $\mu\text{g}/\text{mL}$ ) and deactivated using ethanolamine/HCl (1M). All the SPRi Interactions were performed with circulating ovalbumin on SPRi-Plex II (Horiba Scientific) in 10 mM phosphate buffered saline solution (PBS) under a flow rate of 50  $\mu\text{L}/\text{min}$ . A regeneration step was performed by injecting a chaotropic solution (10 mM glycine, pH 2.5).

## 3. Results and discussion

### 3.1. Surface modification by electrografting of diazonium salt

Gold substrates were modified by electroreduction of 4-carboxybenzene diazonium (CBD) salt using cyclic voltammetry. Figure 1a presents a broad peak starting at 0V/Pt wire corresponding to a one-electron transfer with a redox potential at -0.331 V.

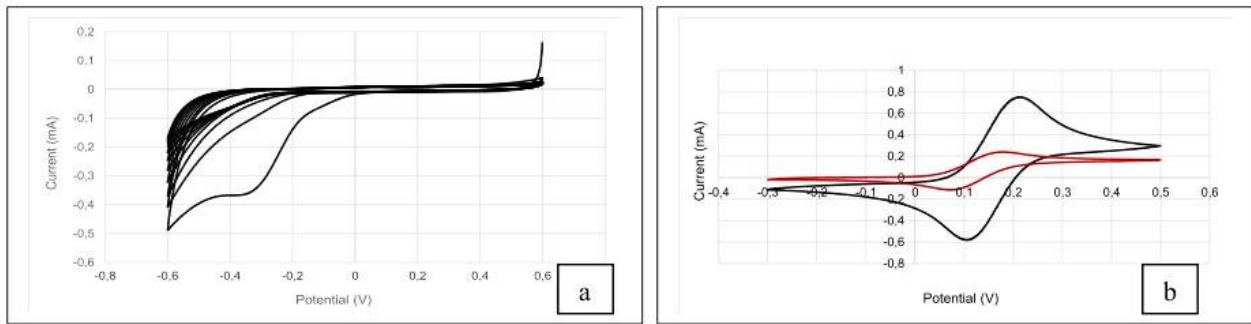


Figure 1: (a) Electrografting of carboxybenzene diazonium salt in acetonitrile by 10 consecutive cycles. Scan rate: 100 mV.sec<sup>-1</sup>. (b) Cyclic voltammograms of ferrocene at bare gold electrode (black curve) and diazonium modified electrode (red curve).

After the first cycle, the current voltage shows a decrement due to the passivation of the surface by the 4-carboxybenzene layer (Figure 1a). After the electrochemical reduction of the diazonium salt, the modified gold surfaces were rinsed to remove the adsorbed molecules and then ferrocene was used as a redox marker to evaluate the conductivity barrier properties of the surface (Figure 1b). The reversible redox curves obtained with Fc/Fc<sup>+</sup> present a lower conductivity on diazonium modified surface than on gold surface confirming the surface grafting [11]. To determine the relationship between the blocking properties and the coating layer, the initial concentration of aryldiazonium (from 5 to 20 mM) and the number of cycles (from 3 to 10 cycles) were modified. As expected, the highest concentration of diazonium salt and number of cycles correspond to the worst case with an important blocking effect. Indeed, the current voltage was decreased from 51  $\mu$ A for 20 mM of CBD to 22  $\mu$ A for 5 mM of CBD. A large concentration of diazonium salt during the first electrochemical reduction, generates a large amount of aryl radical which reacts quickly with the molecules in their neighborhood. Thus, the aryl radical could bond covalently with the gold surface but also with the 4-carboxybenzene layer already attached forming a multilayer surface [10].

For SPR analysis, a plasmon wave should propagate through the modified surface to reach the biomolecules at the liquid/solid interface. The evanescent wave occurs at a regular angle through a thin diazonium layer whereas a thicker diazonium layer passivates completely the surface that shift the resonant angle out of the range of the apparatus. So, the shape and the thickness of the diazonium layer have to be controlled and we engaged this surface characterization by AFM. Plasmon curves were further analyzed on different modified gold surfaces (Figure 2).

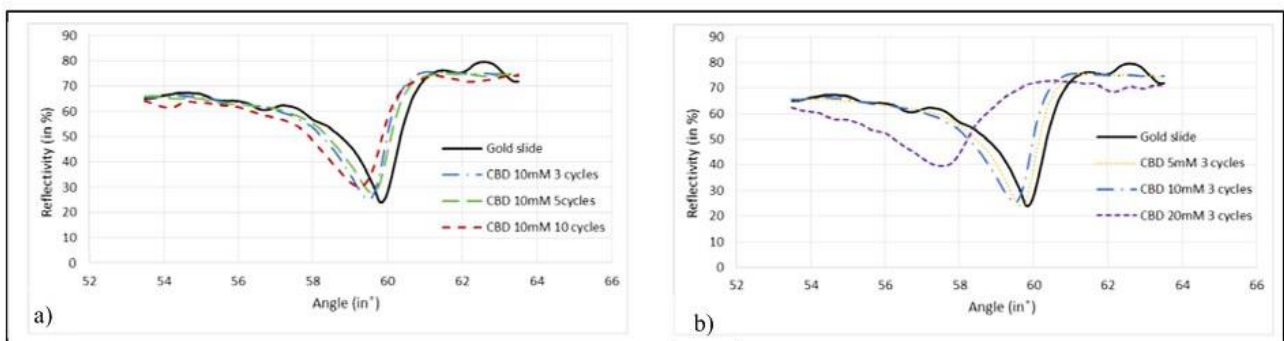


Figure 2: Influence of the number of cycles (a) and initial concentration of diazonium salt (b) on the surface reflectivity.

Diazonium-modified-biochip presents a shift of the plasmon angle to lower value as compared to gold surface. For a low concentration of CBD, this shift is limited indicating that the 4-carboxybenzene layer is closed to a monolayer coating. When the concentration of CBD increased, a multilayer coating was created modifying drastically the plasmon angle.

It could be noted that the number of cycles during electrografting has a limited effect on the plasmon angle except for the experimental condition of 20 mM CBD where no plasmon angle was detected after 10 cycles of electrografting. The diazonium layer was probably too thick to allow the optimal evanescent wave generation conditions. This hypothesis was confirmed by the maximum reflectivity measured for 3 cycles and 5 mM of CBD and its decrease to minimum value for 10 cycles and 20 mM of CBD. No linear relationship could be determined between the reflectivity and the initial concentration of diazonium and the number of cycles probably due to the multilayer profile of the coating. A performant SPR biochip shall present a reflectivity and a plasmon angle close to those noted for a crude gold chip i.e. 24% and 59.9° respectively. According to Table 1, only the modified biochip obtained with 5 mM of CBD and 3 cycles was able to fit with these values.

Table1: Experimental data extracted from reflectivity curves for gold surface and diazonium modified surfaces.

concentration of CBD	Gold surface	5 mM 3 cycles	5 mM 5 cycles	5 mM 10 cycles	10 mM 3 cycles	10 mM 5 cycles	10 mM 10 cycles	20 mM 3 cycles	20 mM 5 cycles	20 mM 10 cycles
Angle (°)	59,9	59,7	59,6	59,6	59,5	59,5	59,3	57,7	57,4	53,8
Reflectivity (%)	24	24,3	24,5	27,4	25,3	27,8	30	40,2	48,8	40,5
$\Delta R^a$ (%)		0,3	0,5	3,4	1,3	3,8	6	16,2	24,8	16,5
$\Gamma^b$ (pg/mm <sup>2</sup> )		55	920	626	239	699	1104	2981	4563	3036

<sup>a</sup> $\Delta R$ : variation of reflectivity; <sup>b</sup> $\Gamma$ : molecules quantities per surface unit

### 3.2. Biomolecular interaction analysis with SPR

To show and validate this concept, anti-OVA antibody was immobilized on diazonium modified biochip by using the fluidics of the SPRi instrumentation. Then, surface was blocked by BSA and deactivated by ethanolamine in order to saturate the unreacted functions. Finally, SPR was utilized to monitor the binding kinetics with antigen target (ovalbumin) in order to evaluate the global affinity constant. Different concentrations of ovalbumin from 5 to 50 nM were injected and the association/dissociation curves were monitored (Figure 3a). As expected, the reflectivity responses increased with the amount of injected ovalbumin until a plateau corresponding to the steady states of the biomolecular interactions.

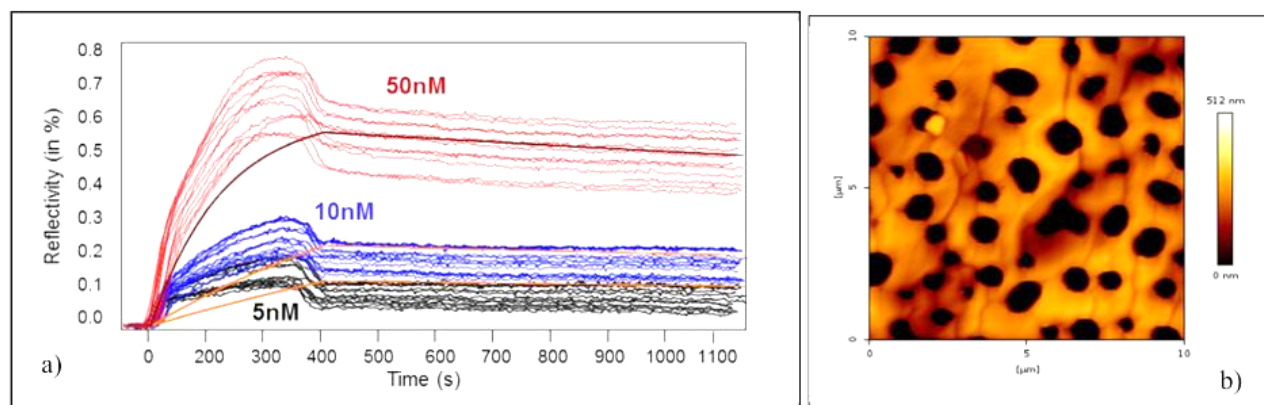


Figure 3: (a) SPR sensorgrams of anti-ovalbumin and circulating ovalbumin (from 5 to 50 nM) at 50  $\mu$ L/min. (b) AFM image of a 4-carboxybenzene modified gold surface after water rinsing.

From these curves, the variation of responses shall be extracted, according to the Langmuir 1:1 binding model, in order to calculate the association rate constant ( $k_a$ ), the dissociation rate constant ( $k_d$ ) and the dissociation constant ( $K_D$ ).  $K_D$  of 1 nM obtained with the diazonium biochip was comparable with the constant value previously reported in the literature [16-18].

Antibody orientation is important to obtain a correct antigen binding. Brogan *et al.* demonstrated that the dissociation rate constant is more important on biochip chemically functionalized with thiolated SAM when the antibodies are randomly orientated than when they are orientated resulting in a poor binding efficiency. In this study, the  $k_d$  of  $1.88 \times 10^{-4} \text{ s}^{-1}$  was obtained with antibodies randomly attached to the diazonium surface. This result was comparable to the  $2.49 \times 10^{-4} \text{ s}^{-1}$  described in literature for protein A immobilized immunosurface [16]. It could be explained by the shape of the 4-carboxybenzene layer coated on gold. Indeed, AFM images of the modified surfaces present a porous carboxybenzene layer with numerous hundred nanometer of diameter holes (Figure 3b). We can emphasize that the ovalbumin diffusion close to the surface was slow down due to the surface organization promoting the anti-OVA-ovalbumin interaction with a weaker dissociation.

#### 4. Conclusion

Diazonium modified biochips were successfully fabricated by electrografting of 4-carboxybenzene diazonium salt. The optimization of the grafting process allows obtaining a grafted diazonium layer suitable for SPRi analysis. The obtained covalent grafting presents a low non-specific binding of protein. This study demonstrates the performance of the diazonium-biochip for studying the interaction between an immobilized antibody and a circulating antigen and then for estimating the kinetic parameters associated to this interaction. Therefore, diazonium-modified chip could be further used to evaluate the nonspecific adsorption of complex matrix, the protein capture in this matrix and to study new biomolecular interactions.

#### 5. Acknowledgements

This work was partially supported by INSA Rouen, Rouen University, CNRS, Labex SynOrg (ANR-11-LABX-0029), the European Battuta Program, the Normandy region (CBS network), European Union (FEDER) and the Evreux Portes de Normandie Agglomeration. We also thank Horiba Scientific for fruitful discussion and their assistance with SPR instrument.

#### References

- [1] H. H. Nguyen, J. Park, et al., *Sensors (Basel, Switzerland)*, 15, (2015) 10481-10510.
- [2] V. Mansuy-Schlick, R. Delage-Mourroux, et al., *Biosensors and Bioelectronics*, 21, (2006) 1830-1837.
- [3] W. Boireau, S. Bombard, et al., *Biotechnology and Bioengineering*, 77, (2002) 225-231.
- [4] A. Berthier, C. Elie-Caille, et al., *Journal of Molecular Recognition*, 24, (2011) 429-435.
- [5] R. J. Green, M. C. Davies, et al., *Biomaterials*, 20, (1999) 385-391.
- [6] K. Uchida, H. Otsuka, et al., *Anal. Chem.*, 77, (2005) 1075-1080.
- [7] E. M. Muñoz, H. Yu, et al., *Anal. Biochem.*, 343, (2005) 176-178.
- [8] O. A. Raitman, E. Katz, et al., *J. Am. Chem. Soc.*, 124, (2002) 6487-6496.
- [9] O. R. Bolduc and J.-F. Masson, *Langmuir*, 24, (2008) 12085-12091.
- [10] M. M. Chehimi, *Aryl Diazonium Salts: New Coupling Agents and Surface Science*, Wiley WCH Verlag GmbH & Co, 2012.
- [11] A. Chira, O.-I. Covaci, et al., *Sci. Bull. B Chem. Mater. Sci. UPB* 74, (2012) 183-192.
- [12] C. A. Mandon, L. J. Blum, et al., *ChemPhysChem*, 10, (2009) 3273-3277.
- [13] S. Abdellaoui, B. C. Corgier, et al., *Electroanalysis*, 25, (2013) 671-684.
- [14] Q. Zou, L. L. Kegel, et al., *Anal. Chem.*, 87, (2015) 2488-2494.
- [15] B. P. Corgier, A. Laurent, et al., *Angew. Chem., Int. Ed. Engl.*, 46, (2007) 4108-4110.
- [16] K. L. Brogan, J. H. Shin, et al., *Langmuir*, 20, (2004) 9729-9735.
- [17] T.-C. Chang, C.-C. Wu, et al., *Anal. Chem.*, 85, (2013) 245-250.
- [18] T.-C. Chang, C.-C. Wu, et al., *Anal. Chem.*, 85, (2013) 10625-10625.

# CHAPTER III

FUNCTIONALIZATION OF SURFACES APPLIED TO DEPOLLUTION OF THE  
ENVIRONMENT



## 1. Introduction

Surface modifications are used to modify chemical, physical or biological properties of any materials to protect them from corrosion<sup>10</sup> or to improve their chemical resistance, biocompatibility, wettability, etc....<sup>180</sup>. In parallel, surface modification of materials is frequently used to develop sensors for environmental and medical applications<sup>9,181</sup>.

In last chapter, I demonstrate that it was possible to graft diazonium salts on gold slide surface for biological applications. Recently, some research works demonstrated that it is also possible to graft diazonium salts on polymeric surface<sup>17,57,54</sup>. However, we observed that it could be difficult to confirm a covalent grafting process on polymeric surfaces using ATR-IRTF spectroscopy. Some expensive techniques such as XPS spectroscopy may help us to evaluate the immobilization process but we do not have this equipment in the Normandy region. Massive are the challenges of functionalizing a surface. The characterization, especially, is even more difficult. In a few decades, numerous studies have been conducted in order to develop efficient tools for the analysis of surfaces.

In my institute, the team of Pr. C. Alfonso was equipped with a new Mass spectroscopy instrument which is hyphenated with ionic mobility and mass spectrometry (IM-MS). They recently demonstrated that this technique is suitable to analyze liquid polymer<sup>182,183</sup>. This equipment is highly sensitive, so maybe it could be used to characterize our grafted surface. The strategy used to validate this hypothesis, called ASAP-IM-MS, is summarized in the first following article, entitled "Atmospheric Solid Analysis Probe-Ion Mobility Mass Spectrometry: An Original Approach to Characterize Grafting on Cyclic Olefin Copolymer Surfaces". In order to validate the concept, the COC surface was modified covalently by different diazonium salts. Then, ASAP-IM-MS experiments highlighted specific ions according to the aryl layer grafted onto the COC surface. ASAP-IM-MS allow to work directly with COC sample without any further

preparation. Chemical datas obtained from ATR-IRTF and ASAP-IM-MS were compared depending on the nature of the aryl layer. In some cases, chemical grafting was difficult to evidence by IRTF spectroscopy while it was easily detected by ASAP-IM-MS. Moreover, this new technique appeared complementary information as compared to IRTF spectroscopy. Indeed, ASAP-IM-MS give some information on the structure of the grafting layer highlighting the multilayer shape of the aryl coating already described by Pinson et al<sup>55</sup>.

In parallel, I investigated if diazonium salts could be grafted on natural materials such as agrowastes. As we known, the use of modified natural materials is becoming a trend in modern civilization<sup>184</sup>, especially when it comes to environmental clean-up. Several technologies are available to remove contamination from environment such as precipitation, membrane separation, reverse osmosis<sup>185,186,187</sup>. These strategies are effectives, but they are expensive and difficult to transfer to a large scale. The use of agrowastes biomass (AWB) as adsorbents has been studied as cost effective and efficient alternative materials for removal of diverse types of pollutants from water and wastewaters<sup>188</sup>. Various AWB parts have been used including straws, shells, leaves, seeds, stalks and husks. Therefore, during my PhD studies, thinking about the possibility of reuse of these agrowastes, my team developed a partnership with the team of Pr E. Djoufac Woumfo, of the Yaoundé University 1 (Cameroun), which are experts in cocoa shell preparation.

The cocoa shell agrowaste is a lignocellulosic material which composes the outer portion of the cocoa bean produced in large scale without any reuse. The strategy is to modify the surface of this residue to add new chemical function to this natural material in order to valorize this product through environmental application.

In order to promote this product, I suggested developing two strategy to modify the surface of cocoa shell. One approach using diazonium salt and another using silylation. In the second

article, entitled “Chemical modification of the cocoa shell surface using diazonium salts”, we presented the grafting process and the characterization we used to demonstrate the covalent grafting of diazonium salt on cocoa shell. The grafting process is made in HCl solution and in presence of a chemical reducer. Thus, diazonium salts are chemically reduced in aryl radical which is able to graft spontaneously and covalently the cocoa shell surface. The surface characterization has been investigated mainly by ATR-IRTF spectroscopy, SEM imaging and its chemical resistance was also evaluated by causing a pH variation. All of the characterization confirmed the surface modification and the chemical resistance of the modified material.

In article 3, entitled "Cobalt nanoparticles embedded into polydimethylsiloxane-grafted cocoa shell: Functional material for CO<sub>2</sub> capture", we demonstrated that silylation and chemical post modification are suitable to transform this agrowaste in a CO<sub>2</sub> sorbent. We incorporated some metallic particles on cocoa shell to enhance the adsorption process. Each one of these functionalization stages has been characterized to see the providing modifications. It was the first time that the functionalization of the cocoa shell using APTES and PDMS with the insertion of cobalt nanoparticles was studied.

## 2. SCIENTIFIC PAPER I

Atmospheric Solid Analysis Probe-Ion Mobility Mass Spectrometry: An Original Approach to Characterize Grafting on Cyclic Olefin Copolymer Surfaces

# Atmospheric Solid Analysis Probe-Ion Mobility Mass Spectrometry: An Original Approach to Characterize Grafting on Cyclic Olefin Copolymer Surfaces

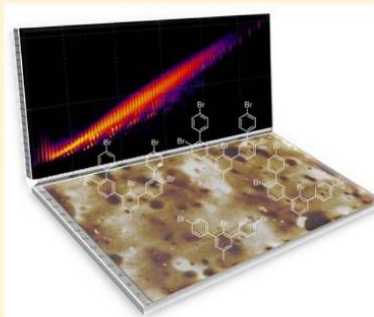
Julien Vieillard,<sup>\*,†</sup> Marie Hubert-Roux,<sup>†</sup> Florian Brisset,<sup>†</sup> Cecile Soullignac,<sup>†</sup> Flavia Fiorese,<sup>†</sup> Nadine Mofaddel,<sup>†</sup> Sandrine Morin-Grognon,<sup>‡</sup> Carlos Afonso,<sup>†</sup> and Franck Le Derf<sup>\*,†</sup>

<sup>†</sup>Normandie Université, COBRA, UMR6014 and FR3038, Université de Rouen, INSA de Rouen, CNRS, 55, rue Saint Germain, 27000 Evreux, France

<sup>‡</sup>Normandie Université, EA3829 MERCI, Université de Rouen, 1 rue du 7ème chasseurs, BP281, 27002 Evreux Cedex, France

## S Supporting Information

**ABSTRACT:** A cyclic olefin copolymer (COC) was grafted with aryl layers from aryl diazonium salts, and then we combined infrared spectrometry, atomic force microscopy (AFM), and ion mobility mass spectrometry with atmospheric solid analysis probe ionization (ASAP-IM-MS) to characterize the aryl layers. ASAP is a recent atmospheric ionization method dedicated to the direct analysis of solid samples. We demonstrated that ASAP-IM-MS is complementary to other techniques for characterizing bromine and sulfur derivatives of COC on surfaces. ASAP-IM-MS was useful for optimizing experimental grafting conditions and to elucidate hypotheses around aryl layer formation during the grafting process. Thus, ASAP-IM-MS is a good candidate tool to characterize covalent grafting on COC surfaces.



## INTRODUCTION

Thermoplastic polymers are suitable for packaging, optical, or biodevice applications.<sup>1–4</sup> Cyclic olefin copolymers (COCs) are of special interest because they are chemically resistant, transparent, and easy to prototype.<sup>5</sup> The chemical composition of a material's surface is important because it defines chemical or physical interactions of the surface with its environment. Depending on the application of the material, it is interesting to modulate the chemical composition of the outermost surface to improve its wettability or interfacial bond strength,<sup>3,6–10</sup> or to reduce unwanted molecular adsorption and biofouling.<sup>10–12</sup> Different strategies aimed at modifying COC properties have been developed. COCs have been coated with chromium, graphite, or organosilicon layers<sup>13,14</sup> to develop optoelectronic or microfluidic devices, respectively. These coatings are promising but they have to be processed in a clean room. Polymer solutions (cellulose derivate, polyacrylamide polymer, or triblock copolymer)<sup>8,15–17</sup> have been physisorbed onto COC surfaces to modulate adsorption, but such modifications were not stable. Covalent grafting is a good alternative to simple coating, yet in many cases, COCs have to be previously activated by ozone oxidation, UV light illumination, electron beam or plasma treatment.<sup>18–23</sup> Recently, we demonstrated that COC surfaces could be covalently grafted with aryl diazonium salt without any preliminary activation.<sup>24</sup>

To characterize COC surface modification, optical methods (fluorescence and Raman microscopy, ATR-FTIR spectroscopy),<sup>6,24</sup> scanning electronic microscopy (SEM),<sup>25,26</sup> X-ray

photoelectron spectroscopy (XPS),<sup>27,28</sup> and a cantilever-based method (AFM)<sup>19,26,29</sup> have been used. Other methods such as contact angle measurement<sup>10,25,27,28</sup> and differential scanning calorimetry (DSC)<sup>23</sup> have also been employed, but they were mainly dedicated to characterizing interactions between COC and its environment. Among these methods, only IR, Raman, and XPS spectroscopy provide information on the chemical composition of the surface. To complete this overview, it is important to note that Ooi et al. characterized a COC surface by <sup>13</sup>C NMR by dissolving the COC substrate in CDCl<sub>3</sub>.<sup>30</sup> To our knowledge, COC has never been characterized by mass spectrometry, although ToF-SIMS or MALDI-ToF-MS has been used to characterize surface modification on various plastics.<sup>31–37</sup>

To characterize the grafting of a COC surface by aryl diazonium salt reduction, we used mass spectrometry with a recent atmospheric ionization method dedicated to the direct analysis of solid samples, called atmospheric solid analysis probe (ASAP) and coupled to ion mobility-mass spectrometry (IM-MS). ASAP was introduced in 2005 by McEwen et al. for rapid analysis without sample preparation.<sup>38</sup> Solid or liquid samples are deposited onto a glass capillary. A heated gas flow of nitrogen thermally desorbs components, which are then ionized with a nitrogen plasma generated by a corona discharge.

Received: September 17, 2015

Revised: November 10, 2015

Published: November 10, 2015

Ion mobility is a post ionization separation method based on the drift of ions in a gas-filled tube under the influence of an electric field.<sup>39,40</sup> Drift time depends on ion charge and collision-cross section (CCS:  $\Omega$ ), which in turn depends on ion size and shape.

Our group recently investigated the application of ASAP-IM-MS to polymer analysis for polyolefin,<sup>41</sup> for blends of polyester and polyethylene<sup>42</sup> or for low-solubility poly(ether ether ketone).<sup>38,43</sup> ASAP yields mainly pyrolysis products except, for instance, for PEEK polymers due to their high thermal stability.

The present work focuses on the ASAP-IM-MS characterization of COC surfaces. A COC surface was modified using aryldiazonium salts, and grafting efficiency was demonstrated by ASAP-IM-MS and attenuated total reflection-FTIR (ATR-FTIR). Chemical data obtained from ATR-FTIR and ASAP-IM-MS were compared depending on the nature of the aryl layer. We thus demonstrated that ASAP-IM-MS is a good candidate tool to characterize thermoplastic surfaces such as COC. ASAP-IM-MS could also be used to characterize an organic layer on a polymeric surface and could be of interest in determining the optimal conditions of the grafting process.

## MATERIALS AND METHODS

**(1). Materials and Reagent.** COC plates (MCS-TOPAS-03) were purchased from Microfluidic Chip Shop, Jena, Germany, in 1 mm thick microscopy slide format cut into 1 × 2 cm plates. The plates were rinsed with acetone in an ultrasonic bath for 20 min and dried before use. Hypophosphorous acid, sodium nitrite, and all the chemicals were purchased from Sigma-Aldrich, Saint Quentin Fallavier (France).

**Synthesis of Aryldiazonium Salts.** 4-Bromobenzenediazonium tetrafluoroborate (BBD) was used in its commercial form. 4-Mercaptobenzenediazonium salt (MBD) and 4-carboxymethylbenzenediazonium salt (CBD) were synthesized from commercial aniline by diazotization as described by Khosroo et al.<sup>44</sup> Briefly, the corresponding para-aniline was dissolved in HBF<sub>4</sub>. The mixture was cooled to 0 °C in an ice water bath. Then sodium nitrite aqueous solution was slowly added. After 20 min, the mixture was cooled to -20 °C to precipitate aryldiazonium salts. Then, the slurry was filtered by suction, and washed with cold tetrafluoroboric acid and cold diethyl ether. Aryldiazonium tetrafluoroborate salts were kept at -20 °C.

**Synthesis of 4-(2-Bromoethyl) Aniline Hydrobromide.** 4-(2-Bromoethyl)aniline was not commercially available, so it was synthesized from 4-(2-hydroxyethyl)aniline by reaction with hydrobromic acid, as described by Liang et al.<sup>45</sup> Briefly, the reactant was dissolved in a 48%-aqueous solution of HBr and heated to reflux for 4 h. After cooling to room temperature, the mixture was kept at -20 °C overnight to precipitate. The slurry was filtered by suction, washed with cold diethyl ether, and then it was recrystallized with EtOH/H<sub>2</sub>O (4:1) and dried before characterization by NMR and MS. Then, the 4-(2-bromoethyl)benzenediazonium (BEBD) salt was synthesized and isolated following the same procedure as the MBD salts.

**Grafting of a COC Surface.** The grafting protocol of aryl diazonium salt on a COC surface is detailed elsewhere.<sup>24</sup> Briefly, COC plates were immersed in acidic aryldiazonium solution (0.1 M) with 10 mol equiv of chemical reducer (H<sub>3</sub>PO<sub>2</sub>) for 1 h. The reactor was kept under UV-visible irradiation throughout the grafting process. Then the surface was rinsed and cleaned by ultrasonic treatment on acetone and dried with nitrogen before characterization.

**(2). Characterization Methods. Infrared Spectroscopy (ATR-FTIR).** ATR-FTIR spectra were recorded with a Tensor 27 (Bruker) spectrometer with a ZnSe ATR crystal. For each spectrum, 20 scans were accumulated with a resolution of 4 cm<sup>-1</sup>. Background spectra were recorded on air before each analysis.

**Atomic Force Microscopy (AFM).** AFM mappings were performed using a PICOSPM (Molecular Imaging, Scientec) in contact mode equipped with silicon nitride cantilevers with a spring constant of 0.3

N/m. AFM imaging (20 × 20 μm<sup>2</sup>) was performed at room temperature in contact mode for each sample before and after chemical modification at a fixed scan rate of 1 line/s with a resolution of 512 × 512 pixels. Arithmetical mean roughness (Ra) was derived from AFM micrographs using SPIP (Scanning Probe Image Processor) software.

**ASAP-IM-MS.** Data acquisition was performed using a SYNAPT G2 HDMS fitted with an ASAP source (Waters Corp., Manchester, UK). This instrument is a hybrid quadrupole/time-of-flight mass spectrometer, which incorporates a traveling wave (T-Wave)-based mobility separation device. The instrument and the T-Wave device are detailed elsewhere.<sup>46</sup> The ASAP source probe was heated at 650 °C for at least 1 h before experiments. A piece of around 2 mm<sup>2</sup> was cut with a wire cutter, placed in a 1.5 mL glass bottle and heated at 350 °C with a sand bath. Then the ASAP capillary tube was dipped into the melted polymer, fixed to the ASAP probe holder, and introduced into the ionization source. For all experiments, ASAP mass spectra were acquired in positive ion mode in the *m/z* 50–1200 range. A blank was recorded for 1 min before introducing samples. A nitrogen flow of 1200 L·h<sup>-1</sup> heated at 650 °C was used for thermal desorption. The corona discharge voltage was 4 kV, and sampling cone voltage was 40 V. TWIM traveling wave height and velocity were set, at 40 V and 700 m·s<sup>-1</sup>, respectively. Helium cell gas flow was set at 180 mL·min<sup>-1</sup>, and IMS gas flow (N<sub>2</sub>) was set at 70 mL·min<sup>-1</sup> at a cell pressure of 3.0 mbar for IMS. For ASAP-MS/MS experiments, the precursor ions were selected with the quadrupole and were collisionally activated in the trap cell using argon as the target gas (flow 1.5 mL·min<sup>-1</sup>; collision energy 50 V). Data acquisition and mass spectrum treatment were provided by MassLynx (version 4.1). DriftScope (version 2.1) software was used for *m/z* versus drift-time map treatments.

## RESULTS AND DISCUSSION

**Characterization of a Pristine COC Surface by ASAP-IM-MS and IR Spectroscopy.** The COC polymers were prepared and analyzed with ASAP probe glass capillary. The drift time versus *m/z* plot obtained from the ASAP-IM-MS analysis of pristine cyclic olefin copolymer is presented in Figure 1a. Two ion series can be seen. The mass spectrum extracted from the main ion series ranging between *m/z* 150 and *m/z* 950 (Figure 1b) showed ions separated by 14 u

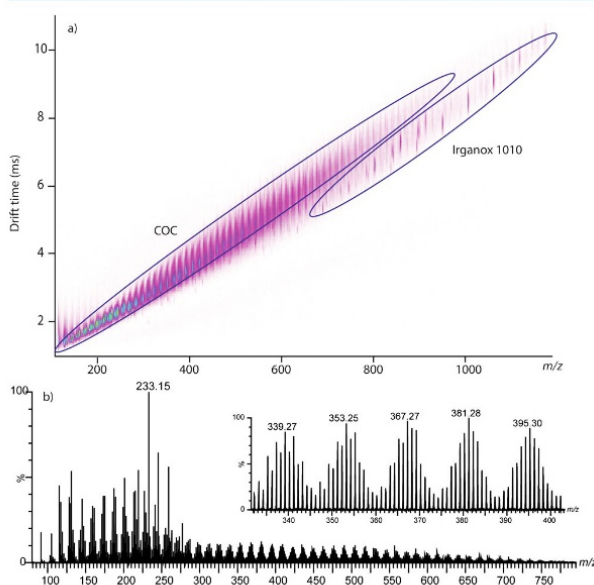


**Figure 1.** ASAP-IM-MS analysis on pristine COC. (a) Drift time vs *m/z* plot; (b) mass spectrum extracted from the COC area.

(CH<sub>2</sub>), that we attributed to pyrolysis products of polyolefin polymers.<sup>41,42</sup> The complexity of the ion distribution was likely due to the formation of different pyrolysis products with various numbers of unsaturation as shown by Lattimer with polyolefins.<sup>47</sup>

The ASAP spectrum of the second ion series (Figure S1) showed ions separated by 56 u (C<sub>4</sub>H<sub>8</sub>), characteristic of the *t*-butyl group. The *m/z* 1176.78 ion was attributed to the molecular ion (M<sup>+</sup>) of a polyphenolic antioxidant, Irganox 1010, and the lower *m/z* values corresponded to its fragment ions.<sup>41</sup> As previously shown,<sup>41</sup> this additive product was well separated from the polymer by ion mobility because of its compact structure.

#### Characterization of 4-Bromobenzenediazonium Grafting on COC Surface by IR-ATR and ASAP IM-MS.

Aryl layers were grafted from aryldiazonium salts containing a heteroatom such as a bromide derivate or thiol molecule. The bromobenzene (BBD) grafted layer exhibited a carbon-bromide bond absorbing at 735 cm<sup>-1</sup> (Figure 2).

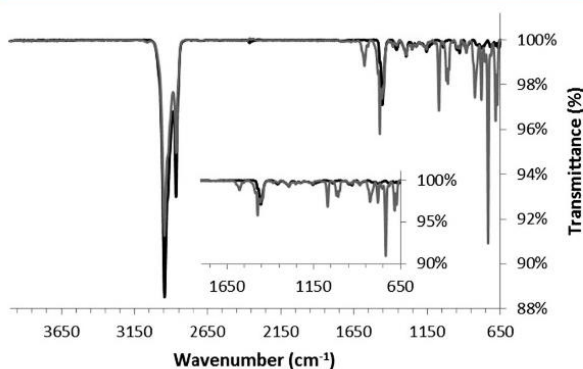


**Figure 2.** ATR-FTIR spectrum of a 4-bromobenzene grafted COC surface (black curve) and a pristine COC (gray curve). The insert focused on the 2000–650 cm<sup>-1</sup> region.

The ATR-FTIR spectrum of pristine COC displayed alkyl vibration at 2947 and 2868 cm<sup>-1</sup>. After grafting, the transmittance of these peaks decreased, demonstrating that the alkyl groups of the outstanding surface are not so easily reached by the IR evanescent wave. Moreover, new peaks at 1582 and 735 cm<sup>-1</sup> appeared corresponding to aryl ring vibration and C–Br stretch, respectively. As ATR-FTIR is a nondestructive method, the same plate was used for ASAP analysis.

The drift time versus *m/z* plot from the ASAP-IM-MS analysis of the COC sample grafted with bromobenzene diazonium salt is presented in Figure 3a, and the corresponding ASAP-MS spectrum in Figure 3b.

The spectrum of the main area between *m/z* 150 and *m/z* 950 (Figure 3b) presented several ions containing bromine atoms, as evidenced by their characteristic isotopic pattern. The *m/z* 309.90 ion was attributed to the molecular ion (M<sup>+</sup>) of dibromo-biphenyl (B<sub>2</sub>P<sub>2</sub>). In the same way, the *m/z* 463.84 ion and the *m/z* 617.78 ion were attributed to the molecular ions (M<sup>+</sup>) of tribromo-triphenyl (B<sub>3</sub>P<sub>3</sub>) and tetrabromo-tetraphenyl (B<sub>4</sub>P<sub>4</sub>), respectively. As regards the surface, bromine distribution may be explained by the growth of a multilayer on the COC surface. In the literature, it is well described that chemical grafting of diazonium salts generally results in multilayer profiles on polymeric surfaces.<sup>48,49</sup> Our ASAP-IM-

MS experiment suggests that up to four aryl layers were coated onto the COC surface after redox reaction. Figure 3 shows that more information on the film may be obtained with ASAP-IM-MS as compared to current literature on aryl film formation. The ions at *m/z* 539.87 and *m/z* 693.82 may be attributed to tribromo-tetraphenyl (B<sub>3</sub>P<sub>4</sub>) and tetrabromo-pentaphenyl (B<sub>4</sub>P<sub>5</sub>), respectively. Such ion series can be either degradation products formed during polymer pyrolysis, or fragment ions produced during ion transfer inside the mass spectrometer ion optics. We performed MS/MS experiments to verify this point. The ASAP-MS<sup>2</sup> spectrum of the *m/z* 617.78 ion (tetrabromo-tetraphenyl) is presented in Figure S2. The *m/z* 459.95 and 302.11 main product ions can be explained by the loss of one and two molecules of Br<sub>2</sub>, respectively. These product ions were not present in the ASAP mass spectrum. Conversely, other ions such as the *m/z* 539.87 ion were present in the mass spectrum but were not present in the MS/MS spectrum. Thus, the *m/z* 593.87 ion and the *m/z* 693.82 ion correspond to species produced in the ASAP source and related to the molecules grafted onto the surface of the polymer; they do not correspond to fragment ions produced in the gas phase through collision-induced dissociation processes.

In the third layer, the coating appeared as mixed, including phenyl rings substituted or not with bromine atoms. Such heterogeneity in the upper layer may have caused important surface roughness. This parameter was evaluated by atomic force microscopy.

**Analysis of the COC Surface by AFM.** Pristine COC and COC grafted by 4-bromobenzenediazonium salt were analyzed by AFM in contact mode. COC grafted by chemical reduction of 4-bromobenzenediazonium salt presented a different structure from pristine COC (Figure S3). The black holes observed in Figure S3b probably originated from some kind of multilayer heterogeneity or from traces left by a nitrogen bubble created during the chemical reduction process. Although this second hypothesis is plausible, it should be ruled out because these black holes were missing when other aryldiazonium salts were grafted on COC.<sup>24</sup> Mean roughness, Ra, and peak-to-peak values, Rz, analyses were evaluated on pristine COC and 4-bromobenzenediazonium-grafted COC (Figure S4). Ra and Rz values were higher in treated COC than in native COC. According to the peak-to-peak analysis, the black holes of the grafted COC had a maximum depth of 630 nm.

**Discrimination between the 4-Bromobenzene Layer and the 4-(2-Bromoethyl)benzene Layer on the COC Surface.** To immobilize proteins on COC through cysteine or methionine,<sup>50</sup> 4-(2-bromoethyl)benzene diazonium (BEBD) salt was synthesized from an aniline precursor and grafted onto a COC surface. As shown in the ATR-IR spectra (Figure S5), bromoethylbenzenediazonium-grafted COC presented low intensity IR peaks at 2947 and 2868 cm<sup>-1</sup> corresponding to molecular vibration as compared with pristine COC. A new peak at 735 cm<sup>-1</sup> corresponding to absorption by a C–Br bond was detected. However, the IR spectra from bromobenzene-diazonium-grafted COC (BBD) and 4-(2-bromoethyl)benzenediazonium-grafted COC (BEBD) were similar. So, this technique is not specific enough to discriminate between the two films, but to further investigate into the question, BEBD-grafted COC was evaluated by ASAP-IM-MS. The results are presented in Figure 4.

In the 2D ASAP-IM-MS plot obtained from the 4-(2-bromoethyl)benzenediazonium-grafted COC sample, the area

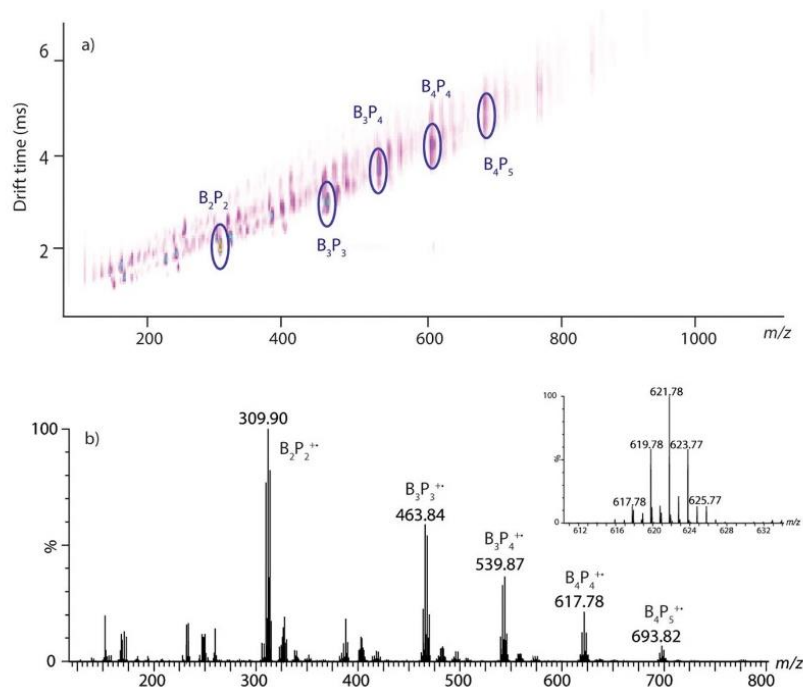


**Figure 3.** ASAP-IM-MS analysis of the COC grafted with 4-bromobenzenediazonium salt: Comparison between (a) the drift time versus  $m/z$  plot and (b) the mass spectrum extracted from bromobenzene area. (the  $m/z$  values indicated on the mass spectrum correspond to the monoisotopic peak and not to the most intense peak of the isotopic pattern).

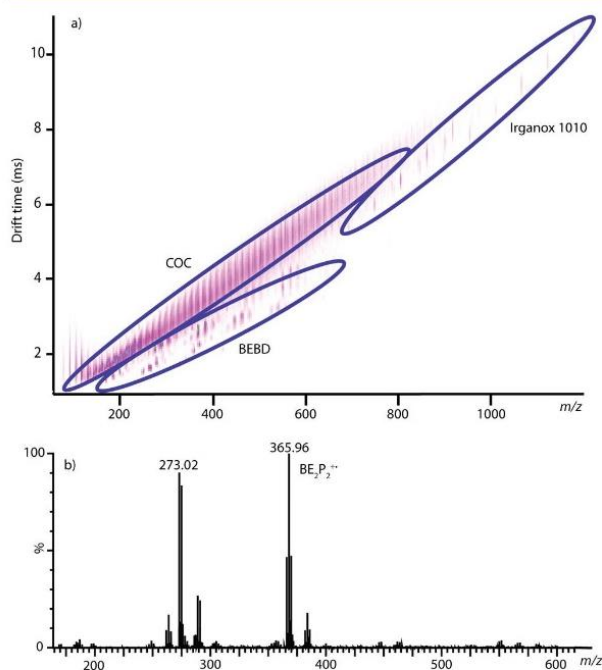


**Figure 4.** ASAP-IM-MS analysis of a 4-(2-bromoethyl)-benzenediazonium-grafted COC (BEBD) sample. (a) Drift time versus  $m/z$  plot, and (b) mass spectrum extracted from the BEBD area. (The  $m/z$  values indicated on the mass spectrum correspond to the monoisotopic peak and not to the most intense peak of the isotopic pattern).

corresponding to COC pyrolysis products is clearly visible (Figure 4a), whereas it is not visible in the plot from the 4-bromobenzenediazonium grafted COC (Figure 3). Nevertheless, characteristic signals related to grafted molecules were observed with lower drift time values. The extracted mass spectrum of this ion series is presented in Figure 4b.

The  $m/z$  365.96 ion is attributed to dibromoethyl-diphenyl ( $\text{BE}_2\text{P}_2$ ). The  $m/z$  273.02 ion was a fragment ion obtained from in-source decomposition of the  $m/z$  365.96 molecular ion, as shown by a tandem mass spectrometry experiment (data not shown). Its isotopic pattern indicated the presence of one bromine atom and probably came from the loss of a  $\bullet\text{CH}_2\text{Br}$  radical through a conventional  $\alpha$  cleavage (Figure S6). So, the successful grafting of BEBD on the COC surface was confirmed by ASAP-IM-MS. Peak attribution indicated that BEBD was grafted with a bilayer profile, whereas BBD was grafted with a four layer profile (Figure 3). Therefore, we assumed that the ethyl function hid the aryl group from the aryl radical limiting the multilayer shape. To confirm that the detected ions were related to grafted molecules, we analyzed 4-(2-bromoethyl)-benzenediazonium tetrafluoroborate powder by ASAP-IM-MS. The  $m/z$  365.96 and  $m/z$  273.02 ions identified in Figure 4 were missing when the diazonium salt was analyzed in the form of a powder or once melted (data not shown). Thus, these ions may be used as a fingerprint of the covalent grafting process. In the same way, an aryl radical was physically adsorbed onto the COC surface for 1 h, then the sample was analyzed by ASAP-IM-MS. The specific  $m/z$  365 and  $m/z$  273 ions of the BEBD-grafted layer were not recovered (data not shown). In a previous work, we indirectly demonstrated that light had to be added to the reaction to graft diazonium salt on COC.<sup>24</sup> Characterization by ATR-FTIR was not sufficient to demon-

strate this requirement unambiguously. So, we tried to graft the 4-(2-bromoethyl)benzenediazonium salt without any light, and then directly analyzed the sample by ASAP-IM-MS. As previously shown, the  $m/z$  365.96 ion corresponding to the dibromo-diphenyl product was not detected in the mass spectrum (data not shown). We thus directly confirmed that light is required to graft aryl radicals onto a COC surface.

To evaluate the versatility of ASAP-IM-MS to characterize the modified COC surface, we grafted various aryldiazonium salts. As ASAP probing occurs at atmospheric pressure, analysis of surfaces coated with oxygenated groups may be difficult. So, we grafted 4-carboxymethylbenzenediazonium salt (CBD) onto the COC surface and then characterized it by ATR-FTIR (Figure 5) and mass spectrometry.

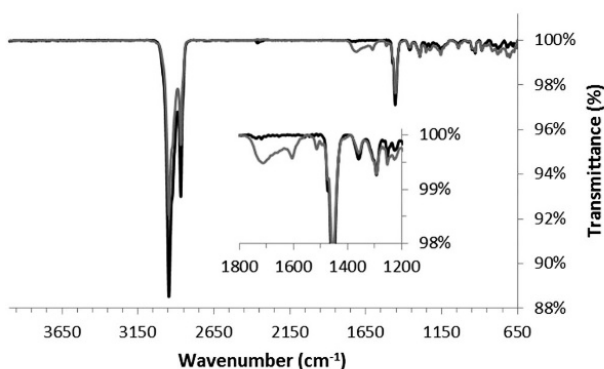


**Figure 5.** ATR-FTIR spectrum of native COC (black curve) and of a 4-carboxymethylbenzenediazonium-grafted COC surface salt (gray curve). The inset is focused on the 2000–650  $\text{cm}^{-1}$  region.

New peaks at 1715 and 1605  $\text{cm}^{-1}$  were detected, respectively associated with carbonyl groups and to aromatic rings. This indicates that COC was indeed covalently grafted by CBD. However, no specific ions were detected by mass spectrometry.

Biomolecules containing a sulfur group may be immobilized on surfaces by substitution using 4-(2-bromoethyl)benzenediazonium (BEBD) or by disulfide bonds using 4-mercaptobenzenediazonium salt (MBD). So, we grafted MBD onto the COC surface. The S–H and C–S stretches presented low intensity peaks in ATR-FTIR, so it was impossible to validate the grafting process through this technique (data not shown). However, mass spectrometry results were unambiguous (Figure 6).

The ASAP mass spectrum (Figure 6) presented several ions consistent with a multilayer shape. The  $m/z$  218.02 ion likely corresponded to the molecular ions of dithio-diphenyl ( $\text{T}_2\text{P}_2$ ) and the  $m/z$  326.03, 434.03, and 542.04 ions to trithio-

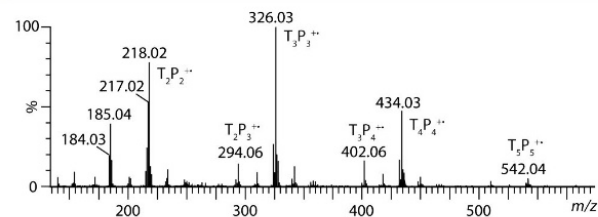


**Figure 6.** Mass spectrum extracted from the ASAP-IM-MS analysis of the 4-mercaptobenzenediazonium-grafted COC.

triphenyl ( $\text{T}_3\text{P}_3$ ); tetrathio-tetraphenyl ( $\text{T}_4\text{P}_4$ ), and pentathio-pentaphenyl ( $\text{T}_5\text{P}_5$ ), respectively. This result is consistent with a film generated on the COC surface with up to five layers of thickness. Ions were also detected in the mass spectrum at  $m/z$  294.06 and  $m/z$  402.06, they can be attributed to dithio-triphenyl ( $\text{T}_2\text{P}_3$ ) and trithio-tetraphenyl ( $\text{T}_3\text{P}_4$ ), respectively. These ions were presented in very low intensity in the MS/MS spectra of  $\text{T}_4\text{P}_4$  and  $\text{T}_5\text{P}_5$  precursor ions, as demonstrated by tandem mass spectrometry experiments (data not shown). Thus, these ions correspond most likely to molecules grafted in the surface of the polymer rather than fragment ions produced in the gas phase. Thus, 4-mercaptobenzenediazonium-grafted COC presented a multilayer profile comparable to 4-bromobenzenediazonium-grafted COC. These results suggest that the multilayer shape of the film was possible only when the heteroatom was directly linked to the phenyl ring.

## CONCLUSION

This Article provides an original approach to characterize surface grafting by mass spectrometry without sample preparation. As a proof of concept, COC surfaces were modified covalently by various diazonium salts. First, we demonstrated that ASAP-IM-MS is a good candidate tool to analyze COC surfaces. Then, ASAP-IM-MS experiments highlighted specific ions according to the aryl layer grafted onto the COC surface. Furthermore, functions such as carbon–sulfur and carbon–halogen, that are difficult to evidence by IR spectrometry, were easily detected by ASAP-IM-MS. So, ASAP-IM-MS is complementary to classical characterization techniques. We also characterized and identified different films by mass spectrometry according to the chemical group on the diazonium cation. Using ASAP-IM-MS, we validated that the lateral group in the para position on the phenyl ring influenced the film formation. When, a small lateral chain was on the phenyl ring, a multilayer film could grow, whereas longer lateral chains limited the multilayer growth. Therefore, ASAP-IM-MS makes it possible to analyze and characterize the nature and the growth profile of the diazonium film grafted onto a COC surface.

## ASSOCIATED CONTENT

### Supporting Information

The Supporting Information is available free of charge on the ACS Publications website at DOI: 10.1021/acs.langmuir.5b03494.

(S1) Mass spectrum of Irganox 1010; (S2) ASAP-MS<sup>2</sup> spectrum of the precursor ion at  $m/z$  617.78; (S3) AFM analysis of BBD-grafted COC; (S4) roughness and peak to peak analysis on BBD grafted COC; (S5) ATR-FTIR spectra of pristine and grafted COC; (S4) proposed mechanism for the formation of the ion at  $m/z$  273.02 (PDF)

## AUTHOR INFORMATION

### Corresponding Authors

\*E-mail: Julien.vieillard@univ-rouen.fr; phone number: (+33) 02.32.29.15.36.

\*E-mail: Franck.lederf@univ-rouen.fr; phone number: (+33) 02.32.29.15.05.

## Author Contributions

The manuscript was written through contributions of all authors. All authors have given approval to the final version of the manuscript.

## Notes

The authors declare no competing financial interest.

## ACKNOWLEDGMENTS

This work was partially supported by INSA Rouen, Rouen University, CNRS, Labex SynORG (ANR-11-LABX-0029) and the Haute Normandie Region (CRUNCH and Sésa networks) and Grand Evreux Agglomération.

## ABBREVIATIONS

CBD, 4-carboxymethylbenzene diazonium salt; BBD, 4-bromobenzene diazonium salt; BEBD, 4-(2-bromoethyl)-benzenediazonium diazonium salt; MBD, 4-mercaptobenzene diazonium salt; ASAP-IM-MS, atmospheric solid analysis probe ionization coupled with ion mobility-mass spectrometry; ATR, attenuated total reflectance; AFM, atomic force microscopy; MALDI, Matrix assisted laser desorption ionization; TOF-SIMS, Time-of-Flight Secondary Ion Mass Spectrometry

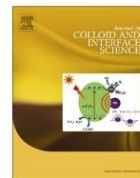
## REFERENCES

- (1) Shinoj, V. K.; Murukeshan, V. M.; Tor, S. B.; Loh, N. H.; Lye, S. W. Design, Fabrication, and Characterization of Thermoplastic Microlenses for Fiber-Optic Probe Imaging. *Appl. Opt.* **2014**, *53*, 1083–1088.
- (2) Sun, Y.; Perch-Nielsen, I.; Dufva, M.; Sabourin, D.; Bang, D. D.; Hogberg, J.; Wolff, A. Direct Immobilization of DNA Probes on Non-modified Plastics by UV Irradiation and Integration in Microfluidic Devices for Rapid Bioassay. *Anal. Bioanal. Chem.* **2012**, *402*, 741–748.
- (3) van Midwoud, P. M.; Janse, A.; Merema, M. T.; Groothuis, G. M.; Verpoorte, E. Comparison of Biocompatibility and Adsorption Properties of Different Plastics for Advanced Microfluidic Cell and Tissue Culture Models. *Anal. Chem.* **2012**, *84*, 3938–3944.
- (4) Kitsara, M.; Ducre, J. Integration of Functional Materials and Surface Modification for Polymeric Microfluidic Systems. *J. Micromech. Microeng.* **2013**, *23*, 033001.
- (5) Diaz-Quijada, G. A.; Peytavi, R.; Nantel, A.; Roy, E.; Bergeron, M. G.; Dumoulin, M. M.; Veres, T. Surface Modification of Thermoplastics—towards the Plastic Biochip for High Throughput Screening Devices. *Lab Chip* **2007**, *7*, 856–862.
- (6) Jena, R. K.; Yue, C. Y.; Anand, L. Improvement of Thermal Bond Strength and Surface Properties of Cyclic Olefin Copolymer (COC) based Microfluidic Device using the Photo-grafting Technique. *Sens. Actuators, B* **2011**, *157*, 518–526.
- (7) Cortese, B.; Mowlem, M. C.; Morgan, H. Characterisation of an Irreversible Bonding Process for COC-COC and COC-PDMS-COC Sandwich Structures and Application to Microvalves. *Sens. Actuators, B* **2011**, *160*, 1473–1480.
- (8) Perez-Toralla, K.; Champ, J.; Mohamadi, M. R.; Braun, O.; Malaquin, L.; Viovy, J. L.; Descroix, S. New Non-covalent Strategies for Stable Surface Treatment of Thermoplastic Chips. *Lab Chip* **2013**, *13*, 4409–18.
- (9) Nikolova, D.; Dayss, E.; Leps, G.; Wutzler, A. Surface Modification of Cycloolefinic Copolymers for Optimization of the Adhesion to Metals. *Surf. Interface Anal.* **2004**, *36*, 689–693.
- (10) Roy, S.; Yue, C. Y.; Lam, Y. C. Influence of Plasma Surface Treatment on Thermal Bonding and Flow Behavior in Cyclic Olefin Copolymer (COC) based Microfluidic Devices. *Vacuum* **2011**, *85*, 1102–1104.
- (11) Sung, D.; Park, J. W.; Jon, S. Facile Immobilization of Biomolecules onto Various Surfaces using Epoxide-containing Antifouling Polymers. *Langmuir* **2012**, *28*, 4507–4514.
- (12) Sung, D.; Yang, S.; Park, J. W.; Jon, S. High-Density Immobilization of Antibodies onto Nanobead-Coated Cyclic Olefin Copolymer Plastic Surfaces for Application as a Sensitive Immunoassay Chip. *Biomed. Microdevices* **2013**, *15*, 691–8.
- (13) Lee, J.-H.; Sang Kyung Kim, S. K.; Park, H.-H.; Kim, T. S. TiO<sub>2</sub> coated microfluidic devices for recoverable hydrophilic and hydrophobic patterns. *J. Micromech. Microeng.* **2015**, *25*, 035032.
- (14) Theelen, M.; Habets, D.; Staemmler, L.; Winands, H.; Bolt, P. Localised Plasma Deposition of Organosilicon Layers on Polymer Substrates. *Surf. Coat. Technol.* **2012**, *211*, 9–13.
- (15) Zhang, J.; Das, C.; Fan, Z. H. Dynamic Coating for Protein Separation in Cyclic Olefin Copolymer Microfluidic Devices. *Microfluid. Nanofluid.* **2008**, *5*, 327–335.
- (16) Sun, X.; Yang, W.; Geng, Y.; Woolley, A. T. A General Microchip Surface Modification Approach using a Spin-Coated Polymer Resist Film Doped with Hydroxypropyl cellulose. *Lab Chip* **2009**, *9*, 949–953.
- (17) Li, C.; Yang, Y.; Craighead, H. G.; Lee, K. H. Isoelectric Focusing in Cyclic Olefin Copolymer Microfluidic Channels Coated by Polyacrylamide using a UV Photografting Method. *Electrophoresis* **2005**, *26*, 1800–1806.
- (18) Sun, Y.; Perch-Nielsen, I.; Dufva, M.; Sabourin, D.; Bang, D. D.; Hogberg, J.; Wolff, A. Direct Immobilization of DNA Probes on Non-Modified Plastics by UV Irradiation and Integration in Microfluidic Devices for Rapid Bioassay. *Anal. Bioanal. Chem.* **2012**, *402*, 741–748.
- (19) Roy, S.; Das, T.; Yue, C. Y. High Performance of Cyclic Olefin Copolymer-Based Capillary Electrophoretic Chips. *ACS Appl. Mater. Interfaces* **2013**, *5*, 5683–5689.
- (20) Ladner, Y.; Bruchet, A.; Crétier, G.; Dugas, V.; Randon, J.; Faure, K. New “one-step” Method for the Simultaneous Synthesis and Anchoring of Organic Monolith inside COC Microchip Channels. *Lab Chip* **2012**, *12*, 1680–1685.
- (21) Stachowiak, T. B.; Rohr, T.; Hilder, E. F.; Peterson, D. S.; Yi, M.; Svec, F.; Fréchet, J. M. Fabrication of Porous Polymer Monoliths Covalently Attached to the Walls of Channels in Plastic Microdevices. *Electrophoresis* **2003**, *24*, 3689–2693.
- (22) Geissler, M.; Roy, E.; Diaz-Quijada, G. A.; Galas, J. C.; Veres, T. Microfluidic Patterning of Miniaturized DNA Arrays on Plastic Substrates. *ACS Appl. Mater. Interfaces* **2009**, *1*, 1387–1395.
- (23) Barakat, H.; Aymes-Chodur, C.; Saunier, J.; Yagoubi, N. Effect of Electron Beam Radio Sterilization on Cyclic Olefin Copolymers used as Pharmaceutical Storage Materials. *Radiat. Phys. Chem.* **2013**, *84*, 223–231.
- (24) Brisset, F.; Vieillard, J.; Berton, B.; Morin-Grognet, S.; Duclairoir-Poc, C.; Le Derf, F. Surface Functionalization of Cyclic Olefin Copolymer with Aryldiazonium Salts: a Covalent Grafting Method. *Appl. Surf. Sci.* **2015**, *329*, 337–346.
- (25) Roy, S.; Yue, C. Y.; Lam, Y. C.; Wang, Z. Y.; Hu, H. Surface Analysis, Hydrophilic Enhancement, Ageing Behavior and Flow in Plasma Modified Cyclic Olefin Copolymer (COC)-Based Microfluidic Devices. *Sens. Actuators, B* **2010**, *150*, 537–549.
- (26) Wang, D.-Y.; Chen, F.-K. Characterization of Hydrogen-Free Diamond-like Carbon Film Deposited on Cyclic Olefin Copolymer. *Diamond Relat. Mater.* **2008**, *17*, 822–825.
- (27) Jena, R. K.; Yue, C. Y. Cyclic Olefin Copolymer based Microfluidic Devices for Biochip Applications: Ultraviolet Surface Grafting using 2-Methacryloyloxyethyl Phosphorylcholine. *Biomicrofluidics* **2012**, *6*, 012822.
- (28) Hwang, S.-J.; Tseng, M.-C.; Shu, J.-R.; Yu, H. H. Surface Modification of Cyclic Olefin Copolymer Substrate by Oxygen Plasma Treatment. *Surf. Coat. Technol.* **2008**, *202*, 3669–3674.
- (29) Chen, R.; Ma, Y.; Zhao, C.; Lin, Z.; Zhu, X.; Zhang, L.; Yang, W. Construction of DNA Microarrays on Cyclic Olefin Copolymer Surfaces using Confined Photocatalytic Oxidation. *RSC Adv.* **2014**, *4*, 46653–46661.
- (30) Ooi, H. W.; Cooper, S. J.; Huang, C.-Y.; Jennins, D.; Chung, E.; Maeji, N. J.; Whittaker, A. K. Coordination Complexes as Molecular Glue for Immobilization of Antibodies on Cyclic Olefin Copolymer Surfaces. *Anal. Biochem.* **2014**, *456*, 6–13.

- (31) Galuska, A. A. Quantitative Surface Analysis of Ethylene–Propylene Polymers using ToF-SIMS. *Surf. Interface Anal.* **1997**, *25*, 1–4.
- (32) Wang, D.; Douma, M.; Swift, B.; Oleschuk, R. D.; Horton, J. H. The Adsorption of Globular Proteins onto a Fluorinated PDMS Surface. *J. Colloid Interface Sci.* **2009**, *331*, 90–97.
- (33) Wu, T.; Hu, H. L.; Du, Y. P.; Jiang, D.; Yu, B. H. Discrimination of Thermoplastic Polyesters by MALDI-TOF MS and Py-GC/MS. *Int. J. Polym. Anal. Charact.* **2014**, *19*, 441–452.
- (34) Groll, J.; Ademovic, Z.; Ameringer, T.; Klee, D.; Moeller, M. Comparison of Coatings from Reactive Star Shaped PEG-stat-PPG Prepolymers and Grafted Linear PEG for Biological and Medical Applications. *Biomacromolecules* **2005**, *6*, 956–962.
- (35) Wang, S.-F.; Li, X.; Agapov, R. L.; Wesdemiotis, C.; Foster, M. D. Probing Surface Concentration of Cyclic/Linear Blend Films Using Surface Layer MALDI-TOF Mass Spectrometry. *ACS Macro Lett.* **2012**, *1*, 1024–1027.
- (36) Zafeiropoulos, N. E.; Vickers, P. E.; Baillie, C. A.; Watts, J. F. An Experimental Investigation of Modified and Unmodified Flax Fibres with XPS, ToF-SIMS and ATR-FTIR. *J. Mater. Sci.* **2003**, *38*, 3903–3914.
- (37) Borysiak, M. D.; Bielawski, K. S.; Sniadecki, N. J.; Jenkel, C. F.; Vogt, B. D.; Posner, J. D. Simple Replica Micromolding of Biocompatible Styrenic Elastomers. *Lab Chip* **2013**, *13*, 2773–2784.
- (38) McEwen, C. N.; McKay, R. G.; Larsen, B. S. Analysis of Solids, Liquids, and Biological Tissues using Solids Probe Introduction at Atmospheric Pressure on Commercial LC/MS Instruments. *Anal. Chem.* **2005**, *77*, 7826–7831.
- (39) Hoskins, J. N.; Trimpin, S.; Grayson, S. M. Architectural Differentiation of Linear and Cyclic Polymeric Isomers by Ion Mobility Spectrometry-Mass Spectrometry. *Macromolecules* **2011**, *44*, 6915–6918.
- (40) Trimpin, S.; Clemmer, D. E. Ion Mobility Spectrometry/Mass Spectrometry Snapshots for Assessing the Molecular Compositions of Complex Polymeric Systems. *Anal. Chem.* **2008**, *80*, 9073–9083.
- (41) Barrère, C.; Maire, F.; Afonso, C.; Giusti, P. Atmospheric Solid Analysis Probe–Ion Mobility Mass Spectrometry of Polypropylene. *Anal. Chem.* **2012**, *84*, 9349–9354.
- (42) Barrère, C.; Selmi, W.; Hubert-Roux, M.; Coupin, T.; Assumani, B.; Afonso, C.; Giusti, P. Rapid Analysis of Polyester and Polyethylene Blends by Ion Mobility-Mass Spectrometry. *Polym. Chem.* **2014**, *5*, 3576–3582.
- (43) Cossoul, E.; Hubert-Roux, M.; Sebban, M.; Churlaud, F.; Oulyadi, H.; Afonso, C. Evaluation of Atmospheric Solid Analysis Probe Ionization Coupled to Ion Mobility Mass Spectrometry for Characterization of Poly(ether ether ketone) Polymers. *Anal. Chim. Acta* **2015**, *856*, 46–53.
- (44) Khoshroo, M.; Rostami, A. A. Characterization of the Organic Molecules Deposited at Gold Surface by the Electrochemical Reaction of Diazonium Salts. *J. Electroanal. Chem.* **2010**, *647*, 117–122.
- (45) Liang, Y.; Meinhardt, T.; Jarre, G.; Ozawa, M.; Vrdoljak, P.; Schöll, A.; Reinert, F.; Krueger, A. Deagglomeration and Surface Modification of Thermally Annealed Nanoscale Diamond. *J. Colloid Interface Sci.* **2011**, *354*, 23–30.
- (46) Giles, K.; Williams, J. P.; Campuzano, I. Enhancements in Travelling Wave Ion Mobility Resolution. *Rapid Commun. Mass Spectrom.* **2011**, *25*, 1559–1566.
- (47) Lattimer, R. P. Pyrolysis Field Ionization Mass Spectrometry of Polyolefins. *J. Anal. Appl. Pyrolysis* **1995**, *31*, 203–225.
- (48) Pinson, J. Attachment of Organic Layers to Materials Surfaces by Reduction of Diazonium Salts. In *Aryl Diazonium Salts: New Coupling Agents in Polymer and Surface Science*; Chehimi, M. M., Ed.; Wiley-VCH Verlag GmbH & Co. KGaA.: Weinheim, Germany, 2012.
- (49) Chehimi, M. M.; Lamouri, A.; Picot, M.; Pinson, J. Surface Modification of Polymers by Reduction of Diazonium Salts: Polymethylmethacrylate as an Example. *J. Mater. Chem. C* **2014**, *2*, 356–363.
- (50) Lundblad, R. L. *Chemical Reagents for Protein Modification*, 4th ed.; CRC Press: Boca Raton, FL, 2014; p 684.

### 3. SCIENTIFIC PAPER II

Chemical modification of the cocoa shell surface using diazonium salts



## Chemical modification of the cocoa shell surface using diazonium salts



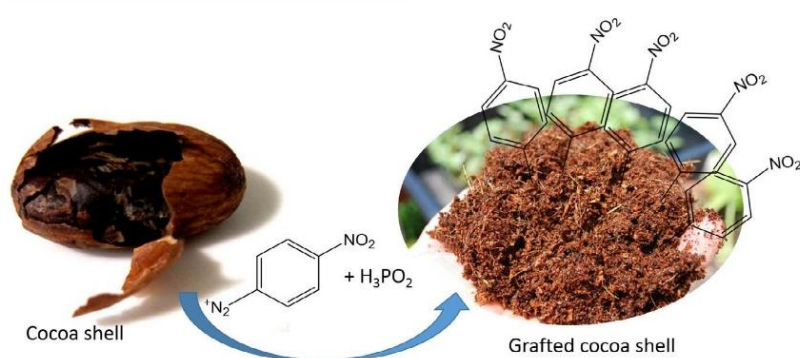
Flavia Fioresi<sup>a</sup>, Julien Vieillard<sup>a,\*</sup>, Radhouane Bargougui<sup>a</sup>, Nabil Bouazizi<sup>a</sup>, Patrick Nkuigwe Fotsing<sup>b</sup>, Emmanuel Djoufac Woumfo<sup>b</sup>, Nicolas Brun<sup>c</sup>, Nadine Mofaddel<sup>a</sup>, Franck Le Derf<sup>a</sup>

<sup>a</sup>Normandie Univ, UNIROUEN, INSA Rouen, CNRS, COBRA (UMR 6014), 76000 Rouen, France

<sup>b</sup>Laboratoire de Chimie Inorganique Appliquée, Département de Chimie Inorganique, Faculté des Sciences, Université de Yaoundé I, B.P. 812 Yaoundé, Cameroon

<sup>c</sup>Institut Charles Gerhardt de Montpellier, UMR 5253 CNRS-ENSCM-UM, Université de Montpellier, 34095 Montpellier, France

## GRAPHICAL ABSTRACT



## ARTICLE INFO

## Article history:

Received 30 November 2016

Revised 19 January 2017

Accepted 20 January 2017

Available online 22 January 2017

## Keywords:

Cocoa shell  
Cocoa husk  
Diazonium  
Grafting  
Lignin

## ABSTRACT

The outer portion of the cocoa bean, also known as cocoa husk or cocoa shell (CS), is an agrowaste material from the cocoa industry. Even though raw CS is used as food additive, garden mulch, and soil conditioner or even burnt for fuel, this biomass material has hardly ever been investigated for further modification. This article proposes a strategy of chemical modification of cocoa shell to add value to this natural material. The study investigates the grafting of aryl diazonium salt on cocoa shell. Different diazonium salts were grafted on the shell surface and characterized by infrared spectroscopy and scanning electronic microscopy imaging. Strategies were developed to demonstrate the spontaneous grafting of aryl diazonium salt on cocoa shell and to elucidate that lignin is mainly involved in immobilizing the phenyl layer.

© 2017 Elsevier Inc. All rights reserved.

**Abbreviations:** NBD, 4-nitrobenzene diazonium salt; BBD, 4-bromobenzene diazonium salt; CS, cocoa shell; NaOH-CS, cocoa shell treated with sodium hydroxide; NBD-CS, cocoa shell modified with 4-nitrobenzene diazonium salt; BBD-CS, cocoa shell modified with 4-bromobenzene diazonium salt; ATR-FTIR, attenuated total reflectance Fourier transformed infrared; SEM, scanning electronic microscopy; EDX, energy dispersive X-ray.

\* Corresponding author at: UMR CNRS 6014 COBRA, Université de Rouen Normandie, 55, rue saint germain, 27000 Evreux, France.

E-mail address: [julien.vieillard@univ-rouen.fr](mailto:julien.vieillard@univ-rouen.fr) (J. Vieillard).

<http://dx.doi.org/10.1016/j.jcis.2017.01.069>

0021-9797/© 2017 Elsevier Inc. All rights reserved.

## 1. Introduction

The cocoa industry generates a large amount of waste byproduct each year. The cocoa shell (CS), which is the nonfood part of the cocoa pod represent the main part of these waste materials that are devoid of any marketable value. Mainly employed as a raw biomass material (as food additive, garden mulch and soil

conditioner) or even burnt for fuel, few strategies have been also investigated to further modify and increase its value. One way consists in developing original composite biomaterials using the cocoa shell and a thermoplastic polymer such as polypropylene [1,2]. However, the poor interfacial compatibility is frequently a limit to produce good composites [3]. CS has also been investigated as a biosorbent for the removal of metal ions. Cadmium, zinc and lead ions have been successfully and quickly adsorbed onto cocoa shell [4–6]. Dye molecules are difficult to remove from industrial wastewater. Numerous methods are described in the literature, and adsorption on lignocellulosic material is one of the finest techniques [7]. In general, CS has to be modified to become an interesting adsorbent. For example, Pua et al. treated cocoa husk with sodium hydroxide to modify its porosity and surface roughness, resulting in a good adsorption capacity [8]. Following the example of coconut shells and other agrowastes, both physical and chemical activations to generate CS-derived activated carbons have been the most commonly used post-treatments to prepare efficient adsorbents for dye removal. Different dyes (methylene blue, crystal violet...) have been successfully adsorbed onto activated cocoa shell [9–13]. In some cases, some post-carbonization treatments are required to complete the activation process. For example, CO<sub>2</sub> increases porosity [14,15] whereas HCl [16] or KOH [17] impregnation modulate the chemical composition of the activated carbon. All of these strategies are efficient but the treatment is rather harsh and costly and the selectivity is limited. In this publication, we suggest another simple modification based on diazonium chemistry. Aryl diazonium salts are bifunctional compounds frequently used to modify the surface properties of different materials [18]. They are easy to prepare, and a wide range of reactive functional groups can be synthesized from aniline derivatives or nitro precursors. Electroreduction or chemical reduction of aryl diazonium generate an aryl radical that bonds to the surface. Although, aryl diazonium salts are frequently used to modify metallic surfaces, some polymeric surfaces have also been covalently grafted [19–22]. The present work focuses on grafting a phenyl diazonium salt on CS, and characterizing its morphology, chemical composition and porosity. We thus demonstrate that grafting a diazonium salt is a convenient method to selectively modulate the chemical properties of cocoa shell.

## 2. Material and methods

**Chemicals:** All the chemicals were purchased from Sigma Aldrich. All the solutions were prepared from double distilled water (Millipore).

**Materials preparation: Cocoa shell conditioning:** The cocoa shells were collected from a local farm managed by the IRAD (Institut de recherche Agricole pour le Développement) at Yaoundé, Cameroon. The shells were cut, washed with acidic water (HCl, 1 M) to remove the organic impurity, sun-dried for 5 days, and then heated at 70 °C overnight to remove moisture. The latter, they were ground and sifted at 160 μm. The diazonium grafting process was carried according to a procedure described elsewhere [23]. Briefly, 4-nitrobenzenediazonium (NBD) and 4-bromobenzene diazonium (BBD) salts were dissolved in acidic solution, and then stirred with hypophosphorous acid (H<sub>3</sub>PO<sub>2</sub>) (90:10 v/v) for 1 h. The products (NBD-CS) or (BBD-CS) were filtered and washed with acetone and double distilled water and then dried at 50 °C for 2 h.

**Material characterizations:** Infrared spectroscopy (ATR-FTIR): ATR-FTIR spectra were recorded using a Tensor 27 (Bruker) spectrometer with a ZnSe ATR crystal. For each spectrum, 20 scans were accumulated with a resolution of 4 cm<sup>-1</sup>. Cocoa shell samples were drilled before IR analysis and background spectra were recorded on air. The scanning electron microscopy (SEM) images

were acquired with a ZEISS EVO 15 electron microscope coupled to an EDX detector for X-ray energy dispersion analysis. CS were metallized by a gold layer at 18 mA for 360 s using a Biorad E5200 device.

## 3. Results and discussion

To modify a non-conductive material such as CS, diazonium salts have to be chemically reduced to obtain an aryl radical. Therefore, cocoa shell was incubated with hypophosphorous acid and NBD or BBD for one hour. When the experiment began the cocoa shell powder rests on the bottom of the beaker. Herein, a few gas bubbles were generated corresponding to N<sub>2</sub> elimination. As sub-product kept forming, the color of the solution turned from transparent to yellow-orange (Fig. S1).

Also, the cocoa shell powder moved from the bottom of the beaker up to the liquid surface during the reaction, corresponding to morphological modifications at the cocoa shell surface. In parallel, no modification was observed when cocoa shell was incubated with HCl and H<sub>3</sub>PO<sub>2</sub>. The above results are confirmed by ATR-FTIR spectroscopy, which provides significant details about the presence of all characteristics band assigning to the CS and NBD group (Fig. 1).

To facilitate the FTIR analysis, the IR bands observed in Fig. 1 are listed in Fig. S2. As expected, the cocoa shell exhibits distinguishable peak patterns which are in good agreement with literature [8]. The bands observed at 1334 and 1517 cm<sup>-1</sup> were attributed to nitro groups attached on the CS surface. Further cleaning by distilled water did not modify the infrared spectra confirming the durable grafting of nitrophenyl layer. Furthermore, the NBD grafting were evaluated by ultrasonic treatment in distilled water and in acetone. As result, no modification was observed on infrared spectroscopy. Chemical resistance was also evaluated by causing the pH to vary from 2 to 9, no modification was observed either.

Fig. 2 showed the SEM images of natural and modified CS. It can be seen that CS is an amorphous material with a smooth porous structure (Fig. 2a). Some components such as polysaccharides, hemicellulose, and lignin are present on its surface. After grafting of NBD, the surface morphology of NBD-CS is strongly modified compared with the natural CS (Fig. 2b and c). Fig. 2d confirmed that acidic solution had no effect on cocoa shell.

As seen, the CS-NBD surface was covered by some films, which suggested that the NBD was grafted into the lattice of the CS and a covalent bond may be formed between NBD and CS. In addition, the chemical grafting provided small cell cavities in the micrograph, producing a developed porosity by activation agent. It is important to note that the whole cocoa shell surface seemed to

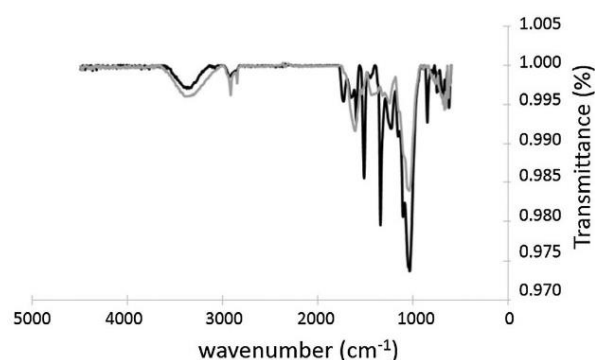
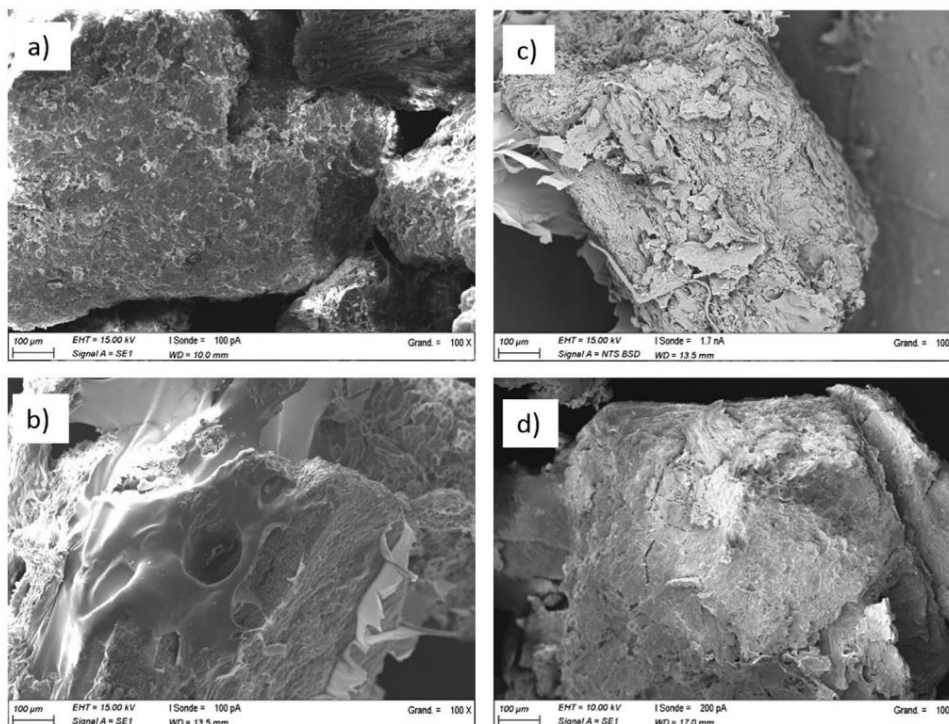


Fig. 1. ATR-FTIR spectra of natural (gray curve) and 4-nitrophenyl-modified cocoa shell (black curve).



**Fig. 2.** SEM images of (a) natural cocoa shell, (b) a thick layer of 4-nitrobenzene film, (c) a foliated layer of the 4-nitrobenzene film, (d) natural cocoa shell treated with acidic solution.

be covered by the phenyl layer, illustrating many bonds between the aryl radicals and the surface. In some areas, SEM images showed a polymeric film spread over the surface that fitted to the large pore of the surface. In other areas, diazonium grafting had a foliated structure expected to increase the roughness of the surface and the specific surface of the CS. Both films were visible for different samples of NBD-CS. The surface heterogeneity probably resulted from different thickness of grafted phenyl layers [19].

It is known that aryldiazonium salts are versatile, as numerous substituent can be synthesized on the phenyl group. Fig. 3 shows the ATR-FTIR spectra and the EDX imaging of CS modified by bromide aryl layer (Fig. 3).

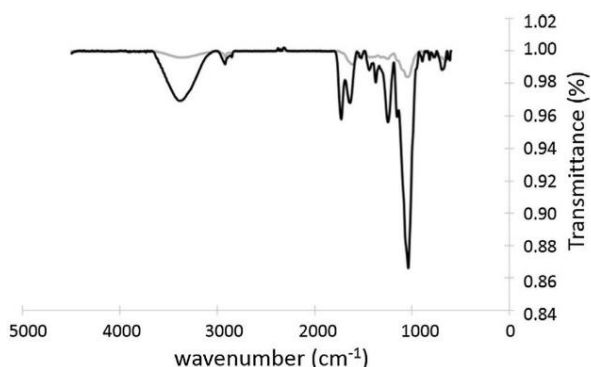


**Fig. 3.** ATR-FTIR analysis of natural cocoa shell (gray curve) and 4-bromobenzene-grafted cocoa shell (black curve).

According to Vieillard et al., the peaks observed at 1582 and 735 cm<sup>-1</sup> is attributed to aryl rings and C-Br stretches respectively [24]. As the peak at 1582 cm<sup>-1</sup> was already present on natural cocoa shell, it was not suitable for identification. The peak at 735 cm<sup>-1</sup> corresponding to C-Br is clearly visible in Fig. 3; its intensity was not modified by ultrasonic cleaning, demonstrating the grafting process. To confirm bromide immobilization on the surface, BBD-CS was characterized by EDX analysis hyphenated with SEM imaging (Fig. 4).

EDX analysis yielded a strong peak at 2.12 keV corresponding to Au atoms resulting from the metallization process. The strong peaks at 0.277 and 0.525 keV probably corresponded to carbon and oxygen atoms from cellulose and lignin. The peak at 1.48 keV corresponded to Br atoms, whereas the peak at 2.4 and 1.74 keV probably corresponded to sulfur and silicon traces, respectively. Elemental (Br) mapping on the grafted cocoa shell (Fig. 4) illustrated the distribution of the 4-bromophenyl film over the surface. Natural cocoa shell was also evaluated; no signal was recorded for Br atoms.

The thickness of the grafted diazonium layer can be controlled by changing the reaction time, the concentration of the reducing agent and the diazonium salt concentration. We modulated the reducing agent concentration from 0 to 9 M equivalent. NBD and CS were incubated in acidic media for 1 h, filtered, dried and then analyzed by ATR-FTIR. During these analyses, the intensity of the NBD peak decrease as a function of the decrease in H<sub>3</sub>PO<sub>2</sub> concentration. However, we also observed weak NBD peaks in the absence of chemical reducer (Fig. 5).

The first part of the article provides observations about the chemical reaction *per se*. The dinitrogen gas bubbles, the movement of the cocoa shell from the bottom to the top of the solution and the change in color also occurred in the absence of

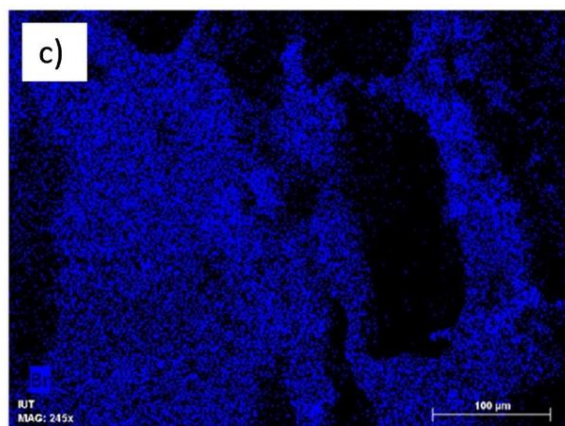
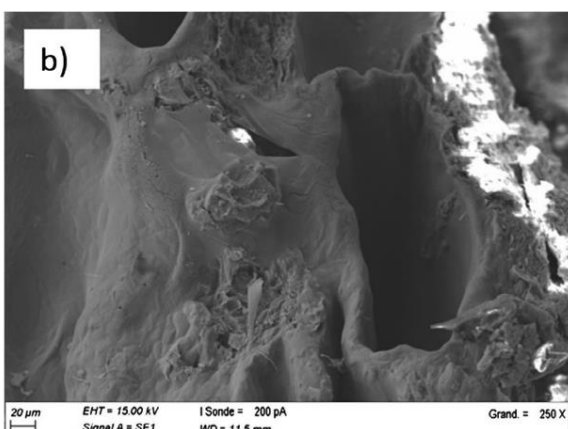
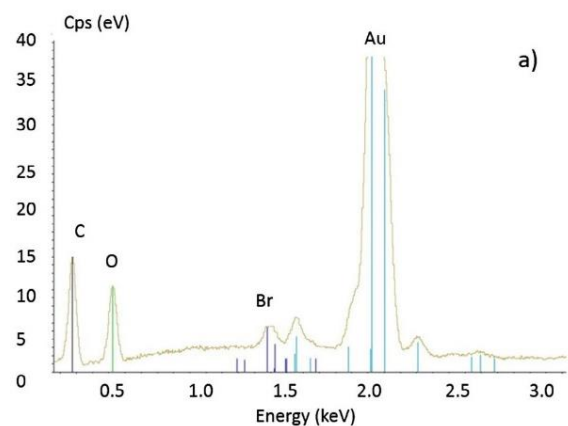


**Fig. 4.** (a) EDX analysis and (b) SEM image of 4-bromobenzene grafted cocoa shell (BBD-CS). (c) Elemental mapping of BBD-CS.

the chemical reducer but the time-course of the reaction differed. When NBD was incubated with a reducing agent, a few minutes were sufficient to produce a visual effect in the solution, whereas more than 30 min were required in the absence of  $H_3PO_2$ . We can hypothesize that 4-nitrobenzenediazonium is simply adsorbed on cocoa shell, but the absence of the stretching  $N_2^+$  mode near  $2280\text{ cm}^{-1}$  invalidates this hypothesis and validates the grafting on CS. Further washing steps failed to eliminate the nitrophenyl layer. We also incubated diazonium salt alone or with

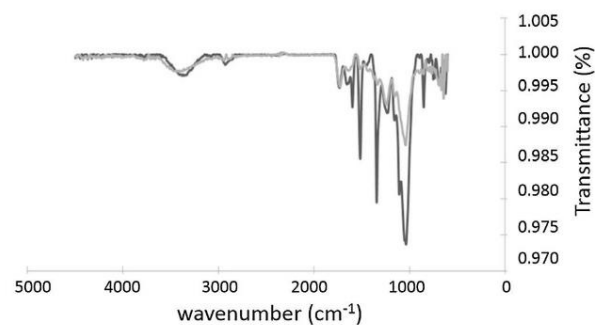


**Fig. 5.** ATR-FTIR analysis of NBD-CS in the presence (black curve) or in the absence (gray curve) of a chemical reducer.

another polymer (a cyclic olefin copolymer surface) and no redox reduction appeared, the stretching  $N_2^+$  mode near  $2280\text{ cm}^{-1}$  being still present in the IR spectra. Such spontaneous processes have been described in literature where diazonium ions are decomposed in acidic media in the presence of a material surface with nucleophilic moieties such as black carbon or metallic surfaces [25–29], or natural fiber [30–33]. Therefore we confirmed that this process may also occur with cocoa shell.

Previous articles detailed the grafting process of diazonium molecules either on cellulose [31,34,35] or lignin [36]. In this study, we employed raw lignocellulosic biomass, *i.e.* cocoa shell, which contains 211 g/kg of lignin, 127 g/kg of hemicellulose and 261 g/kg of cellulose [37]. One may assume that NBD reacted both with the cellulose and the lignin components of CS. To elucidate this hypothesis, CS was treated with alkaline solution to remove the lignin counterpart [8]. SEM images of sodium hydroxide treated cocoa shell (NaOH-CS) sample exhibited a large amount of characteristic fibers of cellulose (Fig. 6a).

These observations were confirmed by ATR-FTIR spectroscopy: the peaks at  $1612$  and  $1232\text{ cm}^{-1}$  corresponding to lignin were

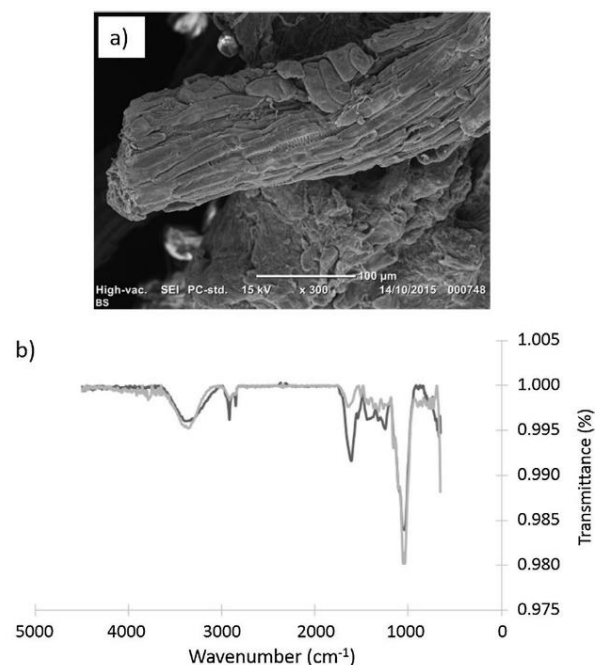


**Fig. 6.** SEM image (a) and ATR-FTIR spectra (b) of cocoa shell treated by sodium hydroxide (NaOH-CS) (gray curve) vs natural cocoa shell (black curve).

significantly less intense (Fig. 6b). After alkaline treatment, the NaOH-CS sample was incubated with NBD as described in the experimental part and analyzed by IR spectroscopy and SEM imaging. Surprisingly, neither FTIR nor SEM could evidence the presence of nitrophenyl layers after lignin removal. This feature strongly suggests the selective grafting of NBD on the lignin component of cocoa shell. Few recent works demonstrated that phenyl diazonium salts could interact with kraft lignin via electrophilic substitution under alkaline conditions, yielding covalent bonds through azo groups [36,38,39]. In our case, we worked in the presence of a chemical reducer at acidic pH. Such conditions should trigger the formation of covalent bonds through the reduction of *in-situ* generated aryl radicals, as demonstrated in literature with carbon surfaces. In our case, one may consider that aryl radicals from diazonium salts could interact with the aromatic rings of the lignin moieties through a similar mechanism. The absence of azo groups suggested by FTIR and EDX analyses (absence of nitrogen atoms) together with the observation of gas bubbles during chemical modification (corresponding to the elimination of N<sub>2</sub>) support such mechanism. Following a similar experimental procedure, the covalent grafting of NBD could be also demonstrated on kraft lignin, supporting our hypothesis. To the best of our knowledge, we showed the first proof of the radical grafting of diazonium salts on the lignin moiety of raw natural materials, providing a new chemical “tool” for the modification of lignin-based materials [40].

#### 4. Conclusion

In this article, we demonstrated the efficient grafting of two different diazonium salts on the surface of a raw agrowaste material, *i.e.* cocoa shells, and its characterization by SEM-EDX and ATR-FTIR analyses. The grafting process is fast, easy to implement and versatile. Moreover, the process was shown to be chemically and mechanically resistant, allowing harsh experimental conditions. It may be triggered by a chemical reducer but also spontaneously, which could be suitable for a low-cost and clean industrial process. Modified cocoa shell may therefore be used as a low-cost adsorbent to entrap pollutants such as heavy metal ions, gases or industrial dye. The versatility of the diazonium salts approach and the variety of potential functional groups might also open perspectives in catalysis [41], electrochemistry [42] and for the synthesis of heteroatom-doped carbons for electrocatalysis [43]. Thus, Palacin et al. reported on the use of 4-nitrobenzenediazonium salts as initiators for the radical polymerization of vinylic monomers from various substrates [27,44]. This Graffast process could be applied to covalently graft polymer films from cocoa shell. Moreover, nitro functional groups could be reduced into amine for the subsequent immobilization of proteins. More recently, nitration of lignin was employed to prepare nitrogen-doped carbons with excellent electrocatalytic activity towards oxygen reduction reaction [43]. Nitrobenzene grafting may also enhance supercapacitor activity [45]. To reach these objectives, we currently intend to convert cocoa shell modified with 4-nitrobenzenediazonium into nitrogen-doped porous carbons. Last but not least, we showed some evidence of the selectivity towards lignin of our grafting process. We are currently conducting additional experiments and characterizations to further support this hypothesis. Further developments of this process are expected to functionalize other biomass materials and even extracted/purified lignin.

#### Author contributions

The manuscript was written through contributions of all authors. All authors have given approval to the final version of the manuscript.

#### Acknowledgment

This work was partially supported by INSA Rouen, Normandy Rouen University, CNRS, Labex SynORg (ANR-11-LABX-0029), the European eramus mundus program EBW+ and Battuta, the French Embassy in Cameroon (879327A), the Haute Normandie Region (CRUNCH and Sésa networks) and Grand Evreux Agglomération.

#### Appendix A. Supplementary material

S1. The color of the solution turned during the grafting experiment; S2. Table to identify IR bands present in Fig. 1. The following files are available free of charge. Supplementary data associated with this article can be found, in the online version, at <http://dx.doi.org/10.1016/j.jcis.2017.01.069>.

#### References

- [1] K. Chun, S. Husseinsyah, H. Osman, Preliminary study of palm oil based coupling agent for polypropylene/cocoa pod husk composites, *Adv. Environ. Biol.* 8 (2014) 2640–2644.
- [2] K.S. Chun, S. Husseinsyah, H. Osman, Utilization of cocoa pod husk as filler in polypropylene biocomposites: effect of maleated polypropylene, *J. Thermoplast. Compos. Mater.* 28 (11) (2015) 1507–1521.
- [3] K.S. Chun, S. Husseinsyah, Agrowaste-based composites from cocoa pod husk and polypropylene: effect of filler content and chemical treatment, *J. Thermoplast. Compos. Mater.* 29 (2016) 1332–1351.
- [4] V.O. Njoku, Biosorption potential of cocoa pod husk for the removal of Zn(II) from aqueous phase, *J. Environ. Chem. Eng.* 2 (2) (2014) 881–887.
- [5] V.O. Njoku, A.A. Ayuk, E.E. Oguzie, E.N. Ejike, Biosorption of Cd(II) from aqueous solution by cocoa pod husk biomass: equilibrium, kinetic, and thermodynamic studies, *Separat. Sci. Technol.* 47 (5) (2012) 753–761.
- [6] B.I. Olu-owolabi, O.U. Oputu, K.O. Adebawale, O. Ogunsolu, O.O. Olujimi, Biosorption of Cd<sup>2+</sup> and Pb<sup>2+</sup> ions onto mango stone and cocoa pod waste: kinetic and equilibrium studies, *Sci. Res. Essays* 7 (15) (2012) 1614–1629.
- [7] S. Rangabhashiyam, N. Anu, N. Selvaraju, Sequestration of dye from textile industry wastewater using agricultural waste products as adsorbents, *J. Environ. Chem. Eng.* 1 (4) (2013) 629–641.
- [8] F.I. Pua, M.S. Sajab, C.H. Chia, S. Zakaria, I.A. Rahman, M.S. Salit, Alkaline-treated cocoa pod husk as adsorbent for removing methylene blue from aqueous solutions, *J. Environ. Chem. Eng.* 1 (3) (2013) 460–465.
- [9] S. Mylsamy, C. Theivarasu, N. Sivakumar, Activated carbon from cocoa (*Theobroma cacao*) shell, an agricultural waste, for the removal of Reactive Red 120 dye by the process of adsorption, *Int. J. Green Herbal Chem.* 2 (2013) 316–323.
- [10] C. Theivarasu, S. Mylsamy, Removal of malachite green from aqueous solution by activated carbon developed from cocoa (*Theobroma Cacao*) shell – a kinetic and equilibrium studies, *E-J. Chem.* 8 (2011) S363–S371.
- [11] C. Theivarasu, S. Mylsamy, Adsorption studies of acid blue-92 from aqueous solution by activated carbon obtained from agricultural industrial waste-cocoa (*Theobroma cacao*) shell, *Asian J. Chem.* 24 (2012) 2187–2190.
- [12] C. Theivarasu, S. Mylsamy, S. N., Adsorptive Removal of Crystal Violet Dye Using Agricultural Waste Cocoa (*Theobroma cacao*) Shell, *Research Journal of Chemical Sciences* 1 (2011) 38–45.
- [13] C. Theivarasu, M. Mylsamy, N. Sivakumar, Cocoa shell as adsorbent for the removal of methylene blue from aqueous solution: kinetic and equilibrium study, *Univ. J. Environ. Res. Technol.* 1 (2011) 70–78.
- [14] F. Ahmad, W.M.A.W. Daud, M.A. Ahmad, R. Radzi, A.A. Azmi, The effects of CO<sub>2</sub> activation, on porosity and surface functional groups of cocoa (*Theobroma cacao*) – shell based activated carbon, *J. Environ. Chem. Eng.* 1 (3) (2013) 378–388.
- [15] O.S. Bello, T.T. Siang, M.A. Ahmad, Adsorption of Remazol Brilliant Violet-5R reactive dye from aqueous solution by cocoa pod husk-based activated carbon: kinetic, equilibrium and thermodynamic studies, *Asia-Pac. J. Chem. Eng.* 7 (3) (2012) 378–388.
- [16] M.C. Ribas, M.A. Adebayo, L.D.T. Prola, E.C. Lima, R. Cataluña, L.A. Feris, M.J. Puchana-Rosero, F.M. Machado, F.A. Pavan, T. Calvete, Comparison of a homemade cocoa shell activated carbon with commercial activated carbon for the removal of reactive violet 5 dye from aqueous solutions, *Chem. Eng. J.* 248 (2014) 315–326.
- [17] A.M. Obuge, O.B. Ebuomwan, Adsorption of methylene blue onto activated carbon impregnated with KOH using cocoa shell, *Int. J. Eng. Tech. Res.* 2 (10) (2014) 11–18.
- [18] J. Pinson, F. Podvorica, Attachment of organic layers to conductive or semiconductive surfaces by reduction of diazonium salts, *Chem. Soc. Rev.* 34 (5) (2005) 429–439.
- [19] F. Brisset, J. Vieillard, B. Berton, S. Morin-Grognet, C. Duclairioir-Poc, F.L. Derf, Surface functionalization of cyclic olefin copolymer with aryldiazonium salts: a covalent grafting method, *Appl. Surf. Sci.* 329 (2015) 337–346.

- [20] S. Gam-Derouich, S. Mahouche-Chergui, M. Turmine, J.-Y. Piquemal, D.B. Hassen-Chehimi, M. Omastová, M.M. Chehimi, A versatile route for surface modification of carbon, metals and semi-conductors by diazonium salt-initiated photopolymerization, *Surf. Sci.* 605 (21–22) (2011) 1889–1899.
- [21] Z. Salmi, S. Sarra Gam-Derouich, S. Mahouche-Chergui, M. Turmine, M. Chehimi, On the interfacial chemistry of aryl diazonium compounds in polymer science, *Chem. Pap.* 66 (2012) 369–391.
- [22] M.M. Chehimi (Ed.), *Aryl Diazonium Salts: New Coupling Agents and Surface Science*, Wiley-VCH, 2012. pp. 335, ISBN Number: 978-3-527-32998-4.
- [23] M.M. Chehimi, A. Lamouri, M. Picot, J. Pinson, Surface modification of polymers by reduction of diazonium salts: polymethylmethacrylate as an example, *J. Mater. Chem. C* 2 (2014) 356–363.
- [24] J. Vieillard, M. Hubert-Roux, F. Brisset, C. Soullignac, F. Fiorese, N. Mofaddel, S. Morin-Grognet, C. Afonso, F. Le Derf, Atmospheric solid analysis probe-ion mobility mass spectrometry: an original approach to characterize grafting on cyclic olefin copolymer surfaces, *Langmuir* 31 (48) (2015) 13138–13144.
- [25] A. Adenier, N. Barré, E. Cabet-Deliry, A. Chaussé, S. Griveau, F. Mercier, J. Pinson, C. Vautrin-UI, Study of the spontaneous formation of organic layers on carbon and metal surfaces from diazonium salts, *Surf. Sci.* 600 (21) (2006) 4801–4812.
- [26] A. Adenier, E. Cabet-Deliry, A. Chaussé, S. Griveau, F. Mercier, J. Pinson, C. Vautrin-UI, Grafting of nitrophenyl groups on carbon and metallic surfaces without electrochemical induction, *Chem. Mater.* 17 (3) (2005) 491–501.
- [27] C. Combellas, M. Delamar, F. Kanoufi, J. Pinson, F.I. Podvorica, Spontaneous grafting of iron surfaces by reduction of aryldiazonium salts in acidic or neutral aqueous solution, application to the protection of iron against corrosion, *Chem. Mater.* 17 (15) (2005) 3968–3975.
- [28] E. Lebègue, T. Brousse, J. Gaubicher, C. Cougnon, Spontaneous arylation of activated carbon from aminobenzene organic acids as source of diazonium ions in mild conditions, *Electrochim. Acta* 88 (2013) 680–687.
- [29] M. Toupin, D. Bélanger, Spontaneous functionalization of carbon black by reaction with 4-nitrophenyldiazonium cations, *Langmuir* 24 (2008) 1910–1917.
- [30] M.M. Haque, M. Hasan, M.S. Islam, M.D.E. Ali, Physico-mechanical properties of chemically treated palm and coir fiber reinforced polypropylene composites, *Bioresour. Technol.* 100 (2009) 4903–4906.
- [31] M.N. Islam, M.R. Rahman, M.M. Haque, M.M. Huque, Physico-mechanical properties of chemically treated coir reinforced polypropylene composites, *Composites A* 41 (2010) 192–198.
- [32] M.R. Rahman, M.M. Huque, M.N. Islam, M. Hasan, Mechanical properties of polypropylene composites reinforced with chemically treated abaca, *Compos. Appl. Sci. Manuf.* 40 (4) (2009) 511–517.
- [33] M.R. Rahman, M.N. Islam, M.M. Huque, S. Hamdan, A.S. Ahmed, Effect of chemical treatment on rice husk (RH) reinforced polyethylene (PE) composites, *Bioresources* 5 (2010) 854–869.
- [34] J. Credou, R. Faddoul, T. Berthelot, One-step and eco-friendly modification of cellulose membranes by polymer grafting, *RSC Adv.* 4 (105) (2014) 60959–60969.
- [35] P. Schroll, C. Fehl, S. Dankesreiter, B. König, Photocatalytic surface patterning of cellulose using diazonium salts and visible light, *Org. Biomol. Chem.* 11 (38) (2013), <http://dx.doi.org/10.1039/c3ob40990b>.
- [36] Y. Deng, H. Zhao, Y. Qian, L. Lü, B. Wang, X. Qiu, Hollow lignin azo colloids encapsulated avermectin with high anti-photolysis and controlled release performance, *Ind. Crops Prod.* 87 (2016) 191–197.
- [37] E.O. Uwagboe, R.A. Hamzat, M. Olumide, L.A. Akinbile, Utilization of cocoa pod husk (CPH) as substitute for maize in layers mash and perception of poultry farmers in Nigeria, *Int. J. Sci. Nat.* 1 (2010) 272–275.
- [38] H. Zhao, Q. Wang, Y. Deng, Q. Shi, Y. Qian, B. Wang, L. Lu, X. Qiu, Preparation of renewable lignin-derived nitrogen-doped carbon nanospheres as anodes for lithium-ion batteries, *RSC Adv.* 6 (81) (2016) 77143–77150.
- [39] A. Duval, H. Lange, M. Lawoko, C. Crestini, Modification of kraft lignin to expose diazobenzene groups: toward pH- and light-responsive biobased polymers, *Biomacromolecules* 16 (9) (2015) 2979–2989.
- [40] D. Kai, M.J. Tan, P.L. Chee, Y.K. Chua, Y.L. Yap, X.J. Loh, Towards lignin-based functional materials in a sustainable world, *Green Chem.* 18 (5) (2016) 1175–1200.
- [41] V.L. Budarin, J.H. Clark, J. Schenck, T.J. Farmer, D.J. Macquarrie, M. Mascal, G. K. Nagaraja, T.H.M. Petchey, Processed lignin as a byproduct of the generation of 5-(chloromethyl)furfural from BIOMASS: A PROMISING NEW MESOPOROUS Material, *ChemSusChem* 8 (24) (2015) 4172–4179.
- [42] F.N. Ajjan, N. Casado, T. Rebis, A. Elfwing, N. Solin, D. Mecerreyes, O. Inganas, High performance PEDOT/lignin biopolymer composites for electrochemical supercapacitors, *J. Mater. Chem. A* 4 (5) (2016) 1838–1847.
- [43] M. Graglia, J. Pampel, T. Hantke, T.-P. Fellingner, D. Esposito, Nitro lignin-derived nitrogen-doped carbon as an efficient and sustainable electrocatalyst for oxygen reduction, *ACS Nano* 10 (4) (2016) 4364–4371.
- [44] G. Deniau, L. Azoulay, L. Bougerolles, S. Palacin, Surface electroinitiated emulsion polymerization: grafted organic coatings from aqueous solutions, *Chem. Mater.* 18 (23) (2006) 5421–5428.
- [45] T. Menanteau, C. Benoit, T. Breton, C. Cougnon, Enhancing the performance of a diazonium-modified carbon supercapacitor by controlling the grafting process, *Electrochem. Commun.* 63 (2016) 70–73.

#### 4. SCIENTIFIC PAPER III

Cobalt nanoparticles embedded into polydimethylsiloxane-grafted cocoa shell:  
functional agrowaste for CO<sub>2</sub> capture



# Cobalt nanoparticles embedded into polydimethylsiloxane-grafted cocoa shell: functional agrowaste for CO<sub>2</sub> capture

Julien Vieillard<sup>1</sup> · Nabil Bouazizi<sup>1</sup> · Flavia Fioresi<sup>1</sup> · Radhouane Bargougui<sup>1</sup> · Nicolas Brun<sup>2</sup> · Patrick Nkuigie Fotsing<sup>3</sup> · Emmanuel Djoufac Woumfo<sup>3</sup> · Olivier Thoumire<sup>4</sup> · Hassan Atmani<sup>4</sup> · Nadine Mofaddel<sup>1</sup> · Franck Le Derf<sup>1</sup>

Received: 16 September 2018 / Accepted: 3 January 2019  
© Springer Science+Business Media, LLC, part of Springer Nature 2019

## Abstract

This paper presents for the first time surface functionalization of cocoa shells (CS) through the covalent grafting of 3-aminopropyltriethoxysilane (APTES) followed by the substitution of poly(dimethylsiloxane) (PDMS) and in situ generation/insertion of cobalt nanoparticles (Co-NP). The immobilization and stability of APTES–PDMS on cocoa shell were confirmed by Fourier transform infrared spectroscopy and differential scanning calorimetry. Morphological analyses by scanning electron microscopy demonstrated that Co-NPs successfully grew on the surface of CS–APTES–PDMS. The CO<sub>2</sub>-adsorption capacity of these new materials was examined at ambient conditions. Both CS–APTES–PDMS and CS–APTES–PDMS–Co showed increased CO<sub>2</sub> adsorption capacities as compared to unmodified cocoa shell. This enhancement was explained by the synergistic behavior of the silane derivate, PDMS grafting, and Co-NP incorporation for CO<sub>2</sub> adsorption. This work represents a new step toward using cocoa shell as an excellent low-cost candidate for a variety of environmental applications such as CO<sub>2</sub> storage at ambient temperature.

## 1 Introduction

Anthropogenic carbon dioxide emissions and the whole energy demand from populations and the industry have been continuously increasing in recent years [1–3]. Thus, sustainable development involving energy storage and conversion, catalysis, adsorption and chemical processing are required

to meet this major global challenge. Amongst them, CO<sub>2</sub> capture has become a significant field of research. In the present article, we propose to employ a low-cost agro waste, i.e. cocoa shell, as a starting material for preparing solid sorbents for carbon capture.

Several materials like zeolites, silica, activated carbons, and alumina have emerged as efficient sorbents for CO<sub>2</sub> capture [4–10], owing to their easy and relatively low-cost synthesis with a low energy request [11]. In order to improve the textural and surface properties of these materials, doping with metal nanoparticles has received considerable attention. In particular, gadolinium currently prompts strong interest in the field of sorbents and sensors because it is a hard and thermally stable element [12–14]. In addition, numerous attempts have been made to improve sorption properties by adding organic fillers [15, 16], e.g. rice husk and polymers [17].

Metal–organic matrices and nanoparticles have recently been studied for CO<sub>2</sub> separation [18–21]. Modifications by polymer grafting have also been investigated, but only closed pores of adsorbent were produced [22]. Moreover, these materials were not studied for CO<sub>2</sub> sorption at ambient conditions.

Biomass agro waste, in particular cocoa shell, are low-cost and abundant primary and renewable energy sources.

**Electronic supplementary material** The online version of this article (<https://doi.org/10.1007/s10854-019-00679-5>) contains supplementary material, which is available to authorized users.

✉ Julien Vieillard  
julien.vieillard@univ-rouen.fr

✉ Nabil Bouazizi  
bouazizi.nabil@hotmail.fr

<sup>1</sup> Normandie Université, UNIROUEN, INSA Rouen, CNRS, COBRA (UMR 6014), 55, rue saint germain, 27000 Evreux, France

<sup>2</sup> Institut Charles Gerhardt Montpellier, Université de Montpellier, ENSCM, CNRS, Montpellier, France

<sup>3</sup> Laboratoire de Physico-Chimie des Matériaux Minéraux, Département de Chimie Inorganique, Faculté des Sciences, Université de Yaoundé I, B.P. 812, Yaounde, Cameroon

<sup>4</sup> Normandie Université, UNIROUEN, CNRS, PBS, UMR 6270, 1 rue du 7<sup>ème</sup> chasseur, 27000 Evreux, France

For example, their gasification to produce syngas has been regarded as one of the most promising options for biomass upgrading [23, 24]. The pore structure and size distribution have been investigated and compared between different families of cocoa shell. Some of them had a major portion of their pores in the micropore range, whereas others had a significant amount of mesopores and macropores [25, 26].

We tested natural cocoa shells (CS), 3-aminopropyltriethoxysilane (APTES)-modified (CS-APTES), APTES-poly(dimethylsiloxane)(PDMS)-modified (CS-APTES-PDMS), and microstructured cocoa shell (CS-APTES-PDMS-Co) as low-cost materials for CO<sub>2</sub> sorption, and investigated their surface morphology, stability and composition. CO<sub>2</sub> adsorption was tested at ambient temperature and normal pressure. To the best of our knowledge, this article is the first report on the preparation of metal nanoparticles embedded into amino-polymer-grafted cocoa shell and their application as solid sorbents for CO<sub>2</sub> capture.

## 2 Experimental procedure

### 2.1 Chemicals

Cobalt nitrate hexahydrate (Co (NO<sub>3</sub>)<sub>2</sub> · 6H<sub>2</sub>O), polydimethylsiloxane (C<sub>6</sub>H<sub>18</sub>OSi<sub>2</sub>), 3-aminopropyltriethoxysilane (APTES), sodium borohydride (NaBH<sub>4</sub>), and pure ethanol (CH<sub>3</sub>CH<sub>2</sub>OH) were purchased from Sigma-Aldrich and used as received. All the solutions were prepared from double-distilled water (Merck, Millipore).

### 2.2 Material preparation and functionalization

The functional CS-APTES-PDMS-Co materials were synthesized as follows:

Firstly, CS were collected from a local farm managed by the IRAD (Institute de recherche agricole pour le développement) at Yaoundé, Cameroon. The shells were cut, washed with acidic water (HCl, 1 M) to remove organic matter, and then sun-dried for 5 days and heated at 70 °C overnight to remove moisture. Finally, they were ground and sifted at 160 μm.

Secondly, 3-aminopropyl-triethoxysilane was chemically grafted using water/ethanol 1:3 (V/V) as a solvent, and a mixture of CS/APTES 1:3 (W/W) at 80 °C for 5 h [27]. The synthesized product, named CS-APTES, was washed, filtered, and then dried at 75 °C overnight.

Thirdly, the siloxane-based polymer was immobilized by a reaction between the amine groups of the grafted APTES and the epoxy groups of the siloxane polymer, as described in the literature [28]. Briefly, 25 mM PDMS was dispersed in 100 mL of isopropanol as a solvent, and then grafted APTES was added. The mixture was placed under reflux and

in contact with a nitrogen flow for 24 h at 75 °C. After that, the resulting product (CS-APTES-PDMS) was filtrated, washed with ethanol, and dried at 80 °C overnight.

Finally, cobalt nanoparticle (Co-NP) dispersion was achieved using 0.3 wt.% of (Co (NO<sub>3</sub>)<sub>2</sub> · 6H<sub>2</sub>O) as a precursor in 40 mL of toluene (99.5%, d=0.865 g mL<sup>-1</sup>) in the presence of 0.03 wt.% of sodium borohydride as a reducing agent. The resulting mixture was stirred at room temperature for 5 h. The final product, named CS-APTES-PDMS-Co, was dried at 70 °C overnight (Scheme 1).

### 2.3 Characterization of the materials

FTIR spectra were recorded using a Tensor 27 (Bruker) spectrometer with a ZnSe ATR crystal. For each spectrum, 20 scans were accumulated with a resolution of 4 cm<sup>-1</sup>. Samples were drilled before IR analysis, and background spectra were recorded on air. For scanning electron microscopy (SEM), CS were metallized by a gold layer at 18 mA for 360 s using a Biorad E5200 device. To obtain SEM images, samples were previously metallized with an evaporated gold layer. Then, SEM images were acquired using a ZEISS EVO 15 electron microscope. Two types of images were recorded: secondary ion images to observe the morphology of the surface, and EDX images to analyze the atomic composition. Differential scanning calorimetry (DSC) of the samples was determined using DSC-92 Setaram with a temperature range from room temperature to 500 °C and a heating rate of 10 °C min<sup>-1</sup>. Zeta potentials were measured using a Malvern nanoZS zetasizer. Samples were prepared by dispersing 0.1 g of sorbents in 10 mL of distilled water.

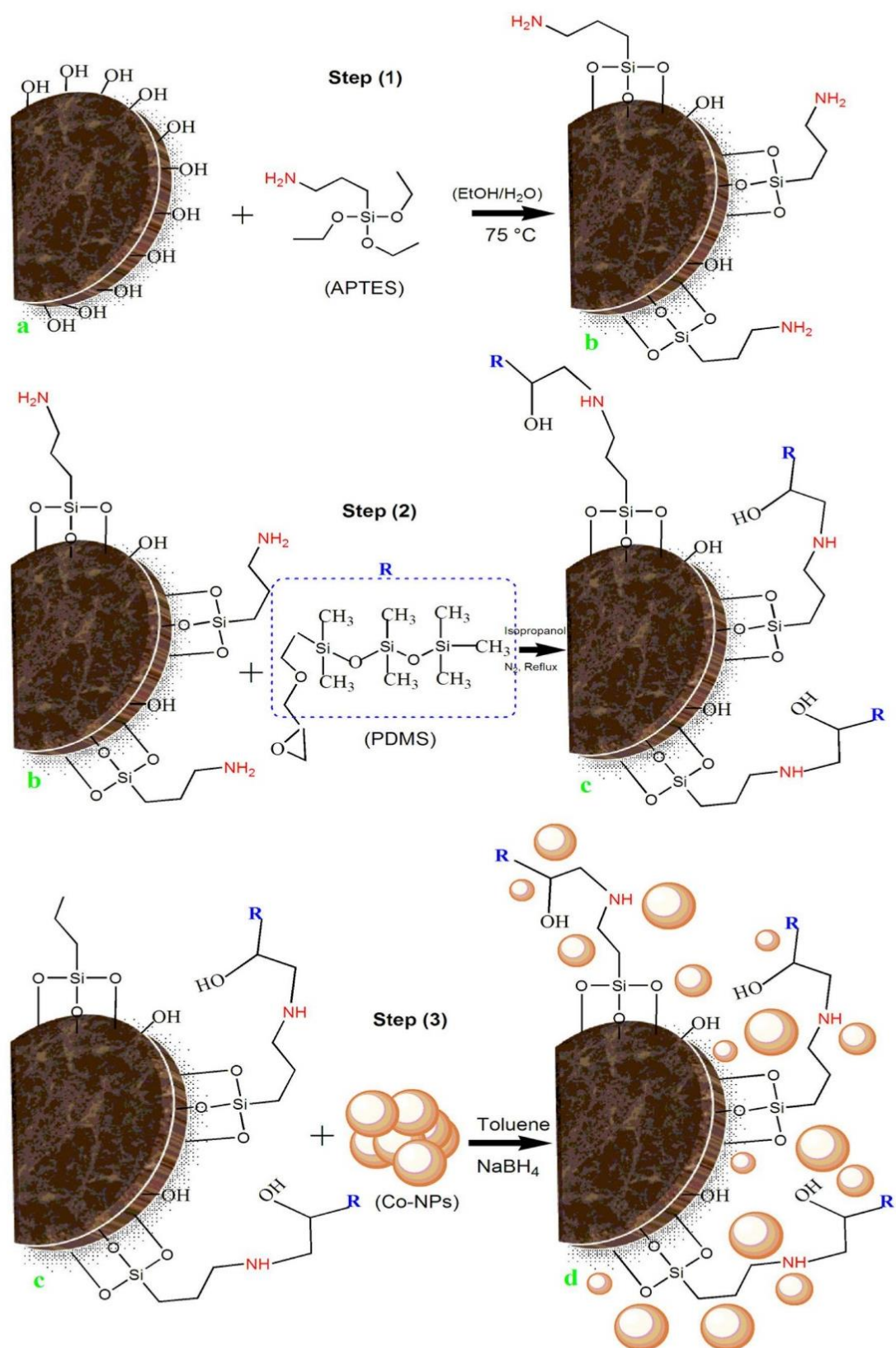
### 2.4 CO<sub>2</sub> adsorption tests

The CO<sub>2</sub> adsorption tests were carried out according to a procedure fully described elsewhere [29]. Typically, 0.1 g of adsorbent was incubated at room temperature and normal pressure with 3 mL of pure carbon dioxide (Air Liquide). Before the incubation step, CO<sub>2</sub> was dried with pumice. The amount of adsorbed CO<sub>2</sub> was measured in triplicate.

## 3 Results and discussion

### 3.1 Chemical grafting of APTES and PDMS

By successfully grafting APTES, we introduced anchoring amine groups (NH<sub>2</sub>) on the cocoa shell surface. Firstly, the chemical grafting strategy is based on the formation of aminosilane layers on the hydroxyl groups naturally present on cocoa shell. Subsequently, these amino groups react with epoxy-terminated PDMS, resulting in PDMS



**Scheme 1** Procedures for the synthesis of CS (a), CS–APTES (b), CS–APTES–PDMS (c), and CS–APTES–PDMS–Co (d)

immobilization onto the cocoa shell surface through a nucleophilic substitution reaction. The stabilization of organo-cocoa shell remains a major challenge because the particles tend to aggregate and lose their properties. Metallic nanoparticle entrapment may favor stabilization through a combination of electrostatic and steric factors [30]. Therefore, Co-NP insertion is expected to provide a convenient strategy to stabilize PDMS-cocoa shell.

Proper grafting and nanoparticle incorporation was first confirmed by FTIR results (Fig. 1). The bands at 1,060 and 800  $\text{cm}^{-1}$  were attributed to the Si–O–Si or Si–O–C stretching vibrations, indicating the successful grafting of APTES on CS [31, 32]. The presence of amine functions on CS–APTES and HC–APTES–PDMS was confirmed by peaks detectable at 3,350 and 1,674  $\text{cm}^{-1}$ , which can be associated to the N–H stretching vibration and  $\text{NH}_2$  bending vibration, respectively [33, 34]. On the other hand, due to PDMS substitution, new peaks appeared between 3,000 and 2,800  $\text{cm}^{-1}$ , confirming the presence of  $(\text{Si}-\text{CH}_2)_2$  and  $\text{CH}_2$  groups. In the 1500–800  $\text{cm}^{-1}$  region, more intense bands associated to the vibration modes for methylene groups and the scissoring mode for  $\text{CH}_2$  were observed [35]. Three new peaks at 1260–1300  $\text{cm}^{-1}$ , 840  $\text{cm}^{-1}$  and 790  $\text{cm}^{-1}$  due to the symmetric bending of the methyl groups connected to the silicon atom ( $\delta\text{Si}-\text{CH}_3$ ) were also observed [36]. Interestingly, the chemical modification that ensued from the reaction with the epoxy ring resulted in the formation of a secondary amine, confirmed by FTIR through the deformation mode of the N–H group at around 1570–1560  $\text{cm}^{-1}$  (Table S1).

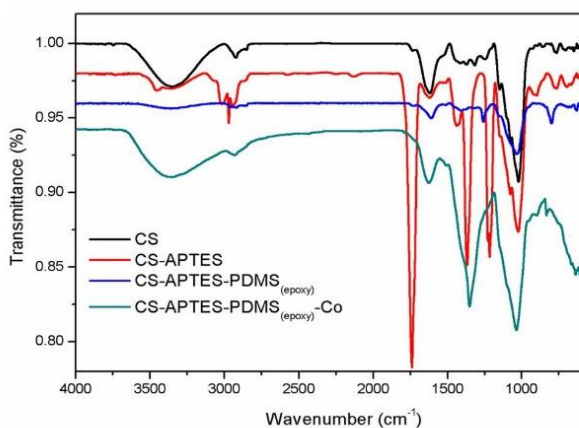


**Fig. 1** FTIR spectra of CS, CS–APTES, CS–APTES–PDMS, and CS–APTES–PDMS–Co

### 3.2 Immobilization of Co-NPs onto CS–APTES–PDMS

Metallic nanoparticle formation resulted from a high dispersive capacity of the host matrices. This property entailed the occurrence of a sufficiently high number of nanoparticle-stabilizing sites. The shift recorded for the OH stretching band from 3350  $\text{cm}^{-1}$  (for CS–APTES–PDMS) to 3320  $\text{cm}^{-1}$  (for CS–APTES–PDMS–Co) confirmed that hydroxyl groups were involved in  $\text{Co}^{2+}$  chelation. Such an IR shift associated with metal cation chelation on cellulose was also observed by Basta et al. [37]. The decrease in the intensity of the IR band at around 750  $\text{cm}^{-1}$  confirmed that silicon atoms were hidden by Co-NPs. Moreover, the shift of the Si–O–Si stretching vibration from 1060–1045  $\text{cm}^{-1}$  to lower frequencies confirmed that Co-NP incorporation was stabilized by the APTES–PDMS layer. These observations suggest that APTES–PDMS aggregated around Co-NPs even in the form of multilayer condensation via intermolecular H-bridges.

We can conclude from these IR data that the main epoxy ending group of PDMS fully reacted with the amine group of APTES via covalent bonding [35, 38], resulting in successful grafting of PDMS on APTES-modified cocoa shell and incorporation of Co-NPs on CS–APTES–PDMS.

### 3.3 Morphological properties

SEM images of CS, CS–APTES, CS–APTES–PDMS, and CS–APTES–PDMS–Co are shown in Fig. 2. At the microscopic scale, CS seemed relatively smooth, with many agglomerated sub-micrometric particles (Fig. 2a). After APTES and PDMS grafting, layers were observed at the edges of the particles, which visibly brought evidence of the existence of APTES–PDMS coating on cocoa shell (Fig. 2b, c). After in situ generation of Co-NPs, a few nanoparticle aggregates were observed, confirming successful impregnation (Fig. 2d). These agglomerates were accompanied by white spots, due to the presence of Co-NPs on the surface of the adsorbent. A few Co-NP agglomerates were also observed uniformly on the whole surface of CS–APTES–PDMS, and the surface morphology was clearly changed (Fig. 2d). The size of the cobalt nanoparticles was estimated to be 50–80 nm from TEM images (Figure S1). This resulted from the displacement of polymer chains to the edge of CS–APTES–PDMS during  $\text{Co}^{2+}$  reduction and in situ generation of metal nanoparticles.

For a detailed characterization, the synthesized samples were analyzed by SEM–EDX spectroscopy. The Au, Cu, and Pd heteroatoms identified in Fig. 3 came from the metallization step required for EDX analysis. Specific peaks for cobalt and silicon atoms were observed, confirming the incorporation of silicon from organosilane grafting and cobalt from

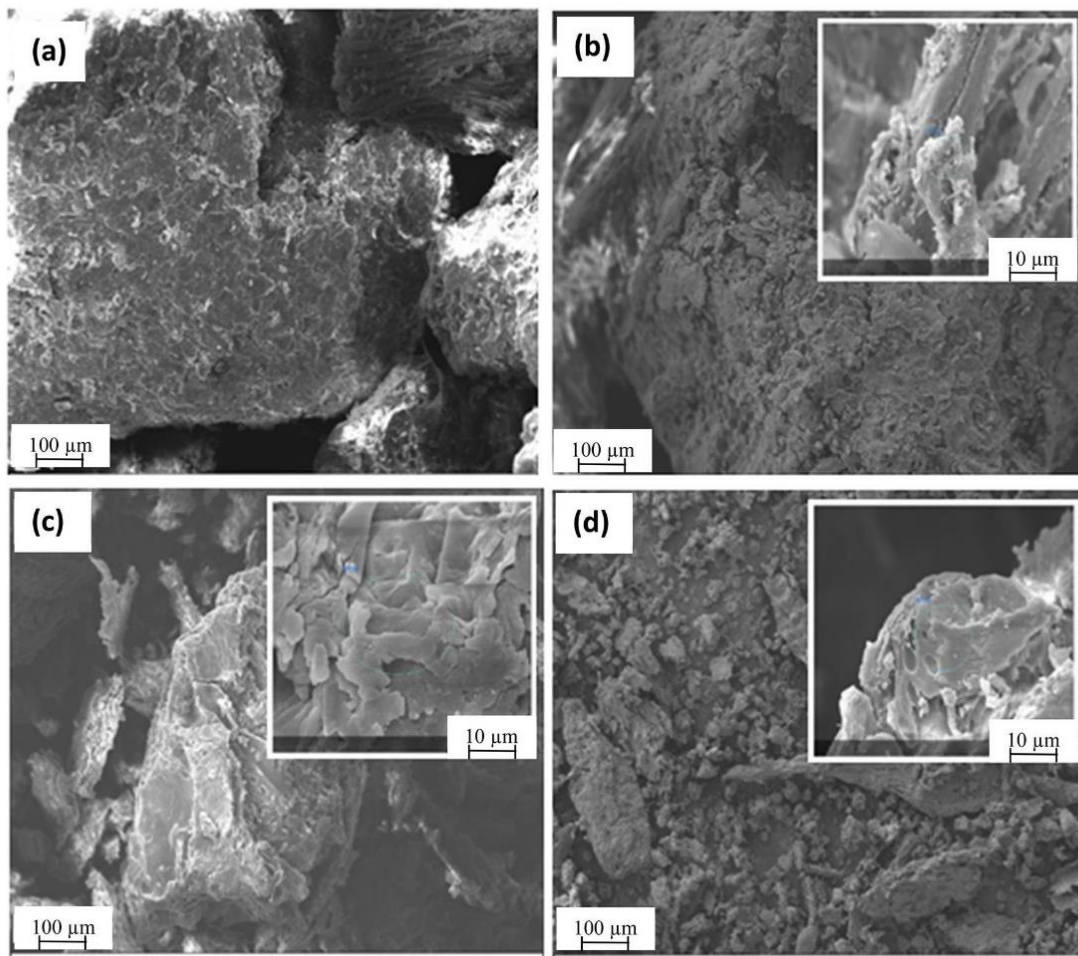


**Fig. 2** SEM images of CS (a), CS-APTES (b), CS-APTES-PDMS (c) and CS-APTES-PDMS-Co (d)

nanoparticle incorporation, as showed in Fig. 3. SEM-EDX (Fig. 4) mapping confirmed that the silicon layer and cobalt nanoparticles covered the whole cocoa shell surface.

### 3.4 Thermal stability of CS-APTES-PDMS-Co

Figure 5 shows a typical DSC curve of cocoa shell before and after treatments by APTES-PDMS coating and Co-NP incorporation. Cocoa shell presented an endothermic peak at around 100 °C corresponding to evaporation of free water from the samples. This peak was missing from the curve associated to the modified materials, probably because they were slightly heated during the grafting process. Two exothermic peaks were visible at 320 and 450 °C on CS-APTES-PDMS-Co, corresponding to cobalt oxide and metallic cobalt [39], respectively.

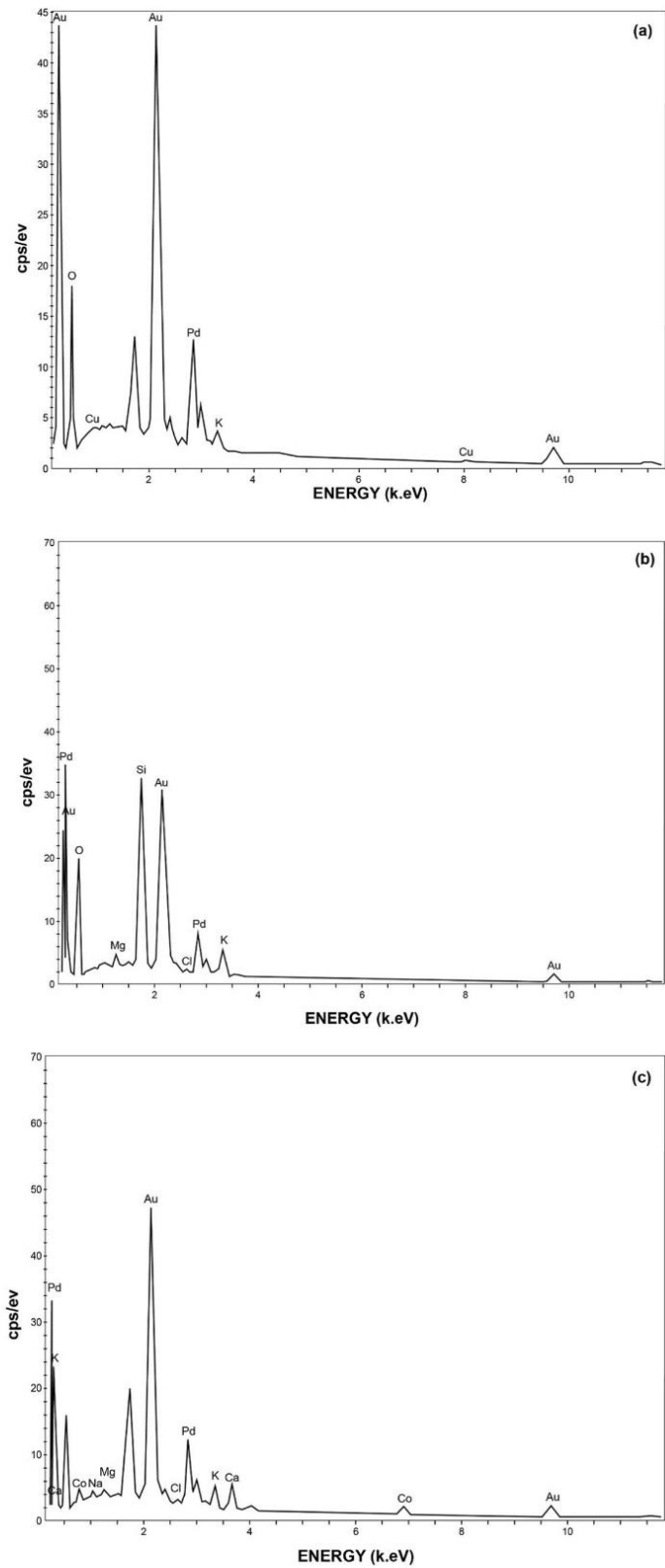
The maximum heat flow was higher for all the modified materials than for the unmodified material. Therefore, increased thermal stability was observed after modification.

This supports that the two aminopropyl groups from aminosilane layers and Co-NPs had a synergetic effect and protected the cocoa shell surface, in good agreement with SEM and FTIR analyses. These results confirm that APTES-PDMS-Co was added on the CS sample, and improved the thermal stability of CS-APTES-PDMS and CS-APTES-PDMS-Co.

### 3.5 Electrical behavior of CS derivatives

The zeta potential may accurately reflect the electrostatic behavior of solid particles for that a tiny change of electric charge in Stern layer can cause the fluctuation of electric potential. Zeta potential analysis provided also important information about the surface charge density of the material and the stability of the nanoparticles dispersion. The average zeta potential for natural cocoa shell was  $-25$  mV (Fig. 6). This negative value may result from the charge contribution of cellulose, lignin and hemicelluloses of CS. After

**Fig. 3** EDX spectra of CS–APTES (a), CS–APTES–PDMS (b), and CS–APTES–PDMS–Co (c)



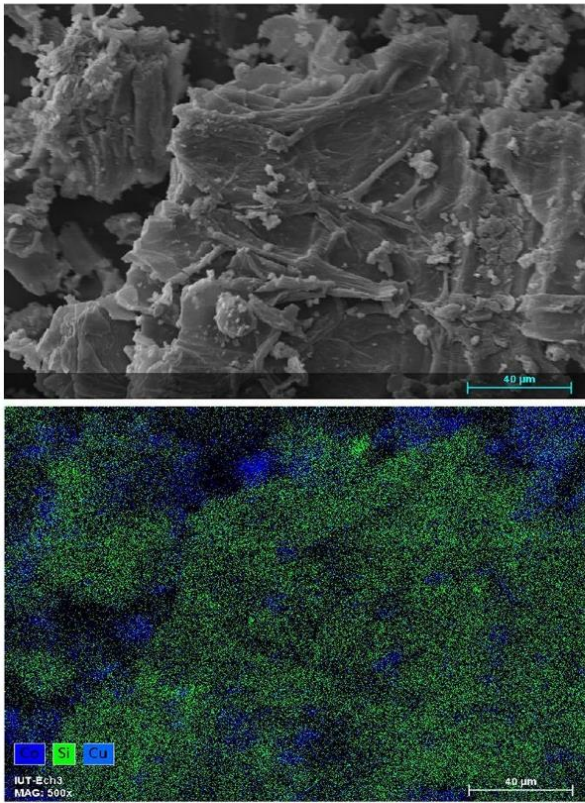


**Fig. 4** SEM image and EDX mapping of the synthesized CS-APTES-PDMS-Co adsorbent

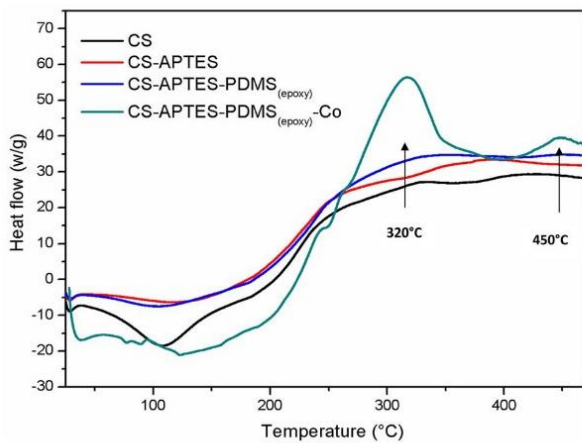


**Fig. 5** DSC profiles of the CS (green), CS-APTES (red), CS-APTES-PDMS (blue), and CS-APTES-PDMS-Co (black) samples. (Color figure online)

APTES and PDMS coating, the increase of the zeta potential revealed a modification of the electrical state of the surface to reach  $-28$  mV and  $-33$  mV respectively. These higher

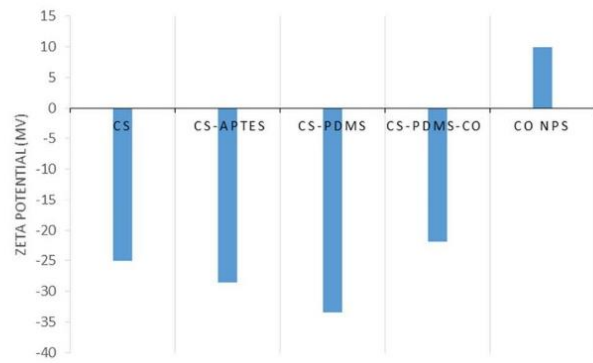


**Fig. 6** Zeta potential of CS derivatives

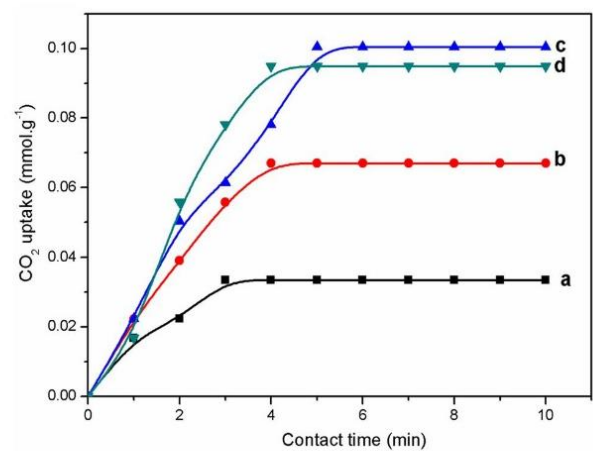


**Fig. 7**  $\text{CO}_2$  uptake recorded for CS (a), CS-APTES (b), CS-APTES-PDMS (c), and CS-APTES-PDMS-Co (d)

values of zeta potential confirmed that APTES and PDMS coating participate to the stabilization of the colloid dispersion of CS particles. The zeta potential of Co nanoparticles was evaluated to 12 mV. Thus, the modification of the zeta potential from  $-33$  mV to  $-22$  mV confirmed the incorporation of Co nanoparticles into CS-PDMS-Co in accordance with SEM and IR analysis.

### 3.6 $\text{CO}_2$ adsorption properties

Figure 7 shows that all samples displayed affinity towards carbon dioxide. Interestingly, CS-APTES, CS-APTES-PDMS and CS-APTES-PDMS-Co demonstrated much better  $\text{CO}_2$  adsorption performances than unmodified cocoa shell. More particularly, CS-APTES-PDMS-Co exhibited a  $\text{CO}_2$  retention capacity of  $0.1 \text{ mmol g}^{-1}$  at room temperature and normal pressure.

Additionally, the functionalized surface area of CS-APTES-PDMS-Co considerably enhanced gas

diffusion due to its larger exposure area and penetration depth for CO<sub>2</sub> molecules. We also compared the CO<sub>2</sub> adsorption properties of various natural unmodified or chemically modified samples reported in the literature with the CS–APTES–PDMS–Co samples prepared in this study (Table 1). CS–APTES–PDMS–Co demonstrated interesting performances towards CO<sub>2</sub> gas capture, with a retention capacity eight-fold higher than bentonite and zeolites (Table 1). The adsorption capacity described in this paper is obviously lower than the adsorption capacity of activated carbon, mesoporous silica or metal–organic frameworks [40], but our aim was to develop a simple (requiring no specific equipment) and low-cost strategy to promote an abundant agro waste resource without any physical activation. This feature could not only be due to the synergetic effect between CS matrices and the cobalt nanoparticles embedded in APTES–PDMS coatings, but also to the well-dispersed cobalt nanoparticles that increase the gas response by providing active CO<sub>2</sub>-capturing sites. We modified cocoa shell step by step. To evaluate the influence of the building blocks, PDMS was directly impregnated onto the cocoa shell surface. In this case, CO<sub>2</sub> adsorption was 75% higher than on cocoa shell but still limited (data not shown). Therefore, silane layers are important to promote PDMS adhesion. The amino groups present on modified matrices increase basicity and thereby favor the chemical formation of carbamate from CO<sub>2</sub> molecules [41, 42]. In parallel, the PDMS layer and cobalt particles induced a modification of the surface probably via compaction of the structure. Thus, CO<sub>2</sub> molecules could be entrapped around cobalt nanoparticles by physical condensation.

### 3.7 Diffusivity and equilibrium adsorption of CO<sub>2</sub> in CS–APTES–PDMS–Co

The amount of adsorbed CO<sub>2</sub> increased as the contact time increased, until it reached a plateau indicating that the samples were saturated with CO<sub>2</sub> gas (Fig. 7). This phenomenon can be explained in terms of the full diffusion of

CO<sub>2</sub> molecules within the materials. Firstly, CO<sub>2</sub> reached the boundary layer at the surface where APTES, PDMS and Co-NPs were immobilized. Thus, CO<sub>2</sub> was quickly adsorbed onto the active site generated by the loading of APTES–PDMS–Co. Meanwhile, the other amounts of CO<sub>2</sub> gas passed through the texture to fill the gaps inside the CS microstructure. Besides diffusion, CO<sub>2</sub> transport was facilitated by the activity of APTES–PDMS–Co that enhanced the adsorption properties of the materials. Afterwards, the aminosilane groups and cobalt nanoparticles on the adsorbent surface were saturated with CO<sub>2</sub> and oxygen atoms, which made the adsorption capacity constant. Thus, the diffusion time was equilibrated, indicating saturation of these materials. Interestingly, the equilibrium time recorded for CS–APTES–PDMS–Co was shorter than the time recorded for the other materials, indicating that cobalt incorporation enhanced gas diffusion into the adsorbent (Table 2). We estimated that PDMS layers induced a compaction of the CS particles facilitating the capture of a higher amount of CO<sub>2</sub> molecules. Nevertheless, those molecules need time to diffuse into the texture of the particles (equilibrium time = 5.4 min). The surrounding of PDMS by cobalt nanoparticles improve the capture of CO<sub>2</sub> molecules due to specific physical condensation. In the same time, cobalt nanoparticles improve the gas diffusion into the particle which could limit the maximum amount of CO<sub>2</sub> molecules captured. To conclude, cobalt catalyzed CO<sub>2</sub> conversion and also increased the cocoa shell surface area [48]. Thus, in situ reduction of metallic cobalt is an interesting field of investigation to develop functional materials for fast gas adsorption.

**Table 2** Time needed for different adsorbents to reach equilibrium

	CS	CS–APTES	CS–APTES–PDMS	CS–APTES–PDMS–Co
Equilibrium time (min)	4.10	4.40	5.30	4.00

**Table 1** Comparison between the CO<sub>2</sub>-retention capacities measured in this study and published results

Adsorbent	CO <sub>2</sub> -retention capacity at room temperature and normal pressure (mmol.g <sup>-1</sup> )	Reference
Bentonite	$3.4 \times 10^{-3}$	[43]
Bentonite–PEI	1	[44]
Cu–organo–bentonite	$2 \times 10^{-3}$	[45]
NaMt–S–N(OH) <sub>2</sub>	$0.283 \times 10^{-3}$	[27]
Montmorillonite	$0.72 \times 10^{-3}$	[43]
TETA–acrylamide–sugarcane bagasse	5	[46]
Metal–organoclay	$1.5 \times 10^{-3}$	[47]
CS–APTES–Co	0.24	[41]
CS–APTES–PDMS–Co	$10 \times 10^{-3}$	This work

## 4 Conclusions

The purpose of the current study was to evaluate the performance of natural and modified cocoa shell for adsorption of CO<sub>2</sub> gas at room temperature and atmospheric pressure. In this respect, CS were functionalized via chemical grafting of APTES and PDMS, followed by Co-NP incorporation. Natural and modified surfaces were characterized by FTIR, SEM, EDX, and DSC. All these analyses demonstrated that both APTES and PDMS were successfully grafted onto CS particles, and elucidated the in situ generation and impregnation of cobalt nanoparticles onto and within the APTES–PDMS coating. While both natural and modified cocoa shell samples demonstrated CO<sub>2</sub> capture abilities, CS–APTES–PDMS–Co offered correct adsorption properties. We demonstrated the key effect of cobalt nanoparticles loaded on CS–APTES–PDMS for fast CO<sub>2</sub> adsorption at ambient temperature. Therefore, the APTES–PDMS grafting and Co-NP incorporation approach offers promising prospects for preparing advanced low-cost materials for CO<sub>2</sub> adsorption and electrocatalysis applications.

**Acknowledgements** We thank Mr Antoine Fontaine for his help to improve the quality of some figures. This work was partially supported by the INSA Rouen, Rouen University, the CNRS, Labex SynOrg (ANR-11-LABX-0029), the European Battuta Program, the Normandy region (CBS network), the European Union (FEDER) and the Evreux Portes de Normandie Agglomeration.

**Author contributions** All authors contributed to the manuscript, and approved of its final version.

## References

- J.D. Figueroa, T. Fout, S. Plasynski, H. McIlvried, R.D. Srivastava, Advances in CO<sub>2</sub> capture technology—the U.S. department of energy's carbon sequestration program. *Int. J. Greenhouse Gas Control* **2**(1), 9–20 (2008)
- C. Azar, K. Lindgren, E. Larson, K. Möllersten, Carbon capture and storage from fossil fuels and biomass—costs and potential role in stabilizing the atmosphere. *Clim. Change* **74**(1), 47–79 (2006)
- D. Aaron, C. Tsouris, Separation of CO<sub>2</sub> from flue gas: a review. *Sep. Sci. Technol.* **40**(1–3), 321–348 (2005)
- Y.L. Tan, M.A. Islam, M. Asif, B.H. Hameed, Adsorption of carbon dioxide by sodium hydroxide-modified granular coconut shell activated carbon in a fixed bed. *Energy* **77**, 926–931 (2014)
- S. Builes, P. López-Aranguren, J. Fraile, L.F. Vega, C. Domingo, Analysis of CO<sub>2</sub> adsorption in amine-functionalized porous silicas by molecular simulations. *Energy Fuels* **29**(6), 3855–3862 (2015)
- P. López-Aranguren, S. Builes, J. Fraile, L.F. Vega, C. Domingo, Understanding the performance of new amine-functionalized mesoporous silica materials for CO<sub>2</sub> adsorption. *Ind. Eng. Chem. Res.* **53**(40), 15611–15619 (2014)
- E. David, J. Kopac, Activated carbons derived from residual biomass pyrolysis and their CO<sub>2</sub> adsorption capacity. *J. Anal. Appl. Pyrolysis* **110**, 322–332 (2014)
- A. Kongnoo, P. Intharapat, P. Worathanakul, C. Phalakornkule, Diethanolamine impregnated palm shell activated carbon for CO<sub>2</sub> adsorption at elevated temperatures. *J. Environ. Chem. Eng.* **4**(1), 73–81 (2016)
- K. Li, S. Tian, J. Jiang, J. Wang, X. Chen, F. Yan, Pine cone shell-based activated carbon used for CO<sub>2</sub> adsorption. *J. Mater. Chem. A* **4**(14), 5223–5234 (2016)
- T. Chen, S. Deng, B. Wang, J. Huang, Y. Wang, G. Yu, CO<sub>2</sub> adsorption on crab shell derived activated carbons: contribution of micropores and nitrogen-containing groups. *RSC Adv.* **5**(60), 48323–48330 (2015)
- S. Sengupta, V. Amte, R. Dongara, A.K. Das, H. Bhunia, P.K. Bajpai, Effects of the adsorbent preparation method for CO<sub>2</sub> capture from flue gas using K<sub>2</sub>CO<sub>3</sub>/Al<sub>2</sub>O<sub>3</sub> adsorbents. *Energy Fuels* **29**(1), 287–297 (2015)
- Y. Liu, N. Zhang, Gadolinium loaded nanoparticles in therapeutic magnetic resonance imaging. *Biomaterials* **33**(21), 5363–5375 (2012)
- X. Zhao, W. Wang, Y. Zhang, S. Wu, F. Li, J.P. Liu, Synthesis and characterization of gadolinium doped cobalt ferrite nanoparticles with enhanced adsorption capability for Congo red. *Chem. Eng. J.* **250**, 164–174 (2014)
- M. Ledwaba, N. Masilela, T. Nyokong, E. Antunes, Surface modification of silica-coated gadolinium oxide nanoparticles with zinc tetracarboxyphenoxy phthalocyanine for the photodegradation of orange G. *J. Mol. Catal. A* **403**, 64–76 (2015)
- A. Pattanayak, S.C. Jana, Thermoplastic polyurethane nanocomposites of reactive silicate clays: effects of soft segments on properties. *Polymer* **46**(14), 5183–5193 (2005)
- E.V. Lebedev, S.S. Ishchenko, V.D. Denisenko, V.O. Dupanov, E.G. Privalko, A.A. Usenko, V.P. Privalko, Physical characterization of polyurethanes reinforced with the in situ-generated silica-polyphosphate nano-phase. *Compos. Sci. Technol.* **66**(16), 3132–3137 (2006)
- H.D. Rozman, Y.S. Yeo, G.S. Tay, A. Abubakar, The mechanical and physical properties of polyurethane composites based on rice husk and polyethylene glycol. *Polym. Test.* **22**(6), 617–623 (2003)
- J. Liu, P.K. Thallapally, B.P. McGrail, D.R. Brown, J. Liu, Progress in adsorption-based CO<sub>2</sub> capture by metal-organic frameworks. *Chem. Soc. Rev.* **41**(6), 2308–2322 (2012)
- J.-Y. Jung, J.W. Lee, Y.T. Kang, CO<sub>2</sub> adsorption characteristics of nanoparticle suspensions in methanol. *J. Mech. Sci. Technol.* **26**(8), 2285–2290 (2012)
- J. Baltrusaitis, J. Schuttlefield, E. Zeitler, V.H. Grassian, Carbon dioxide adsorption on oxide nanoparticle surfaces. *Chem. Eng. J.* **170**(2–3), 471–481 (2011)
- M. Barberio, P. Barone, A. Imbrogno, F. Xu, CO<sub>2</sub> adsorption on silver nanoparticle/carbon nanotube nanocomposites: a study of adsorption characteristics. *Phys. Status Solidi B* **252**(9), 1955–1959 (2015)
- X. Xu, C. Song, J.M. Andresen, B.G. Miller, A.W. Scaroni, Adsorption separation of CO<sub>2</sub> from simulated flue gas mixtures by novel CO<sub>2</sub> “molecular basket” adsorbents. *Int. J. Environ. Technol. Manag.* **4**, 32–52 (2004)
- A. Ergudenler, A.E. Ghaly, Quality of gas produced from wheat straw in a dual-distributor type fluidized bed gasifier. *Biomass Bioenergy* **3**(6), 419–430 (1992)
- Y. Shen, K. Yoshikawa, Recent progresses in catalytic tar elimination during biomass gasification or pyrolysis—a review. *Renew. Energy Rev.* **21**, 371–392 (2013)
- O. Ioannidou, A. Zabaniotou, Agricultural residues as precursors for activated carbon production—a review. *Renew. Sustain. Energy Rev.* **11**(9), 1966–2005 (2007)
- A.R. Mohamed, M. Mohammadi, G.N. Darzi, Preparation of carbon molecular sieve from lignocellulosic biomass: A review. *Renew. Sustain. Energy Rev.* **14**(6), 1591–1599 (2010)

27. A. Azzouz, S. Nousir, N. Bouazizi, R. Roy, Metal–inorganic–organic matrices as efficient sorbents for hydrogen storage. *ChemSusChem* **8**(5), 800–803 (2015)
28. A.F. Pinheiro de Melo, *Development and characterization of polymer-grafted ceramic membranes for solvent nanofiltration*. GVO drukkers & vormgevers B.V. Ponsen & Looijen: 2013
29. N. Bouazizi, M. Khelil, F. Ajala, T. Boudharaa, A. Benghnia, H. Lachheb, R. Ben Slama, B. Chaouachi, A. M'Nif, A. Azzouz, Molybdenum-loaded 1,5-diaminonaphthalene/ZnO materials with improved electrical properties and affinity towards hydrogen at ambient conditions. *Int. J. Hydrog. Energy* **41**(26), 11232–11241 (2016)
30. G. Fritz, V. Schädler, N. Willenbacher, N.J. Wagner, Electrostatic stabilization of colloidal dispersions. *Langmuir* **18**(16), 6381–6390 (2002)
31. M. Yamaura, R. Camilo, L. Sampaio, M. Macedo, M. Nakamura, H. Toma, Preparation and characterization of (3-aminopropyl) triethoxysilane-coated magnetite nanoparticles. *J. Magn. Magn. Mater.* **279**(2), 210–217 (2004)
32. M.N. Sepehr, H. Kazemian, E. Ghahramani, A. Amrane, V. Sivasankar, M. Zarrabi, Defluoridation of water via light weight expanded clay aggregate (LECA): Adsorbent characterization, competing ions, chemical regeneration, equilibrium and kinetic modeling. *J. Taiwan Inst. Chem. Eng.* **45**(4), 1821–1834 (2014)
33. B. Saif, C. Wang, D. Chuan, S. Shuang, Synthesis and characterization of Fe<sub>3</sub>O<sub>4</sub> coated on APTES as carriers for morin-anticancer drug. *J. Biomater. Nanobiotechnol.* **6**(04), 267 (2015)
34. L. Maurizi, A. Claveau, H. Hofmann, Polymer adsorption on iron oxide nanoparticles for one-step amino-functionalized silica encapsulation. *J. Nanomater.* **16**(1), 239 (2015)
35. J. Choi, N.S. Wang, V. Reipa, Electrochemical reduction synthesis of photoluminescent silicon nanocrystals. *Langmuir* **25**(12), 7097–7102 (2009)
36. D. Enescu, V. Hamciuc, L. Pricop, T. Hamaide, V. Harabagiu, B.C. Simionescu, Polydimethylsiloxane-modified chitosan I. Synthesis and structural characterisation of graft and crosslinked copolymers. *J. Polym. Res.* **16**(1), 73–80 (2009)
37. A.H. Basta, W.M. Hosny, H. El-Saied, A.K. Hadi, A., metal chelates with some cellulose derivatives; part IV structural chemistry of HEC complexes. *Cellulose* **3**, 1–10 (1996)
38. D. Enescu, V. Hamciuc, R. Ardeleanu, M. Cristea, A. Ioanid, V. Harabagiu, B.C. Simionescu, Polydimethylsiloxane modified chitosan. Part III: preparation and characterization of hybrid membranes. *Carbohydr. Polym.* **76**(2), 268–278 (2009)
39. H.-Y. Lin, Y.-W. Chen, The mechanism of reduction of cobalt by hydrogen. *Mater. Chem. Phys.* **85**(1), 171–175 (2004)
40. J. Vieillard, N. Bouazizi, R. Bargougui, P.N. Fotsing, O. Thoumire, G. Ladam, N. Brun, J.F. Hochepped, E.D. Woumfo, N. Mofaddel, F.L. Derf, A. Azzouz, Metal–inorganic–organic core–shell material as efficient matrices for CO<sub>2</sub> adsorption: synthesis, properties and kinetic studies. *J. Taiwan Inst. Chem. Eng.* (2018) (in press). <https://doi.org/10.1016/j.jtice.2018.08.020>
41. R. Bargougui, N. Bouazizi, N. Brun, P.N. Fotsing, O. Thoumire, G. Ladam, E.D. Woumfo, N. Mofaddel, F.L. Derf, J. Vieillard, Improvement in CO<sub>2</sub> adsorption capacity of cocoa shell through functionalization with amino groups and immobilization of cobalt nanoparticles. *J. Environ. Chem. Eng.* **6**(1), 325–331 (2018)
42. J. Vieillard, N. Bouazizi, R. Bargougui, N. Brun, P. Fotsing Nkuigie, E. Oliviero, O. Thoumire, N. Couvrat, E. Djoufuc Woumfo, G. Ladam, N. Mofaddel, A. Azzouz, F. Le Derf, Cocoa shell-deriving hydrochar modified through aminosilane grafting and cobalt particle dispersion as potential carbon dioxide adsorbent. *Chem. Eng. J.* **342**, 420–428 (2018)
43. A. Azzouz, N. Platon, S. Nousir, K. Ghomari, D. Nistor, T.C. Shiao, R. Roy, OH-enriched organo-montmorillonites for potential applications in carbon dioxide separation and concentration. *Sep. Purif. Technol.* **108**, 181–188 (2013)
44. C. Chen, D.-W. Park, W.-S. Ahn, Surface modification of a low cost bentonite for post-combustion CO<sub>2</sub> capture. *Appl. Surf. Sci.* **283**, 699–704 (2013)
45. A.V. Arus, M.N. Tahir, R. Sennour, T.C. Shiao, L.M. Sallam, I.D. Nistor, R. Roy, A. Azzouz, Cu<sub>0</sub> and Pd<sub>0</sub> loaded organo-bentonites as sponge-like matrices for hydrogen reversible capture at ambient conditions. *ChemSelect* **1**(7), 1452–1461 (2016)
46. S. Luo, S. Chen, S. Chen, L. Zhuang, N. Ma, T. Xu, Q. Li, X. Hou, Preparation and characterization of amine-functionalized sugarcane bagasse for CO<sub>2</sub> capture. *J. Environ. Manag.* **168**, 142–148 (2016)
47. N. Bouazizi, D. Barrimo, S. Nousir, R.B. Slama, T. Shiao, R. Roy, A. Azzouz, Metal-loaded polyol-montmorillonite with improved affinity towards hydrogen. *J. Energy Inst.* **91**, 110–119 (2016)
48. S. Wang, W. Yao, J. Lin, Z. Ding, X. Wang, Cobalt imidazolate metal–organic frameworks photosplit CO<sub>2</sub> under Mild reaction conditions. *Angew. Chem. Int. Ed.* **53**(4), 1034–1038 (2014)

## 5. Conclusion

In these three papers, we investigated the functionalization of two kinds of surfaces for different applications, the first one a polymer, i.e. cyclic olefin copolymer, and the second an agrowaste material, i.e. cocoa shells. The functionalization of COC and cocoa shell by diazonium salts, in the first two papers, were performed following similar protocols indicating that diazonium reduction is really versatile. Taking into account the advantage of the diazonium chemical reduction, including high reactivity, low cost and a fast process, we performed the covalent grafting of these two surfaces in acidic solution in the presence of a chemical reducer. Parameters such as temperature influence, reagent concentration and light irradiation time, in the case of COC functionalization, were tested in order to provide optimal conditions for the covalent functionalization.

The use of methods such as SEM-EDX, AFM and ATR-IRTF for surfaces characterization, allowed us to show the aryldiazonium grafting through the presence of a thick layer onto the surface, and also prove it to be strong enough to withstand ultrasonic treatment, meaning that the aryldiazonium salts were covalently grafted into the both surfaces.

However, as we showed in the first paper about the COC surface, although we ensure the effectiveness of grafting through the classical methods, some important functions such as carbon-sulfur and carbon-halogen are still difficult to evidence due to the ambiguity presented by the results. Thinking about it, we decided to combine the classical techniques with two different coupled methods. The Ion mobility Mass Spectrometry (IM-MS) and the Atmospheric Solid Analysis Probe Ionization (ASAP) which give rise to the ASAP-IM-MS, where these functions previously mentioned were easily detected. In addition to being able to identify and characterize a small lateral chain in the para position on the phenyl ring, limiting a possible growth of multilayers and so influencing the film formation. After these conclusive studies, we

may introduce the ASAP-IM-MS as a new complementary technique to classical characterization of COC surfaces. Dedicated to the direct analysis of solid samples without sample preparation.

In the parallel studies of functionalization of the cocoa shell surface, in the second paper, we could observe solid evidence of the reaction between the salts of diazonium and the surface of cocoa shell already at the beginning of the experiments. That evidence was given due to the changes in the color of the solution from transparent to yellow-orange and also in the fact that the cocoa shell grains had moved from the bottom of the beaker up to the liquid surface during the reaction process. Which can be attributed to morphological modifications at the cocoa shell surface caused by the attachment of the nitro groups from the diazonium salts on the CS surface.

The efficacy of grafting was confirmed through results obtained using classical surface characterization methods, such as ATR-IRTF spectroscopy. Its chemical resistance was also evaluated by causing a pH variation, where no modification was observed.

After these satisfactory results with the cocoa shell and considering a better use of this raw material, with a complete work and elaborated with the intention of meeting the demands with the current environmental problems of CO<sub>2</sub> capture, we developed the CS-APTES-PDMS-Co functional agrowaste, as shown in the third paper. Where we compared the CO<sub>2</sub> absorption at each stage of CS functionalization, from the beginning with the APTES following by grafting with the PDMS until the incorporation of cobalt nanoparticles, with unmodified CS. The results showed that, besides both CS-APTES-PDMS and CS-APTES-PDMS-Co had shown an increased in the CO<sub>2</sub> adsorption capacities as compared to unmodified cocoa shells, the CO<sub>2</sub>-retention capacity measured in this study are significantly higher compared to published results.



## CONCLUSION AND PERSPECTIVES

This thesis was achieved thanks to the financial support of the Erasmus EBW + program, the Laboratoire en Chimie Organique, Bioorganique, Réactivité et Analytique (COBRA – UMR 6014), the Laboratoire de Microbiologie – Signaux et Microenvironnement (LMSM - EA 4312) and the University of Rouen Normandie.

The aim of this thesis was to study the functionalization of different surfaces using the diazonium salts and we were able to show the feasibility of a direct grafting of aryldiazoniums on different substrates.

The first part of the study was dedicated to the development of an innovative protocol for the grafting of new chemical functions on a surface known for its chemical inertness and optical properties, the gold. The objective was to apply the diazonium chemistry to develop an original SPR biosensor. We succeed to graft diazonium by chemical and electrochemical reduction and after optimization to obtain a carboxybenzene SPR biosensor. The performance of the biochip was demonstrated with antigen/antibody complex and with protein/peptide complex. This work was helpful to Pr. O. Lesouhaitier to validate that the bacterial protein AmiC and CNP hormone were in interaction. We also developed a new generation of SPR biochip promising for the future of the SPR technology.

The perspectives for this research are to determine others unknown dissociation constants ( $K_D$ ) between proteins couples but also with DNA or RNA molecules. The regeneration step has also to be improved to work with complex solution.

The second part of the study was dedicated to environment depollution, such as contaminated waters and air (capture of polluting atmospheric gases). We investigated the functionalization of two kinds of surfaces for different applications, the first one a polymer, i.e. cyclic olefin

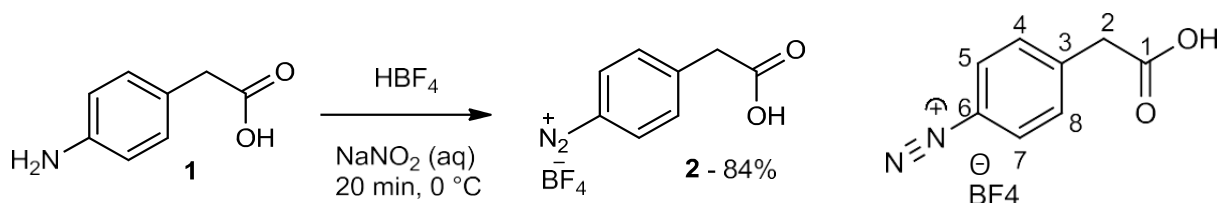
copolymer, and the second an agrowaste material, i.e. cocoa shells.

The functionalization of COC and cocoa shell by diazonium salts, in the first two papers, were performed following similar protocols indicating that diazonium reduction is really versatile. Taking into account the advantage of the diazonium chemical reduction, including high reactivity, low cost and a fast process, we performed the covalent grafting of these two surfaces in acidic solution in the presence of a chemical reducer. Different parameters and diazonium were grafted and the grafting was confirmed through different techniques (SEM, DSC, ATR-IRTF spectroscopy). Now, different perspectives could be emphasized to these works. For instance, COC is suitable for microfluidic application but his chemical inertness was an important problem. So, we can use our diazonium strategy to modulate the surface charge of the microfluidic channel and allow flow migration by electroosmosis. For cocoa shell, the grafting condition has to be optimized to obtain an amino or carboxylic surface suitable to facilitate the adsorption of inorganic or organic pollutant.

As the first analysis with cocoa shell modified by diazonium salt was not satisfactory, we decided to modify this raw material with silane derivatives and metallic particles. So, we developed an original modified cocoa shell called CS-APTES-PDMS-Co. This material present interesting properties to capture CO<sub>2</sub>. We demonstrated that CS-APTES-PDMS and CS-APTES-PDMS-Co show an increased in the CO<sub>2</sub> adsorption capacities as compared to unmodified cocoa shells. The perspective of this work will be to transfer this strategy of modification to activated carbon or other material and to see if APTES could be replaced by aminobenzene diazonium salt.

## EXPERIMENTAL PART

### 4-Carboxymethylbenzene Diazonium Synthesis



Schema 2: The 4-Carboxybenzene diazonium synthesis

The preparation of the compound was conducted according to the method described by Brisset et al.<sup>17</sup>. The 4-aminophenylacetic acid (2.077g, 17 mmol, 1 eq) was dissolved in tetrafluoroboric acid (11.5 mL, 180 mmol) in a three-necked round-bottomed flask. After cooling down the solution to 0°C with an ice bath, a solution of sodium nitrite (1.173 g, 17 mmol, 1 eq.) in 3 mL of water was added over 20 minutes and the reaction was stirred for 15 min. The solution was then kept at -18°C for minimum 3 hr. After precipitation, the diazonium salt was collected as a light brown solid by vacuum filtration. It was washed with cold diethyl ether, dried, and stored at -18°C. The compound was obtained in 84% yield (m = 3.50 g).

**<sup>1</sup>H NMR (300 MHz, CD<sub>3</sub>CN):** δ (ppm) 8.43 (d, J = 9 Hz, 2H, H-5, H-7), 7.83 (d, J = 9 Hz, 2H, H-4, H-8), 3.94 (s, 2H, H-2)

**<sup>13</sup>C NMR (75 MHz, CD<sub>3</sub>CN):** δ (ppm) 170.98 (C-1), 151.81(C-6), 134.12(C-3), 133.30(C-4 et C-8), 113.49(C-5 et C-7), 41.42 (C-2).

## The electro-reduction grafting procedure of diazonium salts

1. Prepare 100 mL of an electrolyte solution in 0.1 mol L<sup>-1</sup> of acetonitrile. The salt can be either N, N, N-tributyl-1-butanaminium tetrafluoroborate (Bu<sub>4</sub>N<sup>+</sup>, BF<sub>4</sub><sup>-</sup>) or N, N, N-tributyl-1-butanaminium hexafluorophosphate (Bu<sub>4</sub>N<sup>+</sup>, PF<sub>6</sub><sup>-</sup>).
2. Prepare 25 mL of a 0.001 mol L<sup>-1</sup> solution of ferrocene in the electrolyte. This solution acts as a reversible electrochemical probe and allows us to visualize the passivation of the surface after deposition.
3. Prepare 10 mL of a 0.005 mol L<sup>-1</sup> solution of aryldiazonium salts in the electrolyte. It is in this solution that the electrodes will be immersed (gold surface is used as working electrode, platinum as counter electrode and Ag/AgCl as reference electrode).
4. The gold surface used for the grafting is analyzed by ATR-IRTF, by cyclic voltammetry in the presence of ferrocene before and after the experiment (ferrocene redox system), and by plasmonic curves after grafting.
5. A first analysis by cyclic voltammetry is carried out in the electrolyte degassed by bubbling nitrogen, with 3 scanning cycles between -0.3 V and 1 V, at 0.1 V/s. This analysis makes it possible to verify the conductivity of the surface and the cleanliness of the electrolyte.
6. A second analysis in the ferrocene of 3 cycles between -0.3 V and 0.5 V per interval of 0.1 V/s makes it possible to determine the E<sup>0</sup> of our cell. Note that the electrodes are rinsed between each analysis with acetonitrile for HPLC.
7. The diazonium salt reduction experiment takes place by cyclic voltammetry.
8. An analysis in ferrocene (ferrocene redox system) of 3 cycles between -0.3 V and 0.5 V, at 0.1 V/s, makes it possible to verify the passivation of the surface.

It should be noted that from step 6, the gold surface is rinsed with acetonitrile between each step to minimize the contaminations that could occur if impurities were present in the electrolyte

and to remove the ferrocene deposits.

### Protocol for antibodies immobilization on SPRi biochips

This protocol presents each step of the antibody immobilization on gold SPR biochip. It was used SPRi-plex array system from *Horiba Scientific-Genoptics*. The steps are described following the order of the experiments.

\*This protocol was optimized to the current surface from Horiba book following its specifications.

\*Chemicals: All the chemicals were purchased from Sigma Aldrich. All the solutions were prepared from double distilled water 18.2 M $\Omega$ .cm (Millipore Thermo Scientific).

#### Antibodies immobilization steps

- Washing the gold biochip with MilliQ deionized water and then drying it;
- In a becker, incubation for 30 min with a mixture of EDC (400 mmol L<sup>-1</sup>/120  $\mu$ L) and Sulfo/NHS (100 mmol L<sup>-1</sup>/120  $\mu$ L)<sup>4, 189, 190</sup>;
- Washing the gold biochip with MilliQ deionized water and then drying;
- Anti-OVA (200  $\mu$ g/ml) incubation in Acetate buffer (10 mmol L<sup>-1</sup>/pH 4.5)<sup>4</sup> in humid atmosphere in order to prevent drying<sup>4</sup>:
  - Deposited as spots (the drop size is dependent of the deposition method. For this deposit is used an automatic spotter (Microarray) of the *Horiba's company* that allows to do spots of diameter 500  $\mu$ m) during 16 hours<sup>4</sup>;
  - The pH immobilization is dependent of the surface. Initially, after to EDC/SulfoNHS activation a pre-concentration test is performed to determine the correct pH. The shift to the left in the plasmon curves give an indication of the amount of immobilized antibody<sup>4</sup>.

- Washing the gold biochip with MilliQ deionized water and then drying;
- In a becker, incubation during 30 min with bovine serum albumin (BSA) 200 µg/mL without agitation, in order to passivate the areas where there is no antibody. This passivated area is used as negative control<sup>20</sup>;
- Washing the gold biochip with MilliQ deionized water and then drying;
- In a becker, incubation during 30 min with ethanolamine.HCl 1 mol L<sup>-1</sup> pH 8.5 without stirring, in order to deactivate the COOH functions which have not interacted with the antibodies and the BSA (bovine serum albumin)<sup>4</sup>;
- Washing the gold biochip with MilliQ deionized water and then drying;
- Then, the gold biochip is ready to use in Surface Plasmon Resonance (SPR) analysis.

#### Installation of the gold biochip in the SPR

- Materials used<sup>4</sup>:
  - Etched prism;
  - Gold biochip from Horiba/Schott;
  - Horiba transparent Oil index (for bonding the gold surface in biochip).

After bonding with Oil index HORIBA, the gold biochip on prism is inserted into the SPR instrument in order to measure the interaction constants between the two couples. The activation and calibration of the SPR are performed using PBS 10 mmol L<sup>-1</sup> and PBS 12.5 mmol L<sup>-1</sup> <sup>4</sup>.

On the SPR, are performed injections (using a syringe/200 µL) of ovalbumin (several concentrations in order to saturate the antibodies) during 4 min at 50 µL/min.

For antibodies regeneration, it is used glycine at 10 mmol L<sup>-1</sup> pH 2 during 4 minutes<sup>4</sup>.

## BIBLIOGRAPHIC REFERENCES Primary Sources

### Secondary Sources

#### Uncategorized References

1. Wang, R.; Tombelli, S.; Minunni, M.; Spiriti, M. M.; Mascini, M., Immobilisation of DNA probes for the development of SPR-based sensing. *Biosensors & bioelectronics* **2004**, *20* (5), 967-74.
2. Rosay, T.; Bazire, A.; Diaz, S.; Clamens, T.; Blier, A. S.; Mijouin, L.; Hoffmann, B.; Sergent, J. A.; Bouffartigues, E.; Boireau, W.; Vieillard, J.; Hulen, C.; Dufour, A.; Harmer, N. J.; Feuilloley, M. G.; Lesouhaitier, O., Pseudomonas aeruginosa Expresses a Functional Human Natriuretic Peptide Receptor Ortholog: Involvement in Biofilm Formation. *mBio* **2015**, *6* (4).
3. Bhalla, N.; Jolly, P.; Formisano, N.; Estrela, P., Introduction to biosensors. *Essays in biochemistry* **2016**, *60* (1), 1-8.
4. Marquart, A., *Surface Plasmon Resonance and Biomolecular Interaction Analysis: Theory and Practice*. Lulu. com: 2008; p 17/19/36/75.
5. Singh, S.; Gupta, A. K.; Gupta, S.; Gupta, S.; Kumar, A., Surface Plasmon Resonance (SPR) and cyclic voltammetry based immunosensor for determination of teliosporic antigen and diagnosis of Karnal Bunt of wheat using anti-teliosporic antibody. *Sensors and Actuators B: Chemical* **2014**, *191*, 866-873.
6. Figueroa, J. D.; Fout, T.; Plasynski, S.; McIlvried, H.; Srivastava, R. D., Advances in CO<sub>2</sub> capture technology—The U.S. Department of Energy's Carbon Sequestration Program. *International Journal of Greenhouse Gas Control* **2008**, *2* (1), 9-20.
7. Azar, C.; Lindgren, K.; Larson, E.; Möllersten, K., Carbon Capture and Storage From Fossil Fuels and Biomass – Costs and Potential Role in Stabilizing the Atmosphere. *Climatic Change* **2006**, *74* (1-3), 47-79.
8. Bargougui, R.; Bouazizi, N.; Brun, N.; Fotsing, P. N.; Thoumire, O.; Ladam, G.; Woumfo, E. D.; Mofaddel, N.; Derf, F. L.; Vieillard, J., Improvement in CO<sub>2</sub> adsorption capacity of cocoa shell through functionalization with amino groups and immobilization of cobalt nanoparticles. *Journal of Environmental Chemical Engineering* **2018**, *6* (1), 325-331.
9. Vilan, A.; Visoly-Fisher, I., Molecular functionalization of surfaces for device applications. *Journal of physics. Condensed matter : an Institute of Physics journal* **2016**, *28* (9), 090301.
10. Vazirinasab, E.; Jafari, R.; Momen, G., Application of superhydrophobic coatings as a corrosion barrier: A review. *Surface and Coatings Technology* **2018**, *341*, 40-56.
11. Nazeer, A. A.; Madkour, M., Potential use of smart coatings for corrosion protection of metals and alloys: A review. *Journal of Molecular Liquids* **2018**, *253*, 11-22.
12. Belanger, D.; Pinson, J., Electrografting: a powerful method for surface modification. *Chemical Society reviews* **2011**, *40* (7), 3995-4048.
13. Lu, M. C.; Wang, R. B.; Yang, A.; Duhm, S., Pentacene on Au(1 1 1), Ag(1 1 1) and Cu(1 1 1): From physisorption to chemisorption. *Journal of physics. Condensed matter : an Institute of Physics journal* **2016**, *28* (9), 094005.
14. Arnold, R. M.; Patton, D. L.; Popik, V. V.; Locklin, J., A dynamic duo: pairing click chemistry and postpolymerization modification to design complex surfaces. *Accounts of chemical research* **2014**, *47* (10), 2999-3008.
15. Kango, S.; Kalia, S.; Celli, A.; Njuguna, J.; Habibi, Y.; Kumar, R., Surface modification of inorganic nanoparticles for development of organic–inorganic nanocomposites—A review. *Progress in Polymer Science* **2013**, *38* (8), 1232-1261.

16. Minko, S., *Grafting on Solid Surfaces: "Grafting to" and "Grafting from" Methods*. 1 ed.; Springer, Berlin, Heidelberg: 2008; p 215-234.
17. Brisset, F.; Vieillard, J.; Berton, B.; Morin-Grognet, S.; Duclairoir-Poc, C.; Le Derf, F., Surface functionalization of cyclic olefin copolymer with aryldiazonium salts: A covalent grafting method. *Applied Surface Science* **2015**, *329*, 337-346.
18. Liu, G.; Liu, J.; Böcking, T.; Eggers, P. K.; Gooding, J. J., The modification of glassy carbon and gold electrodes with aryl diazonium salt: The impact of the electrode materials on the rate of heterogeneous electron transfer. *Chemical Physics* **2005**, *319* (1-3), 136-146.
19. Fioresi, F.; Vieillard, J.; Bargougui, R.; Bouazizi, N.; Fotsing, P. N.; Woumfo, E. D.; Brun, N.; Mofaddel, N.; Le Derf, F., Chemical modification of the cocoa shell surface using diazonium salts. *Journal of colloid and interface science* **2017**, *494*, 92-97.
20. Li, T. B. H., B.; Wang, S.; Chen, C.; Tang, L.; Lu, Q.; Lin, W., Covalent Grafting of Organic Molecules onto Activated Carbon by a Single Step. *BioResources* **2013**, *8*(2), 2300-2309.
21. Shewchuk, D. M.; McDermott, M. T., Comparison of diazonium salt derived and thiol derived nitrobenzene layers on gold. *Langmuir : the ACS journal of surfaces and colloids* **2009**, *25* (8), 4556-4563.
22. Ruffien, A.; Dequaire, M.; Brossier, P., Covalent immobilization of oligonucleotides on p-aminophenyl-modified carbon screen-printed electrodes for viral DNA sensing. *Chemical communications* **2003**, (7), 912-913.
23. Abdellaoui, S.; Corgier, B. C.; Mandon, C. A.; Doumèche, B.; Marquette, C. A.; Blum, L. J., Biomolecules Immobilization Using the Aryl Diazonium Electrografting. *Electroanalysis* **2013**, *25* (3), 671-684.
24. Combellas, C.; Delamar, M.; Kanoufi, F.; Pinson, J.; Podvorica, F., Spontaneous Grafting of Iron Surfaces by Reduction of Aryldiazonium Salts in Acidic or Neutral Aqueous Solution. Application to the Protection of Iron against Corrosion. *Chemistry of Materials* **2005**, pp 3968-3975.
25. Justino, C. I. L.; Freitas, A. C.; Pereira, R.; Duarte, A. C.; Rocha Santos, T. A. P., Recent developments in recognition elements for chemical sensors and biosensors. *TrAC Trends in Analytical Chemistry* **2015**, *68*, 2-17.
26. Voon, C. H.; Sam, S. T., Physical Surface Modification on the Biosensing Surface. *Nanobiosensors for Biomolecular Targeting* **2019**, 23-50.
27. Ragab, D.; Salah Eldin, H.; Taeimah, M.; Khattab, R.; Salem, R., The COVID-19 cytokine storm; what we know so far. *Frontiers in immunology* **2020**, *11*, 1446, 1-4.
28. Seo, G.; Lee, G.; Kim, M. J.; Baek, S. H.; Choi, M.; Ku, K. B.; Lee, C. S.; Jun, S.; Park, D.; Kim, H. G.; Kim, S. J.; Lee, J. O.; Kim, B. T.; Park, E. C.; Kim, S. I., Rapid Detection of COVID-19 Causative Virus (SARS-CoV-2) in Human Nasopharyngeal Swab Specimens Using Field-Effect Transistor-Based Biosensor. *ACS nano* **2020**, *14* (4), 5135-5142.
29. GS, S.; CV, A.; Mathew, B. B., Biosensors: A Modern Day Achievement. *Journal of Instrumentation Technology* **2014**, *2* (1), 26-39.
30. Janissen, R.; Sahoo, P. K.; Santos, C. A.; Da Silva, A. M.; Von Zuben, A. A.; Souto, D. E.; Costa, A. D.; Celedon, P.; Zanchin, N. I.; Almeida, D. B., InP nanowire biosensor with tailored biofunctionalization: ultrasensitive and highly selective disease biomarker detection. *Nano letters* **2017**, *17* (10), 5938-5949.
31. Román, S.; Valente Nabais, J. M.; Ledesma, B.; Laginhas, C.; Titirici, M.-M., Surface Interactions during the Removal of Emerging Contaminants by Hydrochar-Based Adsorbents. *Molecules* **2020**, *25* (9), 2264, 1-12.
32. (a) Scognamiglio, V.; Pezzotti, G.; Pezzotti, I.; Cano, J.; Buonasera, K.; Giannini, D.; Giardi, M. T., Biosensors for effective environmental and agrifood protection and commercialization: from research to market. *Microchimica Acta* **2010**, *170* (3-4), 215-225; (b) Rogers, K. R.; Williams, L. R., Biosensors for environmental monitoring: a regulatory perspective. *TrAC Trends in Analytical Chemistry* **1995**, *14* (7), 289-294.

33. Gong, R.; Sun, Y.; Chen, J.; Liu, H.; Yang, C., Effect of chemical modification on dye adsorption capacity of peanut hull. *Dyes and Pigments* **2005**, *67* (3), 175-181.
34. Peteffi, G.; Fleck, J.; Kael, I.; Rosa, D.; Antunes, M.; Linden, R., Ecotoxicological risk assessment due to the presence of bisphenol A and caffeine in surface waters in the Sinos River Basin-Rio Grande do Sul-Brazil. *Brazilian Journal of Biology* **2019**, *79* (4), 712-712.
35. Bókony, V.; Üveges, B.; Verebélyi, V.; Ujhegyi, N.; Móricz, Á. M., Toads phenotypically adjust their chemical defences to anthropogenic habitat change. *Scientific reports* **2019**, *9* (1), 1-8.
36. Dąbrowski, A.; Podkościelny, P.; Hubicki, Z.; Barczak, M., Adsorption of phenolic compounds by activated carbon—a critical review. *Chemosphere* **2005**, *58* (8), 1049-1070.
37. Fierro, V.; Torné-Fernández, V.; Montané, D.; Celzard, A., Adsorption of phenol onto activated carbons having different textural and surface properties. *Microporous and mesoporous materials* **2008**, *111* (1-3), 276-284.
38. Pan, B.; Xing, B., Adsorption mechanisms of organic chemicals on carbon nanotubes. *Environmental science & technology* **2008**, *42* (24), 9005-9013.
39. Ahmed, M.; Akter, M. S.; Lee, J.-C.; Eun, J.-B., Encapsulation by spray drying of bioactive components, physicochemical and morphological properties from purple sweet potato. *LWT-Food Science and Technology* **2010**, *43* (9), 1307-1312.
40. Elbir, T.; Muezzinoglu, A., Estimation of emission strengths of primary air pollutants in the city of Izmir, Turkey. *Atmospheric Environment* **2004**, *38* (13), 1851-1857.
41. Fu, X.; Wang, S.; Zhao, B.; Xing, J.; Cheng, Z.; Liu, H.; Hao, J., Emission inventory of primary pollutants and chemical speciation in 2010 for the Yangtze River Delta region, China. *Atmospheric Environment* **2013**, *70*, 39-50.
42. Lin, F.; Wang, Z.; Zhang, Z.; He, Y.; Zhu, Y.; Shao, J.; Yuan, D.; Chen, G.; Cen, K., Flue gas treatment with ozone oxidation: an overview on NO<sub>x</sub>, organic pollutants, and mercury. *Chemical Engineering Journal* **2020**, *382*, 123030.
43. Barth, P.; Blaudszun, B. Process and apparatus for the recovery of solvents. 1984.
44. Yu, B.; Liu, X.; Li, N.; Liu, S.; Ji, J., The performance analysis of a purified PV/T-Trombe wall based on thermal catalytic oxidation process in winter. *Energy Conversion and Management* **2020**, *203*, 112262.
45. Mohamed, E. F.; Awad, G.; Andriantsiferana, C.; El-Diwany, A. I., Biofiltration technology for the removal of toluene from polluted air using *Streptomyces griseus*. *Environmental technology* **2016**, *37* (10), 1197-1207.
46. Rao, A. B.; Rubin, E. S., A technical, economic, and environmental assessment of amine-based CO<sub>2</sub> capture technology for power plant greenhouse gas control. *Environmental science & technology* **2002**, *36* (20), 4467-4475.
47. Ahmad, F.; Daud, W. M. A. W.; Ahmad, M. A.; Radzi, R.; Azmi, A. A., The effects of CO<sub>2</sub> activation, on porosity and surface functional groups of cocoa (*Theobroma cacao*) – Shell based activated carbon. *Journal of Environmental Chemical Engineering* **2013**, *1* (3), 378-388.
48. de Quadros Melo, D.; de Oliveira Sousa Neto, V.; de Freitas Barros, F. C.; Raulino, G. S. C.; Vidal, C. B.; do Nascimento, R. F., Chemical modifications of lignocellulosic materials and their application for removal of cations and anions from aqueous solutions. *Journal of Applied Polymer Science* **2016**, *133* (15).
49. Montemore, M. M.; Medlin, J. W., A unified picture of adsorption on transition metals through different atoms. *Journal of the American Chemical Society* **2014**, *258* (26), 17–37.
50. Cordova, E.; Gao, J.; Whitesides, G. M., Noncovalent polycationic coatings for capillaries in capillary electrophoresis of proteins. *Analytical chemistry* **1997**, *69* (7), 1370-1379.
51. Hardenborg, E.; Zuberovic, A.; Ullsten, S.; Soderberg, L.; Heldin, E.; Markides, K. E., Novel polyamine coating providing non-covalent deactivation and reversed electroosmotic flow of fused-silica capillaries for capillary electrophoresis. *Journal of chromatography. A* **2003**, *1003* (1-2), 217-221.

52. Lucy, C. A.; MacDonald, A. M.; Gulcev, M. D., Non-covalent capillary coatings for protein separations in capillary electrophoresis. *Journal of chromatography. A* **2008**, *1184* (1-2), 81-105.
53. Pinson, J.; Podvorica, F., Attachment of organic layers to conductive or semiconductive surfaces by reduction of diazonium salts. *Chemical Society reviews* **2005**, *34* (5), 429-439.
54. Mahouche-Chergui, S.; Gam-Derouich, S.; Mangeney, C.; Chehimi, M. M., Aryl diazonium salts: a new class of coupling agents for bonding polymers, biomacromolecules and nanoparticles to surfaces. *Chemical Society reviews* **2011**, *40* (7), 4143-4166.
55. A. Belmont; Bureau, C.; Chehimi, M. M.; Derouich, S.; Pinson, J., Patents and Industrial Applications of Aryl Diazonium Salts and Other Coupling. In *Aryl Diazonium Salts: New Coupling Agents in Polymer and Surface Science*, Chehimi, M. M., Ed. Wiley-VCH Verlag GmbH & Co.: 2012; pp 309-321.
56. Pinson, J., *Aryl Diazonium Salts: New Coupling Agents in Polymer and Surface Science*. Wiley-VCH Verlag GmbH & Co.: 2012; Vol. 1, p 1-35.
57. Mévellec, V.; Roussel, S.; Tessier, L.; Chancelon, J.; Mayne-L'Hermite, M.; Deniau, G.; Viel, P.; Palacin, S., Grafting Polymers on Surfaces: A New Powerful and Versatile Diazonium Salt-Based One-Step Process in Aqueous Media. *Chemistry of Materials* **2007**, *19* (25), 6323-6330.
58. Chehimi, M. M.; Lamouri, A.; Picot, M.; Pinson, J., Surface modification of polymers by reduction of diazonium salts: polymethylmethacrylate as an example. *Journal of Materials Chemistry C* **2014**, *2* (2), 356-363.
59. Samanta, S.; Bakas, I.; Yilmaz, G.; Cabet, E.; Lilienbaum, A.; Sun, X.; Gosecka, M.; Basinska, T.; Slomkowski, S.; Singh, A., Antibacterial flexible biaxially oriented polyethylene terephthalate sheets through sequential diazonium and hydrophilic polymer surface chemistries. *Journal of Colloid Science and Biotechnology* **2014**, *3* (1), 58-67.
60. Pensa, E.; Cortes, E.; Corthey, G.; Carro, P.; Vericat, C.; Fonticelli, M. H.; Benitez, G.; Rubert, A. A.; Salvarezza, R. C., The chemistry of the sulfur-gold interface: in search of a unified model. *Accounts of chemical research* **2012**, *45* (8), 1183-1192.
61. Xue, Y.; Li, X.; Li, H.; Zhang, W., Quantifying thiol-gold interactions towards the efficient strength control. *Nature communications* **2014**, *5* (1), 1-9.
62. Inkpen, M. S.; Liu, Z. F.; Li, H.; Campos, L. M.; Neaton, J. B.; Venkataraman, L., Non-chemisorbed gold-sulfur binding prevails in self-assembled monolayers. *Nature chemistry* **2019**, *11* (4), 351-358.
63. Liu, G.; Böcking, T.; Gooding, J. J., Diazonium salts: Stable monolayers on gold electrodes for sensing applications. *Journal of Electroanalytical Chemistry* **2007**, *600* (2), 335-344.
64. Plueddemann, E. P., *Silane coupling agents*. Plenum Press, New York. **1982**.
65. Rye, R.; Nelson, G.; Dugger, M., Mechanistic aspects of alkylchlorosilane coupling reactions. *Langmuir : the ACS journal of surfaces and colloids* **1997**, *13* (11), 2965-2972.
66. Haensch, C.; Hoepfner, S.; Schubert, U. S., Chemical modification of self-assembled silane based monolayers by surface reactions. *Chemical Society reviews* **2010**, *39* (6), 2323-2334.
67. Jal, P. K.; Patel, S.; Mishra, B. K., Chemical modification of silica surface by immobilization of functional groups for extractive concentration of metal ions. *Talanta* **2004**, *62* (5), 1005-1028.
68. Ifuku, S.; Yano, H., Effect of a silane coupling agent on the mechanical properties of a microfibrillated cellulose composite. *International journal of biological macromolecules* **2015**, *74*, 428-432.
69. Ratner, B. D.; Hoffman, A. S.; Schoen, F. J.; Lemons, J. E., Introduction – Biomaterials Science: An evolving, multidisciplinary endeavor. In *Biomaterials science* Third ed.; Elsevier: 2013; pp 41-53.
70. Pomerantz, M.; Segmüller, A.; Netzer, L.; Sagiv, J., Coverage of Si substrates by self-assembling monolayers and multilayers as measured by IR, wettability and X-ray diffraction. *Thin Solid Films* **1985**, *132* (1-4), 153-162.
71. Vandenberg, E. T.; Bertilsson, L.; Liedberg, B.; Uvdal, K.; Erlandsson, R.; Elwing, H.; Lundström, I., Structure of 3-aminopropyl triethoxy silane on silicon oxide. *Journal of colloid and interface science* **1991**, *147* (1), 103-118.

72. Abdelmouleh, M.; Boufi, S.; Belgacem, M.; Duarte, A.; Salah, A. B.; Gandini, A., Modification of cellulosic fibres with functionalised silanes: development of surface properties. *International Journal of Adhesion and Adhesives* **2004**, *24* (1), 43-54.
73. Abdelmouleh, M.; Boufi, S.; Salah A. b.; Belgacem MN; Gandini A. *Interaction of Silane Coupling Agents with Cellulose. Langmuir* **2002**, *18*, 3203-3208.
74. Xie, Y.; Hill, C. A.; Xiao, Z.; Militz, H.; Mai, C., Silane coupling agents used for natural fiber/polymer composites: A review. *Composites Part A: Applied Science and Manufacturing* **2010**, *41* (7), 806-819.
75. Cazaurang-Martinez, M. N.; Herrera-Franco, P. J.; Gonzalez-Chi, P. I.; Aguilar-Vega, M., Physical and mechanical properties of henequen fibers. *Journal of Applied Polymer Science* **1991**, *43* (4), 749-756.
76. Asri, R. I. M.; Harun, W. S. W.; Samykano, M.; Lah, N. A. C.; Ghani, S. A. C.; Tarlochan, F.; Raza, M. R., Corrosion and surface modification on biocompatible metals: A review. *Materials science & engineering. C, Materials for biological applications* **2017**, *77*, 1261-1274.
77. Mo, F.; Dong, G.; Zhang, Y.; Wang, J., Recent applications of arene diazonium salts in organic synthesis. *Organic & biomolecular chemistry* **2013**, *11* (10), 1582-1593.
78. Balz, G.; Schiemann, G., Über aromatische Fluorverbindungen, I.: Ein neues Verfahren zu ihrer Darstellung. *Berichte der deutschen chemischen Gesellschaft (A and B Series)* **1927**, *60* (5), 1186-1190.
79. Kochi, J. K., The Mechanism of the Sandmeyer and Meerwein Reactions. *Journal of the American Chemical Society* **1957**, *79* (11), 2942-2948.
80. Heinrich, M. R., Intermolecular olefin functionalisation involving aryl radicals generated from arenediazonium salts. *Chemistry—A European Journal* **2009**, *15* (4), 820-833.
81. Gam-Derouich, S.; Gosecka, M.; Lepinay, S.; Turmine, M.; Carbonnier, B.; Basinska, T.; Slomkowski, S.; Millot, M. C.; Othmane, A.; Ben Hassen-Chehimi, D.; Chehimi, M. M., Highly hydrophilic surfaces from polyglycidol grafts with dual antifouling and specific protein recognition properties. *Langmuir : the ACS journal of surfaces and colloids* **2011**, *27* (15), 9285-9294.
82. (a) Kullapere, M.; Kozlova, J.; Matisen, L.; Sammelselg, V.; Menezes, H. A.; Maia, G.; Schiffrin, D. J.; Tammeveski, K., Electrochemical properties of aryl-modified gold electrodes. *Journal of Electroanalytical Chemistry* **2010**, *641* (1-2), 90-98; (b) Khoshroo, M.; Rostami, A. A., Characterization of the organic molecules deposited at gold surface by the electrochemical reaction of diazonium salts. *Journal of Electroanalytical Chemistry* **2010**, *647* (2), 117-122.
83. Mahouche, S.; Mekni, N.; Abbassi, L.; Lang, P.; Perruchot, C.; Jouini, M.; Mammeri, F.; Turmine, M.; Romdhane, H. B.; Chehimi, M. M., Tandem diazonium salt electroreduction and click chemistry as a novel, efficient route for grafting macromolecules to gold surface. *Surface Science* **2009**, *603* (21), 3205-3211.
84. Polsky, R.; Harper, J. C.; Wheeler, D. R.; Dirk, S. M.; Arango, D. C.; Brozik, S. M., Electrically addressable diazonium-functionalized antibodies for multianalyte electrochemical sensor applications. *Biosensors and Bioelectronics* **2008**, *23* (6), 757-764.
85. Le Floch, F.; Simonato, J.-P.; Bidan, G., Electrochemical signature of the grafting of diazonium salts: A probing parameter for monitoring the electro-addressed functionalization of devices. *Electrochimica Acta* **2009**, *54* (11), 3078-3085.
86. Harper, J. C.; Polsky, R.; Wheeler, D. R.; Brozik, S. M., Maleimide-activated aryl diazonium salts for electrode surface functionalization with biological and redox-active molecules. *Langmuir : the ACS journal of surfaces and colloids* **2008**, *24* (5), 2206-2211.
87. Gorlushko, D. A.; Filimonov, V. D.; Krasnokutskaya, E. A.; Semenischeva, N. I.; Go, B. S.; Hwang, H. Y.; Cha, E. H.; Chi, K.-W., Iodination of aryl amines in a water-paste form via stable aryl diazonium tosylates. *Tetrahedron Letters* **2008**, *49* (6), 1080-1082.

88. Lyskawa, J.; Bélanger, D., Direct modification of a gold electrode with aminophenyl groups by electrochemical reduction of in situ generated aminophenyl monodiazonium cations. *Chemistry of Materials* **2006**, *18* (20), 4755-4763.
89. Baranton, S.; Bélanger, D., In situ generation of diazonium cations in organic electrolyte for electrochemical modification of electrode surface. *Electrochimica Acta* **2008**, *53* (23), 6961-6967.
90. Combellas, C.; Kanoufi, F.; Pinson, J.; Podvorica, F. I., Sterically hindered diazonium salts for the grafting of a monolayer on metals. *Journal of the American Chemical Society* **2008**, *130* (27), 8576-8577.
91. Zhang, X. Electrochemical and Photochemical Functionalization of Au and Si Surfaces by Grafting of Diazonium and Azide Compounds. Dissertation zur Erlangung des akademischen Grades, Humboldt-Universität, Berlin (Germany) 2011.
92. Stewart, M. P.; Maya, F.; Kosynkin, D. V.; Dirk, S. M.; Stapleton, J. J.; McGuinness, C. L.; Allara, D. L.; Tour, J. M., Direct covalent grafting of conjugated molecules onto Si, GaAs, and Pd surfaces from aryldiazonium salts. *Journal of the American Chemical Society* **2004**, *126* (1), 370-378.
93. Girard, A.; Geneste, F.; Coulon, N.; Cardinaud, C.; Mohammed-Brahim, T., SiGe derivatization by spontaneous reduction of aryl diazonium salts. *Applied surface science* **2013**, *282*, 146-155.
94. Mangeney, C.; Qin, Z.; Dahoumane, S. A.; Adenier, A.; Herbst, F.; Boudou, J.-P.; Pinson, J.; Chehimi, M. M., Electroless ultrasonic functionalization of diamond nanoparticles using aryl diazonium salts. *Diamond and Related Materials* **2008**, *17* (11), 1881-1887.
95. Lehr, J.; Williamson, B. E.; Downard, A. J., Spontaneous grafting of nitrophenyl groups to planar glassy carbon substrates: evidence for two mechanisms. *The Journal of Physical Chemistry C* **2011**, *115* (14), 6629-6634.
96. Allongue, P.; de Villeneuve, C. H.; Cherouvrier, G.; Cortes, R.; Bernard, M.-C., Phenyl layers on H-Si (111) by electrochemical reduction of diazonium salts: monolayer versus multilayer formation. *Journal of Electroanalytical Chemistry* **2003**, *550*, 161-174.
97. Lehr, J.; Garrett, D. J.; Paulik, M. G.; Flavel, B. S.; Brooksby, P. A.; Williamson, B. E.; Downard, A. J., Patterning of metal, carbon, and semiconductor substrates with thin organic films by microcontact printing with aryldiazonium salt inks. *Analytical chemistry* **2010**, *82* (16), 7027-7034.
98. Sun, J.; Wang, Z.; Wu, L.; Zhang, X.; Shen, J.; Gao, S.; Chi, L.; Fuchs, H., Investigation of the Covalently Attached Multilayer Architecture Based on Diazo-Resins and Poly (4-styrene sulfonate). *Macromolecular Chemistry and Physics* **2001**, *202* (7), 967-973.
99. Le Floch, F.; Matheron, M.; Vinet, F., Electrochemical grafting on SOI substrates using aryl diazonium salts. *Journal of electroanalytical chemistry* **2011**, *660* (1), 127-132.
100. Skrunts, L.; Kiprianova, L.; Levit, A.; Gragerov, I.; Gordina, T.; Mkhitarov, R., Kinetics and mechanism of the reduction of diazonium salts by hypophosphite. *Theoretical and Experimental Chemistry* **1983**, *19* (1), 98-101.
101. Abiman, P.; Wildgoose, G. G.; Compton, R. G., Investigating the mechanism for the covalent chemical modification of multiwalled carbon nanotubes using aryl diazonium salts. *Int. J. Electrochem. Sci* **2008**, *3* (2), 104-117.
102. Berisha, A.; Chehimi, M.; Pinson, J.; Podvorica, F., Electrode Surface Modification Using Diazonium Salts. In *Electroanalytical Chemistry*, 2015; pp 115-224.
103. Tessier, L. Greffage de films organiques par Polymerisation radicalaire electro-amorcee en milieu aqueux disperse. Thèse de doctorat Physique et Chimie des matériaux,, Université Pierre & Marie Curie, Paris, 2009.
104. Berthelot, T.; Garcia, A.; Le, X. T.; El Morsli, J.; Jégou, P.; Palacin, S.; Viel, P., "Versatile toolset" for DNA or protein immobilization: Toward a single-step chemistry. *Applied Surface Science* **2011**, *257* (8), 3538-3546.
105. Liu, G.; Liu, J.; Davis, T. P.; Gooding, J. J., Electrochemical impedance immunosensor based on gold nanoparticles and aryl diazonium salt functionalized gold electrodes for the detection of antibody. *Biosensors and Bioelectronics* **2011**, *26* (8), 3660-3665.

106. Radi, A. E.; Lates, V.; Marty, J. L., Mediatorless Hydrogen Peroxide Biosensor Based on Horseradish Peroxidase Immobilized on 4-Carboxyphenyl Film Electrografted on Gold Electrode. *Electroanalysis: An International Journal Devoted to Fundamental and Practical Aspects of Electroanalysis* **2008**, *20* (23), 2557-2562.
107. Harper, J. C.; Polsky, R.; Wheeler, D. R.; Lopez, D. M.; Arango, D. C.; Brozik, S. M., A multifunctional thin film Au electrode surface formed by consecutive electrochemical reduction of aryl diazonium salts. *Langmuir : the ACS journal of surfaces and colloids* **2009**, *25* (5), 3282-3288.
108. Gam-Derouich, S.; Mahouche-Chergui, S.; Turmine, M.; Piquemal, J.-Y.; Hassen-Chehimi, D. B.; Omastova, M.; Chehimi, M. M., A versatile route for surface modification of carbon, metals and semi-conductors by diazonium salt-initiated photopolymerization. *Surface science* **2011**, *605* (21-22), 1889-1899.
109. Liu, G.; Luais, E.; Gooding, J. J., The fabrication of stable gold nanoparticle-modified interfaces for electrochemistry. *Langmuir : the ACS journal of surfaces and colloids* **2011**, *27* (7), 4176-4183.
110. Chaussé, A.; Chehimi, M. M.; Karsi, N.; Pinson, J.; Podvorica, F.; Vautrin-UI, C., The electrochemical reduction of diazonium salts on iron electrodes. The formation of covalently bonded organic layers and their effect on corrosion. *Chemistry of Materials* **2002**, *14* (1), 392-400.
111. Adenier, A.; Cabet-Deliry, E.; Lalot, T.; Pinson, J.; Podvorica, F., Attachment of polymers to organic moieties covalently bonded to iron surfaces. *Chemistry of materials* **2002**, *14* (11), 4576-4585.
112. Matrab, T.; Chehimi, M. M.; Perruchot, C.; Adenier, A.; Guillez, A.; Save, M.; Charleux, B.; Cabet-Deliry, E.; Pinson, J., Novel approach for metallic surface-initiated atom transfer radical polymerization using electrografted initiators based on aryl diazonium salts. *Langmuir : the ACS journal of surfaces and colloids* **2005**, *21* (10), 4686-4694.
113. Adenier, A.; Barré, N.; Cabet-Deliry, E.; Chaussé, A.; Griveau, S.; Mercier, F.; Pinson, J.; Vautrin-UI, C., Study of the spontaneous formation of organic layers on carbon and metal surfaces from diazonium salts. *Surface Science* **2006**, *600* (21), 4801-4812.
114. Matrab, T.; Save, M.; Charleux, B.; Pinson, J.; Cabet-Deliry, E.; Adenier, A.; Chehimi, M. M.; Delamar, M., Grafting densely-packed poly (n-butyl methacrylate) chains from an iron substrate by aryl diazonium surface-initiated ATRP: XPS monitoring. *Surface Science* **2007**, *601* (11), 2357-2366.
115. Berisha, A.; Combellas, C.; Kanoufi, F.; Pinson, J.; Podvorica, F. I., Physisorption vs grafting of aryl diazonium salts onto iron: A corrosion study. *Electrochimica Acta* **2011**, *56* (28), 10762-10766.
116. Gam-Derouich, S.; Gosecka, M.; Lepinay, S.; Turmine, M.; Carbonnier, B.; Basinska, T.; Slomkowski, S.; Millot, M.-C.; Othmane, A.; Ben Hassen-Chehimi, D., Highly hydrophilic surfaces from polyglycidol grafts with dual antifouling and specific protein recognition properties. *Langmuir : the ACS journal of surfaces and colloids* **2011**, *27* (15), 9285-9294.
117. Shaulov, Y.; Okner, R.; Levi, Y.; Tal, N.; Gutkin, V.; Mandler, D.; Domb, A. J., Poly (methyl methacrylate) grafting onto stainless steel surfaces: application to drug-eluting stents. *ACS applied materials & interfaces* **2009**, *1* (11), 2519-2528.
118. Alageel, O. S., *Bonding Between Metals and Polymers for Dental Devices*. McGill University, Montréal (Canada) M.S.c in Dental Sciences, 2013; p 111.
119. Le, X. T.; Zeb, G.; Jégou, P.; Berthelot, T., Electrografting of stainless steel by the diazonium salt of 4-aminobenzylphosphonic acid. *Electrochimica acta* **2012**, *71*, 66-72.
120. Liang, H.; Tian, H.; McCreery, R. L., Normal and surface-enhanced Raman spectroscopy of nitroazobenzene submonolayers and multilayers on carbon and silver surfaces. *Applied spectroscopy* **2007**, *61* (6), 613-620.
121. (a) Mirkhalaf, F.; Paprotny, J.; Schiffrin, D. J., Synthesis of metal nanoparticles stabilized by metal-carbon bonds. *Journal of the American Chemical Society* **2006**, *128* (23), 7400-7401; (b) Ghilane, J.; Delamar, M.; Guilloux-Viry, M.; Lagrost, C.; Mangeney, C.; Hapiot, P., Indirect reduction of aryl diazonium salts onto cathodically activated platinum surfaces: Formation of metal-organic structures. *Langmuir : the ACS journal of surfaces and colloids* **2005**, *21* (14), 6422-6429.

122. Ghosh, D.; Pradhan, S.; Chen, W.; Chen, S., Titanium nanoparticles stabilized by Ti– C covalent bonds. *Chemistry of Materials* **2008**, *20* (4), 1248-1250.
123. Combellas, C.; Jiang, D.-e.; Kanoufi, F.; Pinson, J.; Podvorica, F. I., Steric effects in the reaction of aryl radicals on surfaces. *Langmuir : the ACS journal of surfaces and colloids* **2009**, *25* (1), 286-293.
124. Koval'chuk, E. P.; Reshetnyak, O. V.; Pereviznyk, O. B.; Marchuk, I. E.; Smetanets'kyj, V. Y.; Błażejowski, J., Reaction of metals with benzenediazonium tetrafluoroborate in aprotic solvents. *Central European Journal of Chemistry* **2010**, *8* (3), 652-661.
125. Han, S.; Yuan, Y.; Hu, L.; Xu, G., Electrochemical derivatization of carbon surface by reduction of diazonium salts in situ generated from nitro precursors in aqueous solutions and electrocatalytic ability of the modified electrode toward hydrogen peroxide. *Electrochemistry communications* **2010**, *12* (12), 1746-1748.
126. Paulik, M. The Modification of Gold Surfaces via the Reduction of Aryldiazonium Salts. Masters of Science in Chemistry, University of Canterbury (England), 2007.
127. Paulik, M. G.; Brooksby, P. A.; Abell, A. D.; Downard, A. J., Grafting aryl diazonium cations to polycrystalline gold: Insights into film structure using gold oxide reduction, redox probe electrochemistry, and contact angle behavior. *The Journal of Physical Chemistry C* **2007**, *111* (21), 7808-7815.
128. Allongue, P.; Delamar, M.; Desbat, B.; Fagebaume, O.; Hitmi, R.; Pinson, J.; Saveant, J.-M., Covalent modification of carbon surfaces by aryl radicals generated from the electrochemical reduction of diazonium salts. *Journal of the American Chemical Society* **1997**, *119* (1), 201-207.
129. Latus, A.; Noël, J.-M.; Volanschi, E.; Lagrost, C.; Hapiot, P., Scanning electrochemical microscopy studies of glutathione-modified surfaces. An erasable and sensitive-to-reactive oxygen species surface. *Langmuir : the ACS journal of surfaces and colloids* **2011**, *27* (17), 11206-11211.
130. Picot, M.; Lapinsonnière, L.; Rothballer, M.; Barrière, F., Graphite anode surface modification with controlled reduction of specific aryl diazonium salts for improved microbial fuel cells power output. *Biosensors and Bioelectronics* **2011**, *28* (1), 181-188.
131. Corgier, B. P.; Laurent, A.; Perriat, P.; Blum, L. J.; Marquette, C. A., A versatile method for direct and covalent immobilization of DNA and proteins on biochips. *Angewandte Chemie International Edition* **2007**, *46* (22), 4108-4110.
132. Bahr, J. L.; Yang, J.; Kosynkin, D. V.; Bronikowski, M. J.; Smalley, R. E.; Tour, J. M., Functionalization of carbon nanotubes by electrochemical reduction of aryl diazonium salts: a bucky paper electrode. *Journal of the American Chemical Society* **2001**, *123* (27), 6536-6542.
133. Corgier, B. P.; Marquette, C. A.; Blum, L. J., Diazonium– protein adducts for graphite electrode microarrays modification: direct and addressed electrochemical immobilization. *Journal of the American Chemical Society* **2005**, *127* (51), 18328-18332.
134. Allongue, P.; De Villeneuve, C. H.; Pinson, J.; Ozanam, F.; Chazalviel, J.; Wallart, X., Organic monolayers on Si (111) by electrochemical method. *Electrochimica Acta* **1998**, *43* (19-20), 2791-2798.
135. Quinton, D.; Galtayries, A.; Prima, F.; Griveau, S., Functionalization of titanium surfaces with a simple electrochemical strategy. *Surface and Coatings Technology* **2012**, *206* (8-9), 2302-2307.
136. He, T.; He, J.; Lu, M.; Chen, B.; Pang, H.; Reus, W. F.; Nolte, W. M.; Nackashi, D. P.; Franzon, P. D.; Tour, J. M., Controlled modulation of conductance in silicon devices by molecular monolayers. *Journal of the American Chemical Society* **2006**, *128* (45), 14537-14541.
137. Haque, A.-M. J.; Kim, K., Aldehyde-functionalized benzenediazonium cation for multiprobe immobilization on microelectrode array surfaces. *Langmuir : the ACS journal of surfaces and colloids* **2011**, *27* (3), 882-886.
138. Collins, G.; Fleming, P.; O'Dwyer, C.; Morris, M. A.; Holmes, J. D., Organic functionalization of germanium nanowires using arenediazonium salts. *Chemistry of Materials* **2011**, *23* (7), 1883-1891.

139. Lefèvre, X.; Segut, O.; Jégou, P.; Palacin, S.; Jusselme, B., Towards organic film passivation of germanium wafers using diazonium salts: Mechanism and ambient stability. *Chemical Science* **2012**, *3* (5), 1662-1671.
140. Deinhammer, R. S.; Ho, M.; Anderegg, J. W.; Porter, M. D., Electrochemical oxidation of amine-containing compounds: a route to the surface modification of glassy carbon electrodes. *Langmuir : the ACS journal of surfaces and colloids* **1994**, *10* (4), 1306-1313.
141. Han, L.; Ju, H.; Xu, Y., Ethanol electro-oxidation: Cyclic voltammetry, electrochemical impedance spectroscopy and galvanostatic oscillation. *International journal of hydrogen energy* **2012**, *37* (20), 15156-15163.
142. Malmos, K.; Iruthayaraj, J.; Pedersen, S. U.; Daasbjerg, K., General approach for monolayer formation of covalently attached aryl groups through electrografting of arylhydrazines. *Journal of the American Chemical Society* **2009**, *131* (39), 13926-13927.
143. Andrieux, C. P.; Gonzalez, F.; Savéant, J.-M., Derivatization of carbon surfaces by anodic oxidation of arylacetates. Electrochemical manipulation of the grafted films. *Journal of the American Chemical Society* **1997**, *119* (18), 4292-4300.
144. Delamar, M.; Hitmi, R.; Pinson, J.; Saveant, J. M., Covalent modification of carbon surfaces by grafting of functionalized aryl radicals produced from electrochemical reduction of diazonium salts. *Journal of the American Chemical Society* **1992**, *114* (14), 5883-5884.
145. Nguyen, H. H.; Park, J.; Kang, S.; Kim, M., Surface plasmon resonance: a versatile technique for biosensor applications. *Sensors* **2015**, *15* (5), 10481-510.
146. Mansuy-Schlick, V.; Delage-Mourroux, R.; Jouvenot, M.; Boireau, W., Strategy of macromolecular grafting onto a gold substrate dedicated to protein–protein interaction measurements. *Biosensors and Bioelectronics* **2006**, *21* (9), 1830-1837.
147. Berthier, A.; Elie-Caille, C.; Lesniewska, E.; Delage-Mourroux, R.; Boireau, W., Label-free sensing and atomic force spectroscopy for the characterization of protein–DNA and protein–protein interactions: application to estrogen receptors. *Journal of Molecular Recognition* **2011**, *24* (3), 429-435.
148. Liedberg, B.; Nylander, C.; Lundström, I., Biosensing with surface plasmon resonance — how it all started. *Biosensors and Bioelectronics* **1995**, *10* (8), i-ix.
149. Wong, C. L.; Olivo, M., Surface plasmon resonance imaging sensors: a review. *Plasmonics* **2014**, *9* (4), 809-824.
150. Roy, S.; Yue, C.; Lam, Y.; Wang, Z.; Hu, H., Surface analysis, hydrophilic enhancement, ageing behavior and flow in plasma modified cyclic olefin copolymer (COC)-based microfluidic devices. *Sensors and Actuators B: Chemical* **2010**, *150* (2), 537-549.
151. K., T., The Role of Surface Plasmon Resonance in Clinical Laboratories. An evolving platform has the potential to make biosensors more integrated into clinical care. *Clinical Laboratory News* **2019**.
152. Wang, D.-S.; Fan, S.-K., Microfluidic surface plasmon resonance sensors: From principles to point-of-care applications. *Sensors* **2016**, *16* (8), 1175, 1-18.
153. Wijaya, E.; Lenaerts, C.; Maricot, S.; Hastanin, J.; Habraken, S.; Vilcot, J.-P.; Boukherroub, R.; Szunerits, S., Surface plasmon resonance-based biosensors: From the development of different SPR structures to novel surface functionalization strategies. *Current Opinion in Solid State and Materials Science* **2011**, *15* (5), 208-224.
154. Homola, J.; Yee, S. S.; Gauglitz, G., Surface plasmon resonance sensors. *Sensors and Actuators B: Chemical* **1999**, *54* (1-2), 3-15.
155. Sepúlveda, B.; Angelomé, P. C.; Lechuga, L. M.; Liz-Marzán, L. M., LSPR-based nanobiosensors. *nano today* **2009**, *4* (3), 244-251.
156. Petryayeva, E.; Krull, U. J., Localized surface plasmon resonance: Nanostructures, bioassays and biosensing—A review. *Analytica chimica acta* **2011**, *706* (1), 8-24.

157. Menezes, J. W.; Ferreira, J.; Santos, M. J.; Cescato, L.; Brolo, A. G., Large-Area fabrication of periodic arrays of nanoholes in metal films and their application in biosensing and plasmonic-Enhanced photovoltaics. *Advanced Functional Materials* **2010**, *20* (22), 3918-3924.
158. Singh, P., SPR biosensors: Historical perspectives and current challenges. *Sensors and actuators B: Chemical* **2016**, *229*, 110-130.
159. Shankaran, D. R.; Gobi, K. V.; Miura, N., Recent advancements in surface plasmon resonance immunosensors for detection of small molecules of biomedical, food and environmental interest. *Sensors and Actuators B: Chemical* **2007**, *121* (1), 158-177.
160. Nguyen, H. H.; Park, J.; Kang, S.; Kim, M., Surface plasmon resonance: a versatile technique for biosensor applications. *Sensors* **2015**, *15* (5), 10481-10510.
161. Bolduc, O. R.; Masson, J.-F., Monolayers of 3-mercaptopropyl-amino acid to reduce the nonspecific adsorption of serum proteins on the surface of biosensors. *Langmuir : the ACS journal of surfaces and colloids* **2008**, *24* (20), 12085-12091.
162. Li, L.; Chen, S.; Zheng, J.; Ratner, B. D.; Jiang, S., Protein adsorption on oligo (ethylene glycol)-terminated alkanethiolate self-assembled monolayers: the molecular basis for nonfouling behavior. *The Journal of Physical Chemistry B* **2005**, *109* (7), 2934-2941.
163. Raitman, O. A.; Patolsky, F.; Katz, E.; Willner, I., Electrical contacting of glucose dehydrogenase by the reconstitution of a pyrroloquinoline quinone-functionalized polyaniline film associated with an Au-electrode: an in situ electrochemical SPR study. *Chemical communications* **2002**, (17), 1936-1937.
164. Chehimi, M. M., *Aryl diazonium salts: new coupling agents in polymer and surface science*. Wiley: 2012.
165. Chira, A.; Covaci, O.-I.; Radu, G. L., A comparative study of gold electrodes modification methods with aromatic compounds based on diazonium and thiol chemistry *Sci. Bull. B Chem. Mater. Sci. UPB* **2012**, *74*, 183-192.
166. Mandon, C. A.; Blum, L. J.; Marquette, C. A., Aryl diazonium for biomolecules immobilization onto SPRi chips. *ChemPhysChem* **2009**, *10* (18), 3273-3277.
167. Bureau, C.; Pinson, J., Use of a diazonium salt in a method for modifying insulating or semi-conductive surfaces, and resulting products. *PCT Int. Appl.* **2005**, ed. *ALCHIMER*, 51.
168. Yanase, Y.; Hiragun, T.; Ishii, K.; Kawaguchi, T.; Yanase, T.; Kawai, M.; Sakamoto, K.; Hide, M., Surface plasmon resonance for cell-based clinical diagnosis. *Sensors* **2014**, *14* (3), 4948-4959.
169. Kesavan, S.; John, S. A., Spontaneous grafting: a novel approach to graft diazonium cations on gold nanoparticles in aqueous medium and their self-assembly on electrodes. *Journal of colloid and interface science* **2014**, *428*, 84-94.
170. Baranton, S.; Bélanger, D., Electrochemical Derivatization of Carbon Surface by Reduction of in Situ Generated Diazonium Cations. *The Journal of Physical Chemistry B* **2005**, *109* (51), 24401-24410.
171. Laforgue, A.; Addou, T.; Bélanger, D., Characterization of the Deposition of Organic Molecules at the Surface of Gold by the Electrochemical Reduction of Aryldiazonium Cations. *Langmuir : the ACS journal of surfaces and colloids* **2005**, *21* (15), 6855-6865.
172. Lichtenberg, J. Y.; Ling, Y.; Kim, S., Non-specific adsorption reduction methods in biosensing. *Sensors* **2019**, *19* (11), 2488.
173. Ashley, J.; Piekarska, M.; Segers, C.; Trinh, L.; Rodgers, T.; Willey, R.; Tothill, I. E., An SPR based sensor for allergens detection. *Biosensors & bioelectronics* **2017**, *88*, 109-113.
174. Losoya-Leal, A.; Estevez, M. C.; Martinez-Chapa, S. O.; Lechuga, L. M., Design of a surface plasmon resonance immunoassay for therapeutic drug monitoring of amikacin. *Talanta* **2015**, *141*, 253-258.
175. Pillet, F.; Romera, C.; Trévisiol, E.; Bellon, S.; Teulade-Fichou, M.-P.; François, J.-M.; Pratviel, G.; Leberre, V. A., Surface plasmon resonance imaging (SPRi) as an alternative technique for rapid and quantitative screening of small molecules, useful in drug discovery. *Sensors and Actuators B: Chemical* **2011**, *157* (1), 304-309.

176. Chang, T.-C.; Wu, C.-C.; Wang, S.-C.; Chau, L.-K.; Hsieh, W.-H., Using a fiber optic particle plasmon resonance biosensor to determine kinetic constants of antigen–antibody binding reaction. *Analytical chemistry* **2013**, *85* (1), 245-250.
177. Chang, T.-C.; Wu, C.-C.; Wang, S.-C.; Chau, L.-K.; Hsieh, W.-H., Correction to Using A Fiber Optic Particle Plasmon Resonance Biosensor To Determine Kinetic Constants of Antigen–Antibody Binding Reaction. *Analytical chemistry* **2013**, *85* (21), 10625-10625.
178. Brogan, K. L.; Shin, J. H.; Schoenfish, M. H., Influence of surfactants and antibody immobilization strategy on reducing nonspecific protein interactions for molecular recognition force microscopy. *Langmuir : the ACS journal of surfaces and colloids* **2004**, *20* (22), 9729-9735.
179. sprpages, Regeneration. *SPR-Pages* **2006 - 2020**.
180. Ma, Z.; Mao, Z.; Gao, C., Surface modification and property analysis of biomedical polymers used for tissue engineering. *Colloids and surfaces. B, Biointerfaces* **2007**, *60* (2), 137-157.
181. Gonzalez-Macia, L.; Griveau, S.; d'Orlyé, F.; Varenne, A.; Sella, C.; Thouin, L.; Bedioui, F., Electrografting of aryl diazonium on thin layer platinum microbands: Towards customized surface functionalization within microsystems. *Electrochemistry Communications* **2016**, *70*, 78-81.
182. Barrère, C.; Selmi, W.; Hubert-Roux, M.; Coupin, T.; Assumani, B.; Afonso, C.; Giusti, P., Rapid analysis of polyester and polyethylene blends by ion mobility-mass spectrometry. *Polymer Chemistry* **2014**, *5* (11), 3576-3582.
183. Barrère, C.; Hubert-Roux, M.; Afonso, C.; Rcaud, A., Rapid analysis of lubricants by atmospheric solid analysis probe–ion mobility mass spectrometry. *Journal of Mass Spectrometry* **2014**, *49* (8), 709-715.
184. Bhattacharya, A.; Misra, B. N., Grafting: a versatile means to modify polymers: Techniques, factors and applications. *Progress in Polymer Science* **2004**, *29* (8), 767-814.
185. Rodriguez-Narvaez, O. M.; Peralta-Hernandez, J. M.; Goonetilleke, A.; Bandala, E. R., Treatment technologies for emerging contaminants in water: A review. *Chemical Engineering Journal* **2017**, *323*, 361-380.
186. Lu, N. C.; Liu, J. C., Removal of phosphate and fluoride from wastewater by a hybrid precipitation–microfiltration process. *Separation and Purification Technology* **2010**, *74* (3), 329-335.
187. Kumar, M.; Badruzzaman, M.; Adham, S.; Oppenheimer, J., Beneficial phosphate recovery from reverse osmosis (RO) concentrate of an integrated membrane system using polymeric ligand exchanger (PLE). *Water Research* **2007**, *41* (10), 2211-2219.
188. Sophia A, C.; Lima, E. C., Removal of emerging contaminants from the environment by adsorption. *Ecotoxicology and Environmental Safety* **2018**, *150*, 1-17.
189. Usha, R.; Sreeram, K. J.; Rajaram, A., Stabilization of collagen with EDC/NHS in the presence of L-lysine: a comprehensive study. *Colloids and surfaces. B, Biointerfaces* **2012**, *90*, 83-90.
190. Tengvall, P.; Jansson, E.; Askendal, A.; Thomsen, P.; Gretzer, C., Preparation of multilayer plasma protein films on silicon by EDC/NHS coupling chemistry. *Colloids and Surfaces B: Biointerfaces* **2003**, *28* (4), 261-272.

## MODIFICATION DE SURFACE DE DIFFÉRENTS MATÉRIAUX POUR LES APPLICATIONS BIOLOGIQUES ET ENVIRONNEMENTALES

Depuis près d'un siècle, les chercheurs déploient des efforts importants pour apporter de nouvelles propriétés aux matériaux et aujourd'hui la modification de surface des matériaux est plus que jamais un sujet de recherche très attractif lié à une variété d'applications industrielles prometteuses. Le développement d'une méthodologie simple pour caractériser les interactions biomoléculaires a été, au fil des ans, une technologie indispensable pour soutenir les recherches dans les domaines de la biologie et de la microbiologie en raison de son haut degré de sensibilité. La fonctionnalisation de surface par revêtement chimique est une solution prometteuse pour obtenir de nombreuses propriétés bien définies. Cette étude présente la faisabilité de la fonctionnalisation de la surface de l'or en utilisant une chimie basée sur les sels d'aryldiazonium pour le développement de biocapteurs appliqués à la technologie de résonance plasmonique de surface (SPR). Une technique de haute qualité utilisée pour mesurer les interactions biomoléculaires en temps réel dans un environnement label-free.

Depuis de nombreuses années, les activités industrielles sont responsables de la pollution de l'atmosphère. Bien que différents gaz à effet de serre soient impliqués dans la pollution atmosphérique, le CO<sub>2</sub> reste l'un des plus importants en raison de ses concentrations élevées dans l'atmosphère et de sa capacité à provoquer des maladies graves. Plusieurs études dans la littérature ont démontré que certains adsorbants tels que les charbons actifs, les tamis basiques de silice fonctionnalisés, les zéolithes, etc. bien que disponibles dans le commerce sont encore sophistiqués et coûteux limitant leur application. Cependant, il est toujours nécessaire de capter le CO<sub>2</sub> pour des activités à coûts d'exploitation limités. L'objectif de cette étude est de valoriser l'écorce du cacao, une ressource d'agro-déchets prête à l'emploi et facile à modifier, en tant que matériaux peu coûteux pour l'adsorption du CO<sub>2</sub> et l'élimination des toxines des déchets industriels en solution appliquant un traitement chimique à partir des sels de diazonium et des composés de silane pour modifier ses propriétés physico-chimiques.

**Mots clés** : Chimie des surfaces, fonctionnalisation chimique, sels de diazonium, silanes, biocapteurs, résonance plasmonique de surface, agro-déchets.

## SURFACE MODIFICATION OF DIFFERENT MATERIALS FOR BIOLOGICAL AND ENVIRONMENTAL APPLICATIONS

For almost a century, the researchers have been making important efforts in order to bring new properties to materials and nowadays surface modification of materials is more than ever a very attractive research subject related to a variety of promising industrial applications. The development of simple methodology to characterize biomolecular interactions has been, over the years, an indispensable technology to support researches in the areas of biology and microbiology due its high degree of sensitivity. Surface functionalization by chemical coating is a promising solution to obtain numerous well-defined properties. This study presents the feasibility of gold surface functionalization using a chemistry based on aryldiazonium salts to the biosensors development applied to Surface Plasmon Resonance (SPR) technology. A high-quality technique used to measure biomolecular interactions in real time in a label free environment.

Since many years, industrial activities are responsible to the pollution of the atmosphere. Although different greenhouse gases being involved in atmospheric pollution, CO<sub>2</sub> is still one of the most important due its high concentrations in the atmosphere and due to its ability to induce serious health disease. Several studies in the literature have demonstrated that some adsorbents such as activated carbons, basic functionalized silica sieves, zeolites, etc.. although commercially available are still sophisticated and expensive limiting their application. However, there is still a need to capture CO<sub>2</sub> for activities with limited operating cost. The objective of this study is to promote the cocoa shell, an agro-waste resource ready to use and easy to modify, as low-cost materials for CO<sub>2</sub> adsorption and toxins removal from industrial waste in solution applying a chemical treatment from diazonium salts and silane compounds to modify its physic-chemical properties.

**Keywords:** Surface chemistry, chemical functionalization, diazonium salts, silanes, biosensors, surface plasmon resonance, agro-waste.